An *Ab Initio* Density Functional Study of the Structure and Stability of Transition Metal Ozone Complexes

by

Gerhard Venter

Thesis

submitted in fulfilment of the
requirements for the degree

Magister Scientiae

in

Chemistry

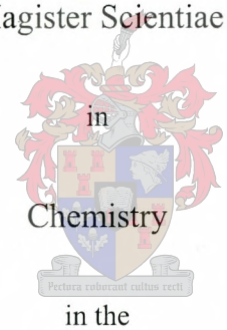

in the

Faculty of Science

at the

University of Stellenbosch

Supervisor: Prof J.L.M. Dillen

December 2002

Declaration

I, the undersigned, hereby declare that the work contained in this thesis is my own original work and that I have not previously in its entirety or in part submitted it at any university for a degree.

Summary

A thorough search through the literature as well as through the *Cambridge Crystallographic Structural Database* resulted in no examples of a neutral ozone acting as ligand in a complex with any metal. Ionic compounds containing ozonide as anionic species, however, are well known throughout the literature and not surprisingly the only result for O_3 and a metal in the CCSD was an ionic rubidium ozonide compound.

What follows is a systematic study into the result of placing an ozone ligand within complexing distance of a transition metal (the first transition row from titanium to copper). Due to the novelty of the system, as first approximation four different orientations of the ozone ligand relative to the metal (a metal cation in these calculations) were investigated. It was found that coordination through the terminal oxygens resulted in energy minima for all the metal cations, although not necessarily the absolute energy minimum on the potential energy surface for the specific cation. A further structural study was done by adding carbonyl and hydrogen ligands to the system, according to the 18-electron rule. For these calculations coordination through the terminal oxygens was employed. In both series the dissociation energy was also calculated. The dissociation energies for the $M(CO)_nH_m(O_3)$ complexes were all positive, indicating that they are theoretically stable structures.

The resulting wave functions were then analysed with the help of three techniques: Atoms in Molecules (AIM), Charge Decomposition Analysis (CDA) and Natural Bond Orbital Analysis (NBO). AIM showed that bonds were indeed formed between the ozone ligand and the transition metal and hinted that the bonding model can be interpreted with the Dewar-Chatt-Duncanson (DCD) model of σ-donation and π-back donation. CDA confirmed that this was the case. NBO results proved erroneous due to the largely delocalized electronic structure of the complexes.

Opsomming

'n Deeglike soektog deur die literatuur en die *Cambridge Crystallographic Structural Database* het geen resultate gelewer van komplekse waarin 'n neutrale osoonligand komplekseer met 'n metaal nie. Ioniese verbindings waarin die osonied as anioon optree, is wel bekend deur die literatuur en die enigste resultaat in die CCSD - vir 'n soektog bevattende osoon en 'n metaal - het 'n rubidiumosonied-verbinding opgelewer.

Wat volg is 'n stelselmatige studie om die effek te ondersoek indien 'n osoonligand naby genoeg aan 'n oorgangsmetaal geplaas word om kompleksering te bevoordeel (metale wat gebruik is, is die eerste oorgangsreeks vanaf titanium tot koper). As gevolg van die onbekendheid van die sisteem is vier verskillende oriëntasies van die osoonligand relatied tot die metal ('n metal katioon in die geval) as beginpunt ondersoek. Daar is gevind dat koördinasie deur die terminale suurstowwe van die osoonligand vir al die metal katione lei tot energie minima, alhoewel dié minima nie noodwendig die globale minima op die potensiële energie oppervlaktes van die katione is nie. 'n Verdere studie is gedoen deur karboniel- en waterstofligande tot die sisteem te voeg, gelei deur die 18-elektron reel. Vir hierdie berekeninge is koördinasie deur die terminale suurstowwe gebruik. In beide reeks is dissosiasie-energieë bereken. Die dissosiasie-energieë van die $M(CO)_nH_m(O_3)$ komplekse was deurgaan positief wat aandui dat die komplekse teoreties stabiel is.

Die verkrygde golffunksies is hierna analiseer deur middel van drie tegnieke: *Atoms in Molecules* (AIM), *Charge Decomposition Analysis* (CDA) en *Natural Bond Orbital Analysis* (NBO). AIM het getoon dat bindings inderdaad gevorm word tussen die osoonligand en die metal en het die moontlikheid laat ontstaan dat die bindingsmodel volgens die Dewar-Chatt-Duncason (DCD) model van σ-donasie en π-terugdonasie geïnterpreteer kan word. Hierdie waarneming is bevestig deur CDA. NBO resultate kon nie suksesvol gebruik word nie as gevolg van die hoë graad van electron delokalisasie van die komplekse.

Acknowledgements

- Professor J.L.M. Dillen, my supervisor, for his guidance and willingness to always explain another theoretical concept and his patience during the writing up of the thesis.
- Dr C. Esterhuysen for her help and encouragement and software.
- Dr S. Cronje for her help in the laboratory and encouragement when writing up.
- Professor J.L.M Dillen, Professor H.G. Raubenheimer, The National Research Foundation and the University of Stellenbosch for their financial support.
- Ernest Lötter for always putting up with my complaints and never refusing to help with the mathematics behind the method.
- My parents for their encouraging words over the phone and especially my mother for making sure that I don't suffer malnutrition.
- My friends for their support, especially Ingrid Strasheim for always calming me down and giving me a pat on the head when things got rough.

Publications and Presentations

- Portions of this work are being written up in the form of an article to be submitted for publication.
- A lecture was presented at the South African Crystallographic Society Annual Meeting, Stellenbosch, 4 & 5 April 2002: "*Modelling Transition Metal Ozone Complexes*".

Table of Contents

Summary i

Opsomming ii

Acknowledgements iii

Publications and Presentations iv

Table of Contents v

Glossary viii

Chapter 1: Introduction 1

Chapter 2: Theoretical Background and Review of Selected Subjects 3

2.1 Introduction 3

2.2 The Computational Method/Level of Theory 3

2.2.1 The Hartree-Fock Method 3

2.2.2 Post-Hartree-Fock Methods 6

2.2.2.1 Configuration Interaction 7

2.2.2.2 Perturbation Theory 8

2.2.2.3 Coupled Cluster Theory 9

2.2.3 Semi-empirical Methods 10

2.2.4 Molecular Mechanics 11

2.2.5 Density Functional Theory 12

2.3 The Basis Set 14

2.3.1 Slater and Gaussian-Type Orbitals 15

2.3.2 Effective Core Potentials 17

2.3.3 The Basis Set Superposition Error 17

2.4 Wave Function Instabilities 18

2.5 Wave Function Analysis 20

2.5.1 Atomic Charges 20

2.5.2 Charge Decomposition Analysis (CDA) 20
2.5.3 Atoms in Molecules (AIM) 22
2.5.4 Natural Bond Orbital Analysis (NBO) 26
2.6 The Cambridge Crystallographic Structural Database (CCSD) 28
2.7 Review of Selected Subjects 28
2.7.1 The Ozone Molecule 28

Chapter 3: Molecular Modelling – Structure Determination and Dissociation Energies 30

3.1 Introduction 30
3.2 Modelling of Ozone 30
3.2.1 Computational Procedure 30
3.2.2 Results 32
3.3 Modelling of $M[O_3]^{2+}$ 33
3.3.1 Computational Procedure 33
3.3.2 Results: Geometries 34
3.3.3 Results: Dissociation Energies 42
3.4 Modelling of $M(CO)_nH_m(O_3)$ 48
3.4.1 Computational Procedure 48
3.4.2 Results: Geometries 50
3.4.3 Results: Dissociation Energies 55

Chapter 4: Electronic Structure and Bonding Analysis 60

4.1 Introduction 60
4.2 The Electronic Structure and Bonding of the Ozone Molecule 61
4.3 The Electronic Structure and Bonding of $M(CO)_mH_n(O_3)$ 62
4.3.1 Atoms in Molecules Analysis 62
4.3.1 Charge Decomposition Analysis 69
4.3.2 Natural Bond Orbital Analysis 79

Chapter 5: Conclusion 84

References 86

Addenda 94

Addendum A: Gaussian98 Input 94

Addendum B: CDA 2.1.2 Output 100

Glossary

AIM	Atoms in Molecules
B3LYP	Becke's three-parameter DFT functional with the correlation-exchange functional of Lee, Yang and Parr.
BSSE	Basis Set Superposition Error
bcp	bond critical point
b	back donation (CDA)
CC	Coupled Cluster
CCSD(T)	Coupled Cluster with Singles and Doubles and Perturbative Triples
CDA	Charge Decomposition Analysis
CI	Configuration Interaction
d	donation (CDA)
Δ	rest term (CDA)
D_e	Dissociation energies, uncorrected for zero-point vibrational energy.
DCD	Dewar-Chatt-Duncanson
DFT	Density Functional Theory
ECP	Effective Core Potential
HF	Hartree-Fock
HOMO	Highest Occupied Molecular Orbital
KS	Kohn-Sham
LUMO	Lowest Unoccupied Molecular Orbital
MBPT	Many Body Perturbation Theory
MO	Molecular Orbital
MP	Møller-Plesset
NBO	Natural Bond Orbital
r	repulsive polarisation (CDA)
RHF	Restricted Hartree-Fock
RKS	Restricted Kohn-Sham
$\rho(r_b)$	Electron density at a bond critical point.

$\rho(r_c)$	Electron density at a critical point
SCF	Self-Consistent-Field
UHF	Unrestricted Hartree-Fock
UKS	Unrestricted Kohn-Sham

Chapter 1: Introduction

Ozone is an unstable, blue diamagnetic gas with a very characteristic metallic odour. In fact, the name ozone, coined by C.F. Schönbein in 1840, comes from the Greek word *ozein*, which means to smell.

A particularly important property of ozone, which is the reason for it receiving much attention the past years, is its ability to strongly absorb in the ultraviolet region of the spectrum, between 220 and 290 nm (λ_{max} 255.3 nm). This leads to a very important atmospheric role it plays. The earth's atmosphere is divided into several layers, the first layer being the troposphere (from the surface to a distance up to about 10 km), the second layer being the stratosphere (between 10 and 50 km up). Most atmospheric ozone is concentrated in a layer in the stratosphere between 15 and 30 km up, where it keeps the surface safe from UVB radiation, which can cause for example skin cancer or cataracts in humans. Concern was expressed in 1974 that interaction between ozone and man-made chlorofluorocarbons (CFC's) would deplete the important equilibrium concentration of ozone with possible disastrous consequences. Chlorofluorocarbons are very stable and only strong UV radiation can cause them to decompose into atomic chlorine which in turn can destroy over 100 000 ozone molecules per atom of chlorine. This concern was confirmed in 1985 by the discovery of a seasonally recurring hole in the ozone layer above Antarctica.

In 1987 the Montreal Protocol was signed, which called for the reduction of CFC production by half by 1998. After the original protocol was signed scientific evidence proved that the damage to the ozone layer was worse than first thought and the parties involved decided to completely end production of hazardous chemicals by the beginning of 1996 in developed countries.

Ozone has other interesting chemical properties as well: its strongly oxidizing nature (acid reduction, E° 2.075 V; alkaline reduction, E° 1.246 V) and its tendency to transfer an oxygen atom with coproduction of O_2. This makes ozone an ideal candidate for oxidation reactions. The acid reduction potential of ozone is only exceeded by fluorine, perxenate, atomic O, the OH radical and a few other such potent oxidants.

In the foreword to the 1991 issue of *Chemical Reviews* on Theoretical Chemistry the author states that "The theory of transition metal chemistry has lagged behind the quantum theory

of organic chemistry because quantitative wave functions are more complicated" (Davidson, 1991). This situation has changed considerably, largely due to the success that gradient-corrected density functional theory has achieved in modelling molecules and the application of small-core relativistic effective core potentials (Frenking and Frölich, 2000). This has made it possible to now study systems of which very little or even no experimental information exists.

There are many examples of ozone forming ionic compounds with the group I alkali metals, eg. LiO_3, KO_3, RbO_3 and CsO_3 (Cotton and Wilkinson, 1988). However, there exists no evidence that ozone forms complexes with transition metals. The aim of this work is to investigate the stability of transition metal complexes containing ozone as ligand with the help of gradient-corrected density functional theory. For the metals the first row transition series from titanium to copper was used.

In **Chapter 2** an overview of the theoretical methods used in this thesis as well as some techniques used in wave function analysis is given. Due to the lack of experimental information on the modelled complexes, only a short overview of some of the work done on the ozone molecule is given. Since no information is available on the structure and possible coordination of ozone to metals, as starting approximation various different possible coordination modes were investigated as described in **Chapter 3**. For this series the "complexes" consisted of only a metal cation and an ozone molecule. Further structural determinations were then done on larger complexes by adding carbonyl and hydrogen ligands and using the 18-electron rule as guide. For both series the dissociation energy was also calculated to present a relative indication of bond strength in the modelled complexes. Once good quality wave functions have been generated they can be used to gain insight into the bonding mechanism present. In **Chapter 4** three popular quantum chemical techniques for analysing the chemical bond are used to gain information about the bonding situation. An overview of the conclusions reached in each chapter is given in **Chapter 5**.

Chapter 2: Theoretical Background and Review of Selected Subjects

2.1 Introduction

An introduction to modern computational chemistry and a short discussion of some of the concepts and techniques used in this thesis are given in **section 2.2 – section 2.5**. The Cambridge Crystallographic Structural Database (CCSD) was searched for compounds containing O_3. The results are shown in **section 2.6**. A review of calculations done on the ozone molecule can be found in **section 2.7**.

2.2 The Computational Method/Level of Theory

2.2.1 The Hartree-Fock Method

The time dependent interactions of electrons can be neglected in most cases. If solutions to the time-independent Schrödinger equation

$$\hat{H}\Psi = E\Psi$$

are generated without any reference to experimental data, the methods are called *ab initio* (Latin: "from the beginning").

The most common type of *ab initio* method is the Hartree-Fock approximation (Hartree, 1928; Fock, 1930). In this approximation it is assumed that the wave function can be determined by using a single *Slater Determinant* (Slater, 1929, 1930) and that the many electron wave function can be written as a product of one-electron spin functions. Spin functions are a combination of a spatial part and an explicitly defined spin part, which can be either α or β. In a Slater determinant the columns represent the different one-electron wave functions (orbitals) with the electron coordinates along the rows. Two requirements of quantum mechanics are thereby satisfied. Firstly, electrons are indistinguishable and by having a linear combination of orbitals in which each electron appears in each orbital it is only possible to say that an electron is put in an orbital, but not which orbital. Secondly, the wave function for fermions must have the property

that it is antisymmetric with respect to the interchange of two particles. When to rows in a determinant are swapped the consequence is a change in the sign of the determinant. This is a consequence of the more familiar *Pauli Principle* (Pauli, 1925).

The Hamiltonian operator for the energy of a system with N electrons and M nuclei in atomic units is

$$\hat{\boldsymbol{H}} = -\sum_{i=1}^{N} \frac{1}{2} \nabla_i^2 - \sum_{A=1}^{M} \frac{1}{2M_A} \nabla_A^2 - \sum_{i=1}^{N} \sum_{A=1}^{M} \frac{Z_A}{|R_A - r_i|} + \sum_{i=1}^{N} \sum_{j>i}^{N} \frac{1}{|r_i - r_j|} + \sum_{A=1}^{M} \sum_{B>A}^{M} \frac{Z_A Z_B}{|R_A - R_B|}$$

where the first two terms are the kinetic energy of the electrons and the nuclei, the third term is the Coulombic electron-nucleus attraction, the third term the Coulombic electron-electron repulsion and the last term is the nucleus-nucleus repulsion. The large mass difference between nuclei and electrons leads to the Born-Oppenheimer approximation (Born and Oppenheimer, 1927) which states that the electronic and nuclear motions can be separated. This allows one to write the energy of a wave function as consisting of two parts

$$E_{tot} = E_{elec} + \sum_{A=1}^{M} \sum_{B>A}^{M} \frac{Z_A Z_B}{|R_A - R_B|}$$

where the first term is the electronic energy given by the electronic Hamiltonian operator

$$\hat{\boldsymbol{H}}_{elec} = -\sum_{i=1}^{N} \frac{1}{2} \nabla_i^2 - \sum_{i=1}^{N} \sum_{A=1}^{M} \frac{Z_A}{|R_A - r_i|} + \sum_{i=1}^{N} \sum_{j>i}^{N} \frac{1}{|r_i - r_j|}$$

and the second part the nucleus repulsion energy.

Further discussion will make use of the notation introduced by Dirac. He introduced the *bra-ket* notation where the vector describing the wave function ψ is called the *ket vector* and given by $|\psi\rangle$. The *bra vector*, $\langle\psi|$, describes the complex conjugate, ψ^*, of the wave function. The integral $\int\ldots\int \psi^* \hat{A} \psi \, d\tau$ using this notation then becomes $\langle\psi|\hat{A}|\psi\rangle$.

The variational theorem (Eckart, 1930) states that the lowest energy E_0 for a certain electronic configuration, ψ_0, is given by

$$E_0 = \frac{\langle \psi_0 | \hat{\boldsymbol{H}} | \psi_0 \rangle}{\langle \psi_0 | \psi_0 \rangle}$$

Substituting the wave function with a Slater determinant and using the fact that the wave functions are orthonormal to one another, the expression

$$\int_{-\infty}^{\infty} \psi_i^* \psi_j dx = \delta_{ij} \qquad \delta_{ij} = \begin{cases} 0 \text{ for } i \neq j \\ 1 \text{ for } i = j \end{cases}$$

gives the expectation value of the Hartree-Fock energy for a closed shell electronic system

$$E_{tot} = 2\sum_{i}^{N/2} H_i^{core} + \sum_{i=1}^{N/2}\sum_{j=1}^{N/2}\left(2J_{ij} - K_{ij}\right) + V_{nn}$$

where H_i is the *one-electron core Hamiltonian*

$$H_i^{core} \equiv \left\langle \phi_i(1) \middle| \hat{\boldsymbol{H}}_i^{core} \middle| \phi_i(1) \right\rangle \equiv \left\langle \phi_i(1) \middle| -\frac{1}{2}\nabla^2{}_i - \sum_{A=1}^{M} \frac{Z_A}{|R_A - r_i|} \middle| \phi_i(1) \right\rangle$$

J_{ij} is the *Coulomb integral* representing the classic electrostatic interaction

$$J_{ij} \equiv \left\langle \phi_i(1)\phi_j(2) \middle| \frac{1}{|r_1 - r_2|} \middle| \phi_i(1)\phi_j(2) \right\rangle$$

and K_{ij} is the *exchange integral* which has no classical analogue

$$K_{ij} \equiv \left\langle \phi_i(1)\phi_j(2) \middle| \frac{1}{|r_1 - r_2|} \middle| \phi_j(1)\phi_i(2) \right\rangle$$

The nucleus-nucleus interaction is given by V_{nn}. The variational energy needs to be minimised in order to find the optimum set of spin orbitals. Lagrange multipliers can be introduced to enforce orthogonality of the spin orbitals. The result of this functional variation with constraints leads to the *Hartree-Fock equations*

$$\hat{\boldsymbol{F}}(1)\phi_i(1) = \varepsilon_i \phi_i(1)$$

where ε_i is the orbital energy and $\hat{\boldsymbol{F}}$ the one-electron *Fock operator* (given here for the coordinates of electron 1)

$$\hat{\boldsymbol{F}}(1) = \hat{\boldsymbol{H}}^{core}(1) + \sum_{j=1}^{N/2}\left[2\hat{\boldsymbol{J}}_j(1) - \hat{\boldsymbol{K}}_j(1)\right]$$

$$\hat{\boldsymbol{H}}^{core}(1) = -\frac{1}{2}\nabla^2{}_1 - \sum_{A=1}^{M} \frac{Z_A}{|R_A - r_1|}$$

$\hat{\boldsymbol{J}}_i$ and $\hat{\boldsymbol{K}}_i$ are the Coulomb and exchange operator analogues to the Coulomb and exchange integrals.

Roothaan (Roothaan, 1951) and Hall (Hall, 1951) proposed that the molecular orbitals be expanded into a set of linear combinations of known one-electron basis functions

$$\phi_i = \sum_{s=1}^{b} c_{si}\chi_s$$

where χ_s represent the b one-electron basis functions and c_{si} the expansion coefficients. Substituting these molecular orbitals into the Hartree-Fock equations and multiplying by χ_s^* leads to the Roothaan equations in matrix form

$$\boldsymbol{FC} = \boldsymbol{SC\varepsilon}$$

where $\boldsymbol{F}$ is the *Fock matrix*, $\boldsymbol{S}$ the *overlap matrix*, $\boldsymbol{C}$ is a square matrix of the expansion coefficients and $\boldsymbol{\varepsilon}$ a diagonal matrix of the orbital energies ε_i. These equations are then iteratively solved to yield the self-consistent-field (SCF) energy and orbitals.

The procedure described above is for closed-shell molecules and called *Restricted Hartree-Fock* (RHF) methods. For open-shell systems two methods can be used: *Unrestricted Hartree-Fock* (UHF) in which the constraint of double occupation of orbitals is removed and the spatial part of the α and β orbitals is allowed to differ, and *Restricted Open-shell Hartree-Fock* (ROHF) in which all the electrons except the unpaired ones are constrained.

2.2.2 Post-Hartree-Fock Methods

The Hartree-Fock model examines the motion of an electron in the average field of the other *N-1* electrons. It does include a form of electron-electron correlation through the use of Slater determinants, but because the instantaneous interaction of the electrons with each other gives a better representation of the repulsion between the electrons than an average interaction, the electronic repulsion is overestimated leading to a higher energy. The *correlation energy* is the energy difference between the exact non-relativistic energy and the HF energy

$$E_{corr} = E_{exact} - E_{SCF}$$

Theoretically three types of correlation corrections can be made:

- *Dynamic correlation* is the inclusion of the ability for the electrons to stay apart.
- *Non-dynamic correlation* can be best described by looking at the H_2 potential energy curve. As the distance between the atoms increases, the electrons start localizing on the two separate atoms, meaning that to correctly describe the system a σ_g (gerade) and σ_u (ungerade) function have to mix in order to preserve spin and spatial symmetry. This type of correlation can also be thought of as the restoration of the atomic character of

the individual atoms as the interatomic distance increases.

- *Static correlation* occurs in cases where a single determinant cannot be an eigenfunction of spin ($\hat{S}^2|SD\rangle \neq S(S+1)|SD\rangle$) since the electron configuration cannot be completely described by only one determinant. A two-determinant reference is therefore preferably needed. In the case of an open-shell singlet, these two determinants would be $|\ldots\phi_n(\alpha)\phi_n(\beta)\boldsymbol{\phi}_{n+1}(\alpha)\boldsymbol{\phi}_{n+2}(\beta)|$ and $|\ldots\phi_n(\alpha)\phi_n(\beta)\boldsymbol{\phi}_{n+1}(\beta)\boldsymbol{\phi}_{n+2}(\alpha)|$.

Static and non-dynamic correlation play a less important role in the heaver transition metals. Due to the increased overlap of the larger *d* and *s* orbitals of the second and third row transition metals, compared to the first row, hybridisation takes place more easily leading to a reduction in the need for configuration mixing to restore the atomic nature of the atoms.

Dynamic correlation plays an important role in complexes where there is a large concentration of electrons in the same region of space. For example in $Cr(CO)_6$ twelve electrons are formally donated to the Cr atom with its six valence electrons. This is clearly a situation in which normal Hartree-Fock calculations will overestimate the electron repulsion and the need for dynamic correlation is emphasised.

Computationally there are three main methods to introduce electron correlation. These are *Configuration Interaction* (CI), *Many Body Perturbation Theory* (MBPT) and *Coupled Cluster Theory* (CC).

2.2.2.1 Configuration Interaction

Configuration interaction can be chemically understood as the mixing of different electronic states. In general, a finite linear combination of Slater determinants constructed from HF-SCF orbitals using unoccupied "virtual" orbitals is employed. If a virtual orbital (j^*) is substituted with an occupied orbital (i) in the HF determinant, the resulting determinant $\Psi_i^{j^*}$ is called *singly excited.* If doubly substituted configurations are used ($k^*, l^* \rightarrow i, j$), the determinant $\Psi_{ij}^{k^*l^*}$ is called *doubly excited.* The general CI wave function is thus given by

$$\Psi_{CI} = \Psi_{HF} + \sum_{i,j^*} a_{ij^*}^{S} \Psi_i^{j^*} + \sum_{i,j,k^*,l^*} a_{ijk^*l^*}^{D} \Psi_{ii}^{k^*l^*}$$

where the coefficients $a_{ij^*}^{S}$ and $a_{ijk^*l^*}^{D}$ regulate the degree of mixing. Since the number of basis

functions used limits the number of constructed occupied and virtual orbitals, the number of possible excited determinants are limited by the size of the basis set. In practice, however, full CI (where all excitations, single, double, triple, etc. are used) is not possible and a limited (truncated) configuration interaction is used. If only double excitations are used the method is called CID (D=double) and with single and double excitations CISD (S=single, D=double). All CI calculations are variational, in other words, they give an upper bound to the exact energy, but have the disadvantage that all methods except full CI are not size consistent. A size consistent quantum mechanical method is one for which the energy and hence the energy error in the calculation increases in proportion to the size of the molecule. Size consistency is important whenever molecules of substantially different sizes are compared.

2.2.2.2 Perturbation Theory

Perturbation theory is another method of evaluating the correlation energy of a system. It is not variational in the sense that it does not result in an upper bound for the exact energy of a system, but it is size consistent.

Møller and Plesset (Møller and Plesset, 1934) introduced a perturbative treatment of atoms and molecules in which the unperturbed wave function is the HF wave function. Within their approach a general electronic Hamiltonian is given by

$$\hat{\boldsymbol{H}} = \hat{\boldsymbol{H}}^{0} + \lambda \hat{\boldsymbol{P}}$$

where $\hat{\boldsymbol{H}}^{0}$ is the unperturbed Hamiltonian, λ is an arbitrary parameter keeping track of the order of perturbation and $\hat{\boldsymbol{P}}$ is the perturbation operator generating the perturbations. The perturbed wave function and resulting energy, expanded as a power series, are

$$\Psi = \Psi^{(0)} + \lambda\Psi^{(1)} + \lambda^{2}\Psi^{(2)} + \ldots = \sum_{n=0}^{\infty} \lambda^{n}\Psi^{(n)}$$

$$E = E^{(0)} + \lambda E^{(1)} + \lambda^{2}E^{(2)} + \ldots = \sum_{n=0}^{\infty} \lambda^{n}E^{(n)}$$

The unperturbed Hamiltonian is defined as the sum over all the spin orbitals of the one-electron Fock operators

$$\hat{\boldsymbol{H}}^{0} = \sum_{i=1}^{n} \hat{\boldsymbol{F}}(i)$$

The perturbation operator is then defined as the difference between the true molecular electronic Hamiltonian and the unperturbed Hamiltonian

$$\hat{P} = \sum_{l} \sum_{m>l} \frac{1}{|r_l - r_m|} - \sum_{m=1}^{n} \sum_{j=1}^{n} \left[\hat{J}_j(m) - \hat{K}_j(m) \right]$$

To improve the Hartree-Fock energy, the second order $E^{(2)}$ (or better) energy correction is needed since the first order correction just gives the normal HF energy. The correction is given by

$$E^{(2)} = \sum_{s \neq 0} \frac{\left| \left\langle \Psi_s^{(0)} \middle| \hat{P} \middle| \Psi^{(0)} \right\rangle \right|^2}{E^{(0)} - E_s^{(0)}}$$

where $\Psi_s^{(0)}$ and the corresponding energy $E_s^{(0)}$ are all possible Slater determinants formed from n different spin orbitals.

The low cost of MP calculations compared to CI makes it an ideal option for correlated calculations. The theory is further extended to include third, fourth and fifth order corrections (MP3, MP4 and MP5).

2.2.2.3 Coupled Cluster Theory

Perturbation methods add all types of corrections (single, double, triple, quadruple, etc.) to the reference wave function to a given order (2, 3, 4, etc.). The idea in *Coupled Cluster* (CC) theory is to include all corrections of a given type to infinite order. Within CC theory the exact ground state nonrelativistic molecular electronic wave function is given by

$$\Psi_{CC} = e^{\hat{T}} \Psi_0$$

where Ψ_0 is the ground state Hartree-Fock wave function and $e^{\hat{T}}$ is defined by a Taylor-series expansion

$$e^{\hat{T}} = 1 + \hat{T} + \frac{1}{2!}\hat{T}^2 + \frac{1}{3!}\hat{T}^3 + \ldots \sum_{k=0}^{\infty} \frac{1}{k!}\hat{T}^k$$

The cluster operator $\hat{T}$ is given by

$$\hat{T} = \hat{T}_1 + \hat{T}_2 + \ldots + \hat{T}_n$$

where n is the number of electrons. $\hat{T}_1$ and $\hat{T}_2$ are the *one-particle excitation operator* and *two-particle excitation operator* and one given by

$$\hat{T}_1\Psi_0 = \sum_{a=n+1}^{\infty}\sum_{i=1}^{n} t_i^a \Psi_i^a$$

$$\hat{T}_2\Psi_0 = \sum_{b=a+1}^{\infty}\sum_{a=n+1}^{\infty}\sum_{j=1+1}^{n}\sum_{i=1}^{n-1} t_{ij}^{ab}\Psi_{ij}^{ab}$$

where Ψ_i^a is a single excited Slater determinant with occupied spin orbital i replaced by virtual spin orbital a and t_i^a is a numerical coefficient, called the amplitude, whose value depends on i and a. Finding the coupled cluster wave function thus reduces to determining the amplitudes. The operator $\hat{T}_1$ converts the Slater determinant into a linear combination of all possible singly excited Slater determinants with similar definitions for $\hat{T}_2$, ..., $\hat{T}_n$.

Once again the size of the basis set influences the calculation since the number of virtual orbitals and hence the number of excited determinants depends on the number of basis functions. Also, instead of using all the operators $\hat{T}_1$, $\hat{T}_2$, ..., $\hat{T}_n$, the operator $\hat{T}$ is approximated by only some of them. Using only $\hat{T}_2$ leads to the *coupled cluster doubles* (CCD) method. Using $\hat{T} = \hat{T}_1 + \hat{T}_2$ leads to the *CC singles and doubles* (CCSD) method. Coupled cluster methods are variational, but not size consistent.

2.2.3 Semi-empirical Methods

The computational cost of *ab initio* HF methods scales with the fourth power of the number of basis functions. This is a result of the number of two-electron integrals needed for computing the Fock matrix. Semi-empirical calculations have the same general structure as HF calculations in that they make use of a Hamiltonian and a wave function. However, within these methods certain pieces of information are approximated or omitted. Usually the core electrons are not used in the calculation and a minimal basis set (more on minimal basis sets in **section 2.6**) is used. Some of the two-electron integrals are also omitted. To correct for the errors resulting from this the methods are parameterized. These parameters are obtained by fitting the results to experimental data or with results obtained from *ab initio* methods.

The advantage of these methods is that they are much faster than *ab initio* calculations. The disadvantage is that they can behave erratically and fewer molecular properties can be

calculated with them since the results they deliver depend much on the set of results they were parameterized from.

Two of the more popular semi-empirical methods in use today are the *Austin Model 1* or AM1 (Dewar et al., 1985) used to model organic molecules and the *Parameterization Method* 3 or PM3 (Stewart, 1989) that is even more popular for organic systems. The *Complete Neglect of Differential Overlap* or CNDO (Segal and Pople, 1966), *Intermediate Neglect of Differential Overlap* or INDO (Pople et al., 1967) and *Modified Intermediate Neglect of Differential Overlap* or MINDO (Bingham et al., 1975) are examples of semi-empirical methods (for more on these methods see Pople and Beveridge, 1970) used to determine initial guess orbitals for *ab initio* calculations.

2.2.4 Molecular Mechanics

The ideal solution to relieve the computational cost associated with *ab initio* methods would be to find a way of determining energy without having to go through the iterative SCF procedure and the associated multitude of basis functions. This is the idea behind *molecular mechanics* (MM) or *Force Field* (FF) methods.

With this method the energy of a molecule is written as a parametric function of the nuclear coordinates. Another difference between *ab intio* and MM methods is that with MM methods bonds between atoms are assumed. The molecules are then modelled as atoms held together by these bonds. It does not use a wave function or electron density, but is based purely on the physical "ball-and-string" model. The energy expression is of the form

$$E_{FF} = E_{stretch} + E_{bend} + E_{torsion} + E_{non-bond} + E_{coupling}$$

where $E_{stretch}$ is the energy expression for the stretching of a bond between two atoms, E_{bend} for the bending of an angle, $E_{torsion}$ for the torsional energy of rotation around a bond, $E_{non\text{-}bond}$ for non-bonded interactions such as Van der Waals forces and $E_{coupling}$ for coupling between the before mentioned forces. The constants needed for the above-mentioned forces are obtained from spectroscopic methods or *ab initio* calculations. In order to achieve a good transferability of parameters between different atomic systems, force fields use atom types, such as considering atoms as sp^2 or sp^3 hybridized, or even the functional group as an indication of the

parameterization. Once again, as with semi-empirical methods, the performance of these methods is dependent on the specific parameterization used.

Examples of some popular MM methods are *Assisted Model Building with Energy Refinement* or AMBER (Cornell et al., 1995), used to model proteins and nucleic acids, *Chemistry at Harvard Macromolecular Mechanics* or CHARMM (Brooks et al., 1983), which is the name of a force field as well as the program incorporating it used to model large biomolecules, MM3 (Allinger et al., 1989) and MM4 (Allinger et al., 1996) used to model organic molecules and the *Universal Force Field* or UFF (Rappé et al., 1992).

2.2.5 Density Functional Theory

The Hohenberg-Kohn Theorem (Hohenberg and Kohn, 1964) states that for molecules with a non-degenerate ground state the ground state wave function, energy and all other properties are uniquely determined by the ground state electron probability density $\rho_0(r)$,

$$E_0 = E_0[\rho_0].$$

Any other density that is not the true density will necessarily lead to a higher energy. Levy (Levy, 1979, 1982) proved this theorem for non-degenerate ground states. This idea, that the energy of an electronic system can be calculated from its electron density, dates as far back as the 1920's with the work of Thomas (Thomas, 1927) and Fermi (Fermi, 1927).

The Hohenberg-Kohn Theorem does not tell us what the exact relation between the electron density and the wave function as well as the resulting energy is. This relationship is not trivial and the aim of *Density Functional Theory* (DFT) is to establish it. The energy functional for the purely electronic energy depending on the electron density can be divided into three parts, a kinetic energy part $T[\rho]$, attraction between the nuclei and the electrons $E_{ne}[\rho]$, and attraction between electrons, $E_{ee}[\rho]$ (nucleus-nucleus repulsion is constant due to the Born-Openheimer approximation). A practical approach based on the Hohenberg-Kohn Theorem and similar in structure to the Hartree-Fock method was developed by Kohn and Sham (Kohn and Sham, 1965). Following their, work the energy of an electronic system consisting of N electrons and M nuclei can be written as

$$E_0 = E[\rho] = -\frac{1}{2}\sum_{i=1}^{N}\int\theta_i^*(\boldsymbol{r}_1)\nabla^2\theta_i(\boldsymbol{r}_1)d\boldsymbol{r}_r + \sum_{a=1}^{M}\int\frac{Z_a}{\boldsymbol{R}_a-\boldsymbol{r}_1}\rho(\boldsymbol{r}_1)d\boldsymbol{r}_1 + \frac{1}{2}\iint\frac{\rho(\boldsymbol{r}_1)\rho(\boldsymbol{r}_2)}{\boldsymbol{r}_1-\boldsymbol{r}_2}d\boldsymbol{r}_1 d\boldsymbol{r}_2 + E_{XC}[\rho]$$

where the Kohn-Sham (KS) orbitals are given by θ_i and the electron density $\rho(\mathbf{r}_1)$ is given by

$$\rho(\boldsymbol{r}_1) = \sum_{i=1}^{N} \theta_i^*(\boldsymbol{r}_1)\theta_i(\boldsymbol{r}_1) = \sum_{i=1}^{N} |\theta_i|^2$$

$E_{XC}[\rho]$ is the exchange-correlation functional and is defined as the difference between the kinetic energy and Coulomb electron-electron repulsion energy of the real system and the non-interacting reference system. An accurate description of this functional is the major challenge behind DFT.

Before any of the terms describing the electronic energy can be evaluated the electron density has to be calculated. This can be found once the Kohn-Sham orbitals and the exchange-correlation functional are known. Finding the KS orbitals is done in a similar fashion as finding the HF orbitals. The Kohn-Sham equations have the form

$$\hat{\boldsymbol{h}}_{KS}\theta_i = \varepsilon_i\theta_i$$

where the operator $\hat{\boldsymbol{h}}_{KS}$ is given by

$$\hat{\boldsymbol{h}}_{KS}(1)\theta_i(1) = \left[-\frac{1}{2}\nabla_1^2 - \sum_{a=1}^{M} \frac{Z_a}{|\boldsymbol{R}_a - \boldsymbol{r}_1|} + \int \frac{\rho(\boldsymbol{r}_2)}{|\boldsymbol{r}_1 - \boldsymbol{r}_2|} d\boldsymbol{r}_2 + \upsilon_{XC}(1) \right] \theta_i(1)$$

and the potential $\upsilon_{XC}(1)$ by

$$\upsilon_{XC}(1) = \frac{\delta E_{XC}[\rho(\boldsymbol{r}_1)]}{\delta\rho(\boldsymbol{r}_1)}$$

The remaining challenge is the exchange-correlation functional which can be written as consisting of an exchange and a correlation part. Describing the electron density as a homogeneous (uniform) gas, leads to the *Local Density Approximation* (LDA). An exchange functional based on this approximation was developed by Vosko, Wilk and Nusair (1980). A better approximation can be made by treating the electron gas as non-uniform and including derivatives of the electron density. Functionals developed in this fashion are called *Gradient-corrected* functionals. Commonly used gradient-corrected exchange functionals of this type are B or B88 (Becke, 1988), PW91 (Perdew, 1991; Burke, Perdew, Wang, 1998), B86 (Becke, 1986) and P or P86 (Perdew and Wang, 1986). Among the most widely used correlation functionals are the correlation counterpart of the Perdew exchange functional P or P86 (Perdew, 1986), the PW91 correlation functional by Perdew and Wang (1992) and the most widely used one LYP (Lee, Yang and Parr, 1988). Exchange and correlation functionals can also be paired resulting in

methods like BLYP or BP86. Finally, hybrid functionals can also be constructed, which use a formula for the exchange energy based on the KS orbitals (similar to the HF exchange energy) together with other exchange and correlation functionals described above. The most popular hybrid functional is the B3LYP functional suggested by Stevens et al. (1994) which is based on the B3PW91 functional of Becke (1993a, 1993b) but replaces the PW91 functional with LYP.

As with SCF methods the KS method approximates the KS orbitals as a linear combination of basis functions. If a complete set of basis functions is used then in principle the exact solution can be found. Numerical "basis functions" can be used to determine the orbitals, the solutions are then given as a table of numbers over a grid of points. An algorithm to solve the KS equations with numerical basis sets has been developed by Becke (1989) and Dickson and Becke (1993). This has made it possible to calculate the error introduced by using finite basis sets.

2.3 The Basis Set

Solving the Schrödinger equation according to the Roothaan-Hall approximation is essentially the same as determining the molecular orbitals associated with a molecule. The exact form of the molecular orbitals are not known and therefore *basis functions* $\chi_s(\boldsymbol{r})$ are introduced to facilitate with the calculations

$$\phi_i(\boldsymbol{r}) = \sum_{s=1}^{b} c_{si}\chi_s(\boldsymbol{r})$$

Basis sets are a collection of functions in either spherical or Cartesian coordinates and are used to approximate one electron orbitals of which the molecular orbitals are built. Expanding an unknown function such as a molecular orbital into a set of known functions such as basis functions is not an approximation if a *complete* set is used. However, using an infinite set of functions is not possible, and since the computational complexity scales with n^4, choosing a basis set with the lowest possible number of functions without compromising accuracy is of great importance. It is important to note that even high-level methods such as MP*n*, CI and CC *will not overcome an inadequate basis set.*

2.3.1 Slater and Gaussian-Type Orbitals

Two types of basis functions are commonly used in electronic calculations. *Slater-Type Orbitals* (STO) introduced by Slater (1930) and *Gaussian-Type Orbitals* (GTO) introduced by Boys (1950). Slater-type orbitals are of the general form

$$\phi_{\zeta,n,l,m}(r,\theta,\varphi) = NY_{l,m}(\theta,\varphi)r^{n-1}e^{-\zeta r}$$

where N is a normalisation constant, $Y_{l,m}$ is the spherical harmonic function describing the angular momentum ("shape" of the orbital), ζ the exponent, and r, θ and φ are spherical coordinates. Slater-type orbitals have the disadvantage that the two electron integrals needed to compute the energy cannot be solved analytically. The shape of a STO can be approximated by a summation of a number of GTO's with different exponents and coefficients. Even if ten GTO's are used the calculation will still proceed faster than with one STO. Gaussian-type orbitals have the general forms (in polar and Cartesian coordinates)

$$\phi_{\zeta,n,l,m}(r,\theta,\varphi) = NY_{l,m}(\theta,\varphi)r^{2n-2-1}e^{-\zeta r^2}$$

$$\phi_{\alpha,l_x,l_y,l_z}(x,y,z) = Nx^{l_x}y^{l_y}z^{l_z}e^{-\alpha r^2}$$

In the Cartesian representation N is a normalisation constant and α is the exponent. The type of orbital described is determined by the values of l_x, l_y and l_z, e.g. $l_x = 1$, $l_y = l_z = 0$ for a p_x orbital and $l_x = 1$, $l_y = 1$, $l_z = 0$ for a d_{xy} orbital. There are six *d*-type GTO's with factors x^2, y^2, z^2, xy, xz and yz. If desired five linear combinations of these functions can be made to simulate the five real *d*-type orbitals, with factors xy, xz, yz, x^2-y^2 and $3z^2$-$(x^2 + y^2 + z^2)$. The sixth combination is $x^2 + y^2 + z^2$ and is like a 3*s*-type function.

Although the valence orbitals play the most important role in chemical bonding it is the core orbitals that contribute the most to the energy. Thus using many basis functions to describe the chemically unimportant but energetically important core orbitals has led to the introduction of *Contracted Gaussian-Type Orbitals* (CGTO's). Contracted basis functions are formed from a linear combination of uncontracted Gaussian functions (primitives). Such functions then have their exponents as well as the contraction coefficients fixed during the optimisation. Each contraction is then seen as a single basis function.

As mentioned above a sum of functions is used to describe a certain atomic orbital. The smallest number of one-electron functions needed is referred to as a *minimal basis set*, e.g. for

hydrogen it would be one *s*-type function, for oxygen two *s*-types (1*s* and 2*s*) and one set of *p*-type functions ($2p_x$, $2p_y$, $2p_z$). An improvement is to use two functions to describe each atomic orbital, called *Double Zeta* (DZ) basis sets. Chemical bonding occurs between valence orbitals, therefore, core orbitals play little role and approximating them with more than one function is rarely done. Double Zeta basis sets where only the basis functions for the valence electrons are doubled are called *split valence sets* (also referred to as VDZ). Naturally other types are *Triple Zeta* (TZ or VTZ), *Quadruple Zeta* (QZ) and *Quintuple Zeta* (5Z).

To better describe a system more basis functions can be added. If functions describing orbitals of higher angular momentum than the ones present in the ground state configuration are added, they are called *polarisation functions*. These functions also play an essential role when electron correlation methods are used. Basis sets can also be augmented with functions having small values of the exponent, ζ. These are called *diffuse functions* and are needed whenever loosely bound electrons are present, e.g. anions or excited states.

The contraction schemes lead to the names of popular basis sets, e.g. 6-31G of Pople and co-workers consists of six primitive Gaussians contracted for the core, three for the "inner" valence region and one for the "outer" valence region. In general the notation-scheme is *n-ij*G or *n-ijk*G, where *n* is the number of primitives contracted for the inner shells and *ij* or *ijk* the number of primitives for the outer or valence shell. The sets can also be augmented with polarisation functions, *d*-type or *f*-type for heavy atoms and *p*-type for hydrogen. This is then shown as *n-ij*G(d) or *n-ij*G(d,f) or *n-ij*G(d,p). The notation *n-ij*G* is synonymous to *n-ij*G(d) and *n-ij*G** is synonymous to *n-ij*G(d,p). Adding diffuse functions on non-hydrogen atoms are shown as *n-ij*+G and adding diffuse functions on all atoms, hydrogen and heavy atoms, are shown as *n-ij*++G.

Throughout this work the notation adopted to describe the contractions is, for example $(10s,4p,1d) \rightarrow [3s,2p,1d]$, which means that 10 *s*-type functions in total were contracted to a total of three, four *p*-type functions were contracted to a total of two and one uncontracted *d*-type function. This however does not explain how the contractions were done. To do this, for example the notation (631,31,1) is adopted, which says that there are three *s*-type contracted functions, the first consisting of six primitives, the second of three and the last one. Likewise, there are two *p*-type contracted functions, the first one consisting of three primitives, the second of one. The different shells are separated by commas.

Some review articles on basis sets have been written by Wilson (1987), by Davidson and Feller (1986), by Feller and Davidson (1990) and by Helgaker and Taylor (1995).

2.3.2 Effective Core Potentials

When modelling transition metal compounds, the computational chemist always needs to work with elements of the third or higher rows. These elements pose two problems: their huge number of core electrons and relativistic effects. Both these problems can be solved (or at least approximately "solved") with the use of *Effective Core Potentials* (ECP).

The ECP is an one-electron operator that replaces the two-electron Coulomb and exchange operators in the valence electrons' Hartree-Fock equation that results from interactions between the core electrons and the valence electrons. ECP's are therefore not basis sets, but rather a modification to the Hamiltonian. The inner electrons are replaced by averaged potentials and basis functions are only needed for the outer (valence) electrons reducing computation time considerably. The form of the ECP's is determined by a numerical fit of HF or relativistic Dirac-Hartree-Fock calculations to a suitable set of Gaussian functions. ECP's are given as parameters of the following:

$$ECP(r) = \sum_{i=1}^{M} d_i r^{n_i} e^{-\zeta r^2}$$

where M is the number of terms in the expansion, d_i is a coefficient for each term, n_i the power of r (the distance to the nucleus) and ζ the exponent. ECP's were reviewed by Krauss and Stevens (1984), Frenking et al. (1996) and Cundari et al. (1996).

2.3.3 The Basis Set Superposition Error

When energies of fragments or molecules are compared, for instance to calculate dissociation energy, it is important that the same basis set is used for all the relevant calculations. However, an error is introduced due to the fact that the basis sets are centred on one nucleus. The incompleteness of the basis sets due to the limit of finite functions leads to the phenomenon that the electron density around one nucleus may be described by basis functions centred on another nucleus. This effect is known as the *Basis Set Superposition Error* (BSSE) and leads to a non-

physical lowering in the energy that needs to be compensated for. As the basis set approaches the complete set so does the BSSE tend to zero. A way to estimate the BSSE is the *Counterpoise Correction* (CP) of Boys and Bernard (1970).

Consider two fragments ***A*** and ***B*** having basis sets centred on their respective nuclei, denoted by ***a*** and ***b***. These two fragments form a complex ***AB*** with a combined basis set ***ab***. The geometry of the fragments will be different in the complex compared to their isolated state, the complex geometry is denoted with a *. The complexation energy is then given by

$$\Delta E_{complexation} = E(AB)^{*}_{ab} - E(A)_{a} - E(B)_{b}$$

The counterpoise correction to estimate the BSSE is

$$\Delta E_{cp} = E(A)^{*}_{ab} + E(B)^{*}_{ab} - E(A)^{*}_{a} - E(B)^{*}_{b}$$

The energy of one fragment is thus calculated with the basis functions of the other fragment present, but without any particles from the other fragment. This calculation is done for both the fragments. This gives an indication of the energy lowering due to the electrons of the particular fragment occupying basis functions of the other fragment. From their sum is subtracted the sum of the energies of the fragments with only basis functions centred on their own nuclei present. All calculations are done at the geometry of the optimised complex.

The success of the CP method has been under doubt for some time but is currently accepted as the most successful way to calculate BSSE (Chalasinski and Szczesniak, 1994; Van Duijneveldt et al., 1994).

2.4 Wave Function Instabilities

In general orbitals are determined completely independently of the spin of the occupying electron (in the case of one-electron orbitals). Spin can be introduced only later by writing *spin orbitals* as a product of a spatial function and a spin part, being either one of α or β (see **section 2.2.1**).

When determining the lowest possible electronic energy for a given system (using HF theory) by variation of the orbital coefficients of the contracted Gaussians and thereby determining the composition of the molecular orbitals, certain constraints are introduced. Firstly the assumption can be made that the molecular orbitals can be divided into α and β one-electron MO's consisting of purely α functions or β functions. This is the case in UHF theory. Secondly,

the constraint can be introduced that the orbitals are restricted to being real functions, determined by real constants. Lastly, no distinction can be made between α and β orbitals and each molecular orbital can be constrained to being doubly occupied. This is the case with RHF theory.

When the energy of a system is thus calculated through the SCF approach, a number of predetermined simplifications are always present. This leads to the problem that the determined molecular orbital coefficients might not be an optimum in an unconstrained space. Lifting some restrictions might lead to a lower energy situation. A solution to the Roothaan-Hall equations is then called unstable if the energy can be lowered by allowing some constraints to be relaxed. However, it is important to remember that the determination of the energy is still only an approximation, and by lifting constraints one can only then better the approximation, but still not get to the exact solution.

Equations have been derived by Seeger and Pople (1977) from which one can determine whether a lower energy solution exists. An appropriate matrix can be constructed from which the negative eigenvalues can be used to indicate a direction in which the search for a lower energy wave function should be directed.

Only instabilities relating to closed shell KS-DFT equations are of practical value. Open shell systems appear to be less crucial since they are of unrestricted type and in general break spin and spatial symmetry. In the KS expression of the total energy, only the kinetic energy part depends explicitly on the orbitals (basis functions) whereas the remainder is a functional of the electron density. Analogous to HF theory methods exist (Bauernschmitt and Ahlrichs, 1996) with which one can determine whether a lower energy solution exists and how to proceed in finding it.

The *Gaussian98* (Frisch et al., 1998) software can check for instabilities in wave functions by allowing an RHF determinant to become UHF, allowing the orbitals to be complex and, therefore, have complex coefficients and by reducing the symmetry of the orbitals relative to the symmetry of the molecule.

2.5 Wave Function Analysis

2.5.1 Atomic Charges

A property that can be used to interpret structural and reactivity differences is *atomic charges*. One of the earliest and still widely used methods today to determine atomic charges is the *Mulliken Population Analysis* (Mulliken, 1962). Mulliken proposed a method that partitions the electrons of an n electron molecule into net populations n_r in each basis function χ_r and overlap populations $n_{r\text{-}s}$ for all possible pairs of basis functions. For a set of basis functions χ_1, χ_2, ..., χ_b each MO has the form

$$\phi_i = \sum_s c_{si}\chi_s$$

Integrating the probability density for one electron in orbital ϕ_i (given by $|\phi_i|^2$) and using the fact that both the MO's and basis functions are normalised leads to

$$c_{1i}^2 + c_{2i}^2 + \ldots + 2c_{1i}c_{2i}S_{12} + 2c_{1i}c_{3i}S_{13} + 2c_{2i}c_{3i}S_{23} + \ldots = 1$$

where $S_{kl} = \int \chi_k \chi_l \mathrm{d}\upsilon_1 \mathrm{d}\upsilon_2$ is an overlap integral. One electron in ϕ_i thus contributes $c_{1i}{}^2$ to the net population in basis function χ_1 and 2 c_{1i} $c_{2i}S_{12}$ to the overlapping region between χ_1 and χ_2, etc. If there are n_i electrons in MO ϕ_i, then the contribution of electrons in ϕ_i to the net population in χ_r and to the overlapping region between χ_r and χ_s are

$$n_{r,i} = n_i c_{ri}^2 \qquad n_{r-s,i} = n_i \left(2c_{ri}c_{si}S_{rs}\right)$$

Summing over the occupied MO's then gives the net population in χ_r and the overlap population between basis functions χ_r and χ_s. Addition of the net population of all the basis functions centred on an atom gives the atomic population. The charge is given by subtracting the total atomic population from the atomic number.

There are many problems associated with the method (Bachrach, 1994) and a much better approach to determining atomic charges is discussed in **section 2.5.4**.

2.5.2 Charge Decomposition Analysis (CDA)

A very important field in chemical research is the interpretation of chemical bonding in transition metal complexes. The Dewar-Chatt-Duncanson DCD (Dewar, 1951; Chatt and

Duncanson, 1953) model is used to describe metal-ligand interaction by considering two main contributions, σ-donation from the ligand to an empty *d* orbital of the metal, and π-back donation from a filled metal *d* orbital to the ligand (**fig. 2.1**).

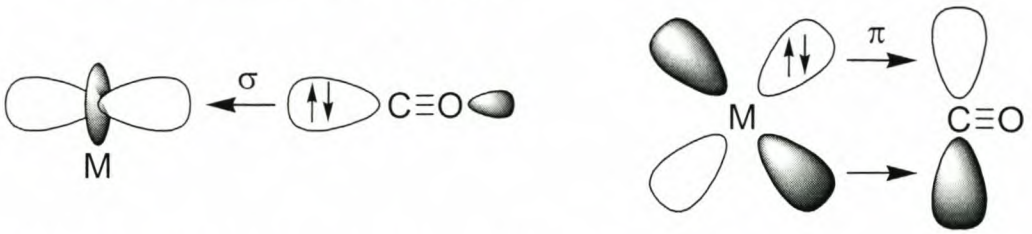

Figure 2.1 The important orbital interactions of the DCD model.

Frenking and Dapprich (1992) have developed a method based on analysis of the molecular orbitals of the fragments in the complex to determine whether the DCD model can be used to interpret the bonding. Within this method the wave function of a complex L_nM-X, is written as a linear combination of the molecular orbitals of the metal fragment L_nM, and the ligand X. It is important that both fragments are expressed in closed-shell configurations.

To carry out the analysis the following steps are taken:

- The MO's of the complex are computed in its equilibrium geometry.
- The MO's of the fragments are computed with their geometry as in the complex.
- The MO's are combined by calculating their direct sum.
- The eigenvectors of the complex are calculated in the basis of the fragment MO's (in normal HF theory the eigenvectors in the basis of the atomic orbitals are the MO coefficients, and the eigenvalues the MO energies).
- The overlap integrals are calculated in the basis of the fragment MO's (normally done through a similarity transformation).
- The donation *d*, back donation *b*, repulsive polarisation *r* and the rest term Δ are computed.

The orbital contributions of the fragments to the total wave function are divided into four terms: (i) mixing of the occupied MO's of the ligand with the unoccupied MO's of the metal fragment (σ-donation, *d*); (ii) mixing of the unoccupied MO's of the ligand with the occupied MO's of the metal fragment (π-back donation, *b*); (iii) mixing of the occupied MO's of the ligand with the occupied MO's of the metal fragment (repulsive polarization, *r*); (iv) mixing of the unoccupied

MO's of the ligand with unoccupied orbitals of the metal fragment (rest term, Δ). The different terms are given by

$$d_i = \sum_{k}^{\text{occ,A}} \sum_{l}^{\text{vac,B}} m_i c_{ki} c_{li} \langle \Phi_k | \Phi_l \rangle$$

$$b_i = \sum_{m}^{\text{occ,B}} \sum_{n}^{\text{vac,A}} m_i c_{mi} c_{ni} \langle \Phi_m | \Phi_n \rangle$$

$$r_i = \sum_{k}^{\text{occ,A}} \sum_{m}^{\text{occ,B}} m_i c_{ki} c_{mi} \langle \Phi_k | \Phi_m \rangle$$

$$\Delta_i = \sum_{n}^{\text{vac,A}} \sum_{l}^{\text{vac,B}} m_i c_{ni} c_{li} \langle \Phi_n | \Phi_l \rangle$$

where the two fragments are denoted *A* and *B*, m_i is the occupation number of the specific MO ϕ_i, Φ_k, Φ_l, Φ_m and Φ_n are the fragment basis functions and c_{ki}, c_{li}, c_{mi} *and* c_{ni} are the fragment coefficients.

Positive values for these terms correspond to charge concentrated in the respective areas of overlap, negative values correspond to charge being removed from these areas. The repulsive polarization should always be negative, since the overlap between two filled orbitals is repulsive. The rest term is perhaps the most important term in the calculation. To coincide with the idea of donor-acceptor interaction both fragments are given in closed shell configuration. *If the rest term differs greatly from zero this indicates that the empty fragment orbitals should not be modelled as unfilled and that a closed shell description, and hence donor-acceptor behaviour, is incorrect.*

2.5.3 Atoms in Molecules (AIM)

A theoretical approach to analyze the electronic structure that is not based on molecular orbitals but on the wave function, is *Atoms in Molecules* (AIM) of Bader (1990). The theory of AIM takes the electron density, which is derived directly from the wave function, as its main source of information.

For a fixed arrangement of nuclei the probability of finding each electron out of a total of *n* electrons in an infinitesimal volume element is given by

$$\psi^* \psi \, dq_1 dq_2 ... dq_k ... dq_N$$

where q_k is the set of four coordinates describing the k^{th} electron. These coordinates are the three

spatial coordinates, $\tau_k = (x_k, y_k, z_k)$ and one spin coordinate which can be either α or β. The volume element for the k^{th} electron can then be written as $d\tau_k = dx_k dy_k dz_k$. The physical meaning of this probability is the chance of finding a particular configuration in which each electron is in a particular position and has a given spin. The probability of finding an electron in a volume element independent of the instantaneous positions and spins of the other N-1 electrons is given by summing up over all spin coordinates and integrating over all spatial coordinates except that of one electron, which electron is taken is irrelevant, since all electrons are identical. The example given is the probability of electron 1 being in the volume $d\tau_1$, independent of the instantaneous positions of the other electrons (Popelier, 2000).

$$\sum_{\text{spins}} \left[\int d\tau_2 \int d\tau_3 \ldots \int d\tau_N \psi^* \psi \right] d\tau_1$$

The total "probability" (strictly this is not a probability since the maximum this quantity can obtain is N, where mathematical probabilities are between zero and one) to find any of the N electrons in $d\tau_1$, is given by multiplying the equation by N. This probability can be turned into the corresponding probability density (the density per unit volume) to result in the equation for electron density ρ:

$$\rho(\boldsymbol{r}_1) = N \sum_{\text{spins}} \left[\int d\tau_2 \int d\tau_3 \ldots \int d\tau_N \psi^* \psi \right]$$

Each topological feature of $\rho(\boldsymbol{r})$, whether it is a maximum, minimum or saddle point, has associated with it a critical point (cp), a point where the first derivative of the electron density $\nabla\rho(\boldsymbol{r})$ equals zero. These points can be denoted by the coordinate $\boldsymbol{r}_c$. The collection of nine second derivatives of $\rho(\boldsymbol{r})$, the Hessian matrix, is symmetrical and can be diagonalised to yield three eigenvalues and eigenvectors. The eigenvalues correspond to the three principle curves of $\rho(\boldsymbol{r})$ and the eigenvectors to their directions in space. The curvatures are negative at a maximum and positive at a minimum. The rank of a critical point, denoted by ω, is the number of non-zero curves at that point and its signature, denoted by σ, is the sum of their algebraic signs. The critical point is thereby labelled by assigning these two values in the notation (ω,σ). There are four possible critical points of rank three:

- (3, -3): All eigenvalues (curvatures) are negative and $\rho(\boldsymbol{r})$ is a local maximum at $\boldsymbol{r}_c$. These critical points correspond with the nuclei and are called *nuclear attractors*. At the exact location of the centre of the nucleus the first derivative is not defined (the

exact electron density shows a cusp at the nuclear centre), therefore, the cp does not correspond to the exact location, but rather to a position very close to it.

- (3, -1): Two eigenvalues are negative and $\rho(\boldsymbol{r})$ is a local maximum at $\boldsymbol{r}_c$ in the plane defined by the eigenvectors corresponding to the negative eigenvalues. The third eigenvalue is positive and $\rho(\boldsymbol{r})$ is a local minimum along the associated eigenvector at $\boldsymbol{r}_c$. A critical point of this form is called a *bond critical point*. These points play a very important role in the analysis of the bonding modes and henceforth the coordinate associated with them will be denoted $\boldsymbol{r}_b$.
- (3, 1): Two eigenvalues are positive and $\rho(\boldsymbol{r})$ is a minimum at $\boldsymbol{r}_c$ in the plane defined by their associated eigenvectors. The third eigenvalue is negative and corresponds to a maximum in $\rho(\boldsymbol{r})$ at $\boldsymbol{r}_c$ along the associated eigenvector. A critical point of this form is called a *ring critical point*.
- (3, 3): All eigenvalues are positive and $\rho(\boldsymbol{r})$ is a minimum at $\boldsymbol{r}_c$. A critical point of this form is called a *cage critical point*.

A gradient path is defined as a curve to which the gradient vector is tangential at each of its points. The area spanned by the gradient field consisting of gradient paths originating at infinity and terminating at a nucleus is called an atomic basin. This highlights another interesting feature of the AIM theory in that the area spanned by each of the atoms can be distinguished. A collection of gradient paths originating at infinity and terminating at a bond critical point forms a boundary between two atoms and is called an *interatomic surface* (IAS). The dot product between the gradient vector and the normal ($\nabla\rho.\mathbf{n}$) of the IAS is equal to zero for *every* point on the IAS, hence the surface is also referred to as a *zero-flux surface*.

Two gradient paths, each terminating at a nucleus, can be traced from a bond critical point. These two paths form a line that is called the *atomic interaction line* (AIL). When an AIL exists in an environment where the atoms are in equilibrium (such as at an energy minimum, where the forces on the nuclei are zero) it is called a *bond path* (BP) and considered as quantum mechanical proof that the appropriate nuclei are bonded (Popelier and Bader, 1998).

A plot of the Laplacian of the electron density ($\nabla^2\rho$) can be used to give an indication of areas where the electron density is locally concentrated (the Laplacian is negative, illustrated by solid lines) or locally depleted (the Laplacian is positive, illustrated by dotted lines). It has been

shown that the areas of concentration determined by the Laplacian correlate well with the different shells inside an atom.

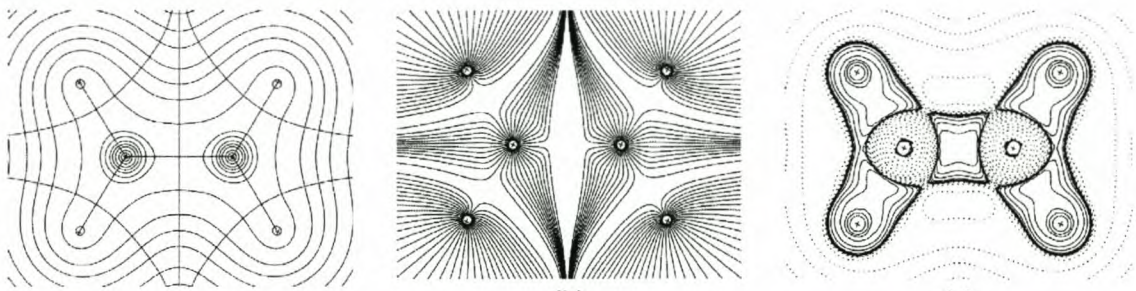

(a) (b) (c)

Figure 2.2 (a) Contour plot of the electron density of ethene. The bond paths and zero flux surfaces are shown. (b) The atomic basins of the atoms. (c) Contour plot of the Laplacian of the electron density. Solid lines indicate charge concentration where $\nabla^2\rho < 0$, dotted lines indicate charge depletion where $\nabla^2\rho > 0$.

Integration of a relevant function over the spin coordinates of all electrons and the spatial coordinates of all but one electron (this type of integration, which also occurs in the expression for the electron density, is written as dτ') and over the region spanned by the atomic basin of an atom yields the value of that property for the specific atom. Examples of functions which can be integrated are

- $K(\boldsymbol{r}) = -\frac{1}{4} N \int d\tau' \left[\psi^* \nabla^2 \psi + \psi \nabla^2 \psi^* \right]$, the Hamiltonian kinetic energy density, which is defined to be everywhere negative.
- $G(\boldsymbol{r}) = \frac{1}{2} N \int d\tau' \nabla \psi^* . \nabla \psi$, the Lagrangian kinetic energy density.
- $V(\boldsymbol{r}) = N \int d\tau' \psi^* \left(-\hat{r} . \nabla \hat{V} \right) \psi$, the Virial field, or potential energy density.

A bond critical point has another important application. The value of the Laplacian or the total energy density at the bond critical point can give information about the nature of the bond. Cremer and Kraka (1984) have shown that a negative value of H_b (the total energy density, defined as $G(\boldsymbol{r}) + V(\boldsymbol{r}) = -K(\boldsymbol{r})$, at the bond critical point) indicates covalent character and a positive or zero value is typical for closed-shell interactions. Popelier (2000) has suggested that a negative value of the Laplacian, in other words a charge concentration, is a sign of covalent bonding, and a positive value, in other words charge depletion, a sign of closed-shell interaction. In a covalent bond electrons are shared between two atoms and the electronic charge is concentrated in the internucleur region and therefore concentrated at the bond critical point. With

closed-shell interactions the charge is predominantly contracted towards one of the nuclei. Therefore the concentration is found not on the bond critical point but closer to the atom that acts as acceptor.

2.5.4 Natural Bond Orbital (NBO) Analysis

Natural Bond Orbital (NBO) analysis, developed by Reed, Weinstock and Weinhold (Reed et al., 1988, Weinhold, 1998) originated as a technique for studying hybridisation and covalent effects in polyatomic wave functions. NBO's, which are in essence built up out of *Natural Atomic Orbitals* (NAO), were conceived as a basis set that would correspond to the picture of localized bonds and electron pairs, in accordance with theories such as those of Lewis.

The analysis arises from a set of transformations of the input basis set (AO) to various localised basis sets: *Natural Atomic Orbitals* (NAO's), *Natural Hybrid Orbitals* (NHO's), *Natural Bond Orbitals* (NBO's) and *Natural Localised Molecular Orbitals* (NLMO's) which can be transformed to delocalised *Natural Orbitals* (NO's) or *Canonical Molecular Orbitals* (MO's). Each set of one-centre (NAO, NHO) and two-centre (NBO, NLMO) orbitals constitutes a complete orthonormal basis set.

Natural orbitals refer to the intrinsic orbitals that arise as eigenfunctions of the first-order reduced density operator

$$\hat{\Gamma}(1|1') = N\int\psi(1,2,...,N)\psi^{*}(1',2,...,N)d\tau_2 d\tau_3 ... d\tau_N \,.$$

The eigenorbitals $\{\phi_i^{NO}\}$ are then given by the eigenequation

$$\hat{\Gamma}\phi_i^{NO} = q_i\phi_i^{NO}$$

where the eigenvalues q_i are the occupation numbers, their values being strictly between zero and two. These orbitals are "natural" to the N electron wave function ψ. The natural orbitals however are highly unsuitable for chemical analysis since they transform as irreducible representations of the full symmetry group of the operator and thus appear delocalised over all nuclear centres making them highly non-transferable. In contrast to this, NBO's attain the high occupancy of NO's but have local one-centre and two-centre properties.

To determine the NAO's the density matrix is first written in terms of blocks of basis functions belonging to the same centre. Each of these blocks is then diagonalised to produce a set

of non-orthogonal "pre-NAO's". On basis of occupation these orbitals can be divided into two sets, a "natural minimal set" corresponding to the atomic orbitals of the isolated atom and a "Rydberg" set consisting of the formal unoccupied orbitals. The second step is to orthogonalise the strongly occupied pre-NAO's for each centre to all the strongly occupied pre-NAO's on the other centres. This is done through an *Occupancy-Weighted Symmetric Orthogonalisation* (OWSO) procedure which assigns higher weight to preserving the form of the strongly occupied pre-NAO's. Thirdly, the weakly occupied pre-NAO's are made orthogonal to the strongly occupied pre-NAO's by Gram-Schmidt orthogonalisation. Finally the OWSO procedure is used to make the weakly occupied pre-NAO's orthogonal.

Once the density matrix has been transformed to the NAO basis, each one-centre block is searched for NAO's with high occupancy (>1.999e) and they are removed as core orbitals. The next step is to search for lone pair eigenvectors. NAO's with occupancies >1.90e are designated lone pairs and removed from the density matrix. Next the two-centre blocks are searched for eigenvectors exceeding a certain threshold (normally 1.90e). If an insufficient number of NBO's is found the criteria may be lowered until a sufficiently large number of electrons has been assigned to bonds. Lastly, the search is done for three-centre bonds.

Each bond-type b_{AB} may be decomposed into its constituent normalised atomic hybrids (h_A, h_B) and polarisation coefficients (c_A, c_B)

$$b_{AB} = c_A h_A + c_B h_B .$$

Since an initial bond orbital b_{AB} found in the (A,B) block might slightly overlap with another bond orbital, e.g. b_{AC} found in block (A,C), the hybrids are reorthogonalised to form the final set of NHO's.

The NBO basis density matrix is of very nearly diagonal form, with diagonal elements of nearly 2 for each Lewis-type NBO (strongly occupied NBO's) and near 0 for each non-Lewis-type NBO (weakly occupied NBO's) with only small off-diagonal elements connecting the Lewis and non-Lewis blocks. A sequence of 2x2 Jacobi rotations can be used to zero these off-diagonal elements, bringing the trace of the Lewis block to N and the non-Lewis block to 0. The transformed orbitals are then true molecular orbitals (NLMO's) with occupations of either 2 or 0.

The natural population of the orthonormal NAO orbital ϕ_i^A is given by the matrix element

$$q_i^A = \left\langle \phi_i^A \middle| \hat{\boldsymbol{\Gamma}} \middle| \phi_i^A \right\rangle .$$

The total natural charge on atom A with atomic number Z^A is then given by

$$Q^A = Z^A - \sum_i q_i^A \ .$$

2.6 The Cambridge Crystallographic Structural Database (CCSD)

The Cambridge Crystallographic Structural Database (Allen and Kennard, 1993) was searched for compounds containing O_3 and a row three to row five element. The only result found was a rubidium ozonide crown ether, with the reference code JEWVEM. The compound was synthesized by Korber and Jansen (1990) and is shown in **figure 2.3**. This compound however is an ionic ozonide $Rb^+O_3^-$ and attains its nature as a complex through the crown ether interaction.

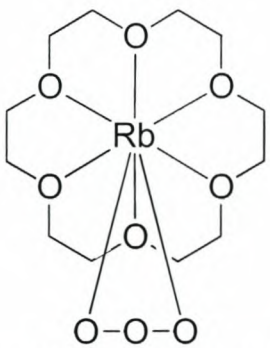

Figure 2.3 The result from a CCSD search for compounds containing O-O-O.

2.7 Review of Selected Articles

Since the complexes modelled in this work are completely novel compounds in this section an overview is given of some calculations done on the ozone molecule .

2.7.1 The Ozone Molecule

Ozone has been the subject of many theoretical studies (Raghavachari et al., 1989; Yamaguchi et al., 1968; Lee et al., 1987; Scuseria et al., 1989; Lee and Scuseria, 1990) due to the difficulties in obtaining an accurate wave. This is a consequence of the fact that the ground state of ozone has to

be described with more than one electronic configuration to obtain accurate results (see **section 3.2.1**). Large basis sets and extensive computation of correlation energies are needed to successfully predict the structure and properties of this molecule (Koch et al., 1993).

Adler-Golden et al. (1985) used the *Complete Active Space Self Consistent Field* (CASSCF) method together with a double zeta plus polarisation basis set and a triple zeta basis set to calculate the ozone vibrational infrared intensities. An agreement of between 2% and 11% with experimental values were obtained for the vibrational frequencies. Stanton et al. (1989) used perturbation theory and CC methods to investigate the potential energy surface of ozone. A double zeta basis set augmented with six polarisation functions were used, together with a larger [5*s*3*p*2*d*] set described in Stanton and Magers (1988). The vibrational frequencies calculated with CCSD and MBPT showed reasonable agreement with the experimental values. However, the asymmetric stretching frequency was found to oscillate wildly between 2373 cm^{-1} for MBPT(2) to 680 cm^{-1} for CCSDT-1 in comparison with the experimental value of 1089 cm^{-1}. The most accurate work on the vibrational frequencies has been done by Lee (1990) who calculated the problematic asymmetric frequency to be 1053 cm^{-1} using CCSD(T) theory and an enormous [5*s*4*p*3*d*3*f*] ANO (Almlöf and Taylor, 1987) basis set.

Several DFT calculations on the geometry of ozone have been done (Fournier et al., 1989; Jones, 1985; Versluis and Ziegler, 1988; Morin et al., 1985). Murray et al. (1993) used density functional theory together with DZP, TZ2P and TZ2p+*f* basis sets to model ozone. A review of some calculations on the vibration frequencies of ozone can be found in their work. The DFT methods fared remarkably well in comparison with the highly correlated CC methods. Using the BLYP functional the problematic asymmetric frequency was calculated to be at 1026 cm^{-1}.

Chapter 3: Molecular Modelling – Structure Determination and Dissociation Energies

3.1 Introduction

As mentioned in **Chapter 1** transition metal ozone complexes are completely novel compounds. Since no experimental or other information is available on the structure and bonding of ozone in complexes the determination of their structure was approached by first calculating in which orientation the ozone ligand is most likely to bond to the transition metal. This was done by modelling complexes in which the only species present are the transition metal cation and the ozone ligand. These computations are described in **section 3.3**. After the most likely orientation had been determined the complexes were enlarged to contain other ligands, described in **section 3.4**. All structural determinations and DFT energy calculations were done with the *Gaussian98* (Frisch et al., 1998) program package. Graphical representations were done with *Gaussview2.08* and *Molden3.7* (Schaftenaar and Noordik, 2000). Example input files are given in **Addendum A**.

3.2 Modelling of Ozone

3.2.1 Computational Procedure

The structure of ozone was determined using B3LYP (Becke, 1993) and the 6-31G(d) basis set of Pople et al. (Ditchfield, Hehre and Pople, 1971; Hehre, Ditchfield and Pople, 1972; Hariharan and Pople, 1973; Gordon, 1980; Hariharan and Pople, 1974). The 6-31G(d) valence double zeta basis set consists of a (10*s*,4*p*,1*d*) → [3*s*,2*p*,1*d*] contraction for the oxygen atom, augmented with a *d*-type polarisation function with exponent 0.800. The contraction is done (631,31,1).

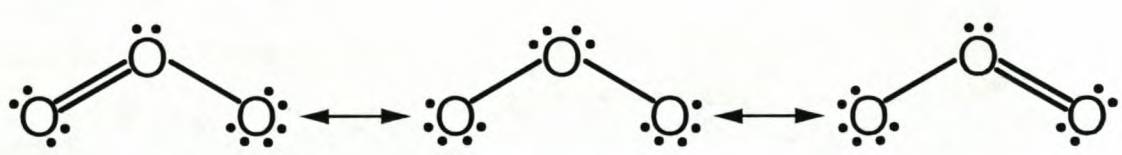

Figure 3.1 A representation of ozone, showing how it can be seen as a diradical.

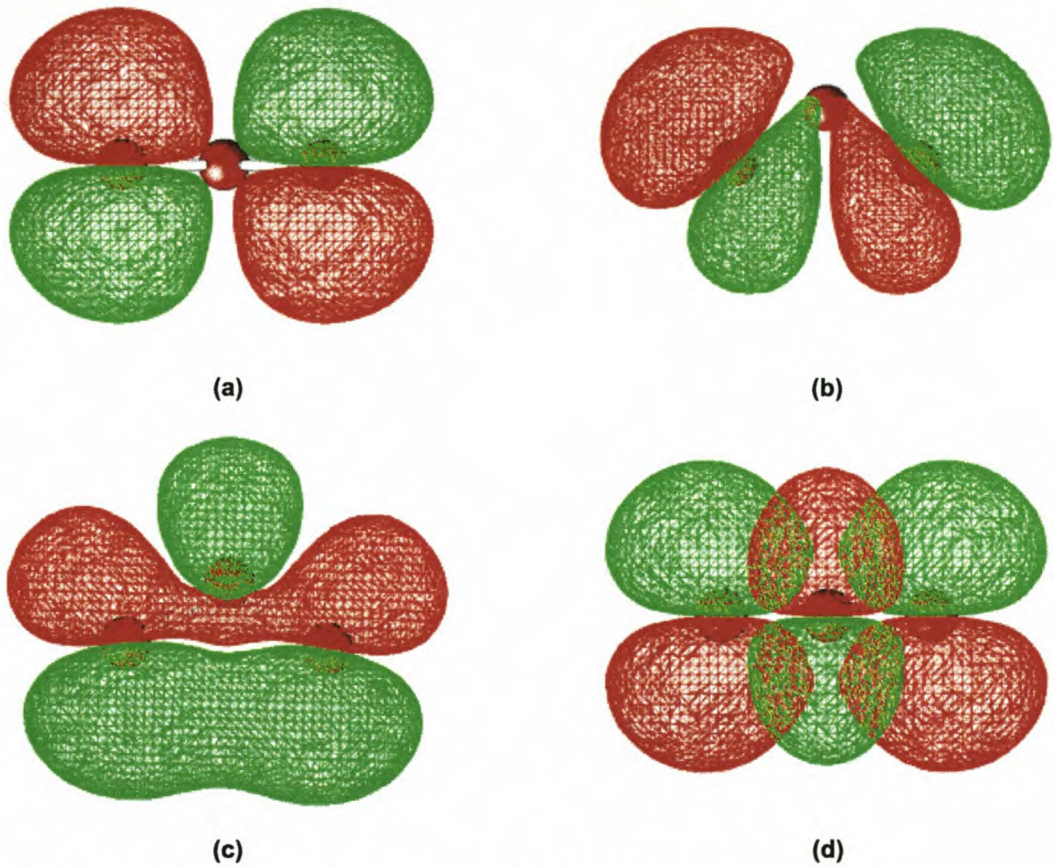

Figure 3.2 The (a) $1a_2$, (b) $4b_2$, (c) $6a_1$ and (d) $2b_1$ MO's of ozone.

The schematic representation of ozone (**fig. 3.1**) reveals that the molecule can be described by three resonance structures. One of these electronic representations shows that ozone can be seen as consisting of two singlet-coupled π-electrons, each one residing on one of the terminal oxygens. In MO-theory, within the symmetry point group C_{2v}, these three structures can be represented by the two electron configurations $[core]1a_2^2 4b_2^2 6a_1^2$ plus the doubly excited $[core]1a_2^2 4b_2^2 2b_1^2$. This property of ozone that more than one electronic structure is needed to accurately describe the molecule plays an important role when the choice of level of theory to model the molecule is made. The effect of static correlation is important and since DFT takes correlation implicitly into account with the exchange-correlation functional, it is a well suited method.

The two electronic configurations which can be written for the ground state of ozone indicate that an appropriate HOMO should have both b_1 and a_1 character. This can be achieved

by mixing the HOMO and LUMO. *Gaussian98* calculations can be instructed to mix these two orbitals using the `guess=mix` instruction. This situation however does not necessarily lead to the lowest energy. Ground state ozone is a singlet and will therefore be described using RHF theory (Strictly speaking the terms RHF and UHF refer to wave functions calculated with Hartree Fock theory, and one should refer to DFT wave functions as UKS and RKS, Unrestricted/Restricted Khon-Sham. The terms RHF and UHF are therefore used in general context). As mentioned earlier closer inspection of the electronic structure reveals that ozone is an *open-shell singlet* and therefore the lowest energy cannot be found by modelling with an RHF wave function, an UHF or ROHF wave function is needed. To obtain the lowest ground state the `stable=opt` instruction has to be used. This calls the routine that checks for wave function instabilities, as described in **section 2.4**. On finding an instability, the routine will search for a lower energy, in the case of ozone this can then be achieved by allowing the singlet wave function, which is determined under RKS conditions, to become UKS.

Ozone was also modelled with the basis set of Dunning and Huzinaga (Dunning, Hay, 1976). This is a full double zeta basis set with no added polarization functions. This set uses a $(9s,5p) \rightarrow [4s,2p]$ contraction for oxygen, done (6111,41). The reason for the use of this basis set is that the lanl2dz basis set was used for calculations on the complexes, and within this set atoms of the first row are described with the Dunning/Huzinaga basis set (see **section 3.4**). Therefore, ozone needed to be calculated with the same basis set to determine dissociation energies.

3.2.2 Results

The results obtained with the 6-31G(d) basis set proved to be much more reliable than those of the Dunning/Huzinaga basis set. The bond distance of 1.264 Å as well as the bond angle of 117.92° calculated using the 6-31G(d) set compare very well with experimental results of 1.272 Å and 116.78° obtained via microwave spectroscopy (Colmont, Demaison and Cosléou, 1995). The energy for the molecule was calculated as -225.4087 Hartree. It is interesting to note that an energy lowering of 1.412 kcal mol^{-1} is obtained when the wave function is allowed to become UKS. The vibrational frequencies of ozone have proved to be very sensitive (Murray, Handy and Amos, 1993) to basis set and level of theory. In this study the three frequencies were calculated to be 708.9 cm^{-1} (a_1), 1046.9 cm^{-1} (b_2) and 1216.7 (a_1). The values were multiplied by a scaling

factor of 0.9614, as suggested by Scott and Radom (1996), for calculations with B3LYP/6-31G(d). The values correspond poorly to the experimental values of 716 cm^{-1}, 1089 cm^{-1} and 1135 cm^{-1} as reported by Scott and Radom (1996). In their article they also mention that ozone is a problematic case and report deviations of 110 cm^{-1} from the experimental values.

Using the Dunning/Huzinaga basis set the bond distance is 1.328 Å and the bond angle 117.94°. As in the case of the 6-31G(d) optimisation the wave function was found to have an RHF → UHF instability. However the search for a lower energy was unsuccessful.

3.3 Modelling of $M[O_3]^{2+}$

3.3.1 Computational Procedure

The $M[O_3]^{2+}$ fragments were modelled using the B3LYP functional and the 6-31G(d) basis set. This basis set makes use of a (22*s*,16*p*,4*d*,1*f*) → [5*s*,4*p*,2*d*,1*f*] contraction for the transition metals, contracted in a (66631,6631,31,1) fashion. A polarisation function with exponent 0.800 was used for the transition metals. The optimisations were done without symmetry constraints.

Complexes of the form $M[O_3]^{2+}$ were built, where M = [Ti, V, Cr, Mn, Fe, Co, Ni, Cu]. All complexes had a charge of +2 and spin states of either singlets, for the fragments that had an even number of total electrons (Ti^{2+}, Cr^{2+}, Fe^{2+}, Ni^{2+}), or doublets, for the fragments having an uneven number of total electrons (V^{2+}, Mn^{2+}, Co^{2+}, Cu^{2+}). The choice of a +2 valence for the ions was done based on articles where similar types of computations were done, transition metal complexes consisting of a metal ion and either CO_2 (Sodupe, Branchadell, Rosi and Bauschlicher, 1997; Fan and Liu, 1999) or NO (Blanchet, Duarte and Salahub, 1997; Thomas, Bauschlicher, Jr. and Hall, 1997) as ligand or alternatively metal oxide cations as coordinating centre (Nakao, Hirao and Taketsugu, 2001). In these examples the complexes were modelled as +1 cations. Modelling the species as cations also adds the extra effect of Coulomb forces, which are not evident in neutral species.

Once again the HOMO's and LUMO's were mixed for the MO's of the starting guesses and the wave functions of the final structures were checked for instabilities. If instabilities were found the wave functions were reoptimised. The importance of testing wave functions of unknown molecules/ions for stability is described by Klapötke and Schultz (1998). Vibrational frequencies were calculated to determine the nature of the stationary point.

Four different input orientations were used in the calculation (**fig. 3.3**). For the first three orientations all the atoms are in the same plane. In the first case, the ozone ligand is placed with the terminal oxygens facing the metal (*A*). In the second orientation the ligand is placed with the central oxygen facing the metal (*B*). In the third orientation the ligand is placed with one of the terminal oxygens facing the metal, in an end-on configuration (*C*). In the final orientation the ozone ligand is placed in a plane not containing the metal atom (*D*).

Figure 3.3 The four different input geometries, labelled A, B, C and D, used for the $M[O_3]^{2+}$ optimisations.

3.3.2 Results: Geometries

The results for each $M[O_3]^{2+}$ complex are shown in **table 3.1**. The columns of the structure types leading to the lowest energy are highlighted. The energies are given as determined once a stationary point had been established, as well as after the wave function had been tested for stability, and if needed reoptimised. *All results following are based on the wave function which has been deemed stable.*

The expectation values of the $\langle S^2 \rangle$ operator are also listed in the table of results. This is done to give an indication of the amount of spin contamination evident in the UKS wave functions and to thereby assess their quality. Because UHF and also UKS wave functions are not eigenfunctions of the spin operator, the value of $\langle S^2 \rangle$ may not be the same as for the pure spin state. Koch and Hollhausen (2000), however warn that one must be careful not to overstress the parallelism between HF theory and KS theory. In HF theory the Slater determinant constructed is in fact the approximate wave function used and the greater the spin contamination gets the more questionable the wave function becomes. In KS theory the Slater determinant is not the true wave function for the system and the relation between spin contamination in the Slater determinant and the true wave function is not known. It must be kept in mind that molecular orbitals derived from DFT calculations are purely mathematical constructs to facilitate the solution of the KS-SCF

procedure (Cramer, Dulles, Giesen and Almlöf, 1995). Pople et al. (1995) argued that DFT wave functions which *do not* contain spin contamination are actually wrong! Nonetheless, the values are reported and can be compared with the $<S^2>$ values for pure spin states, given in **table 3.2**.

The vanadium(II) complex was the first in the series to present problems. When the B3LYP/6-31G(d) method did not result in a minimum, other basis sets were explored, such as STO-3G, 3-21G, 4-21G or the larger 6-311+G**. Some tests were also done on using other levels of theory, such as normal HF or CI methods. This however did not result in better performance and was not done for the other complexes.

To give an indication of the form of the resulting lowest energy structures, the structures of three of the $Ti[O_3]^{2+}$ complexes and one of the $Co[O_3]^{2+}$ complexes are shown in **figure 3.4**. The other metals yielded complexes that are generally the same in form.

Titanium(II), $Ti[O_3]^{2+}$

The lowest energy structure was obtained starting from *D*. Starting from *A* resulted in a planar structure, the energy of this structure being 0.8 kcal mol^{-1} higher than the energy of the structure obtained from *D*. A stationary point was obtained for the *B* structure, but a frequency analysis showed that it was an energy maximum which could be lowered by rotating the ligand to obtain an *A*-type structure. Starting from *C* yielded an *A*-type structure.

Vanadium(II), $V[O_3]^{2+}$

Two different stationary points were obtained for the *A*-type structure, having a symmetric and an asymmetric geometry. A frequency analysis of the symmetric structure revealed the existence of one imaginary frequency, showing that a better geometry can be obtained by distorting one of the terminal oxygen-metal bonds. This distortion yielded the second stationary point on the potential energy surface of $V[O_3]^{2+}$, the energy being lower by 0.1 kcal mol^{-1}. The optimisation of the *B*-type structure yielded a stationary point having two imaginary frequencies. The one frequency was an out-of-plane vibration of the central oxygen, the other a rotation of the ozone ligand in the molecular plane. Following these vectors led to the *D* form minimum. The *C* optimisation converged to an *A* structure.

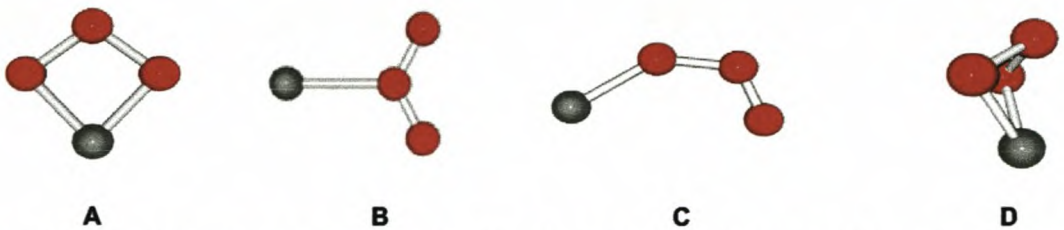

Figure 3.4 The minimum energy structures for $Ti[O_3]^{2+}$, starting from the *A*, *B* and *D* structures in **figure 3.3** as well as the *C* type converged structure for $Co[O_3]^{2+}$.

Chromium(II), $Cr[O_3]^{2+}$

For this fragment the *A* structure resulted in the lowest energy. Neither the *B* nor the *C* structure converged. For both of these optimisations the atoms moved away to result in structures in which the oxygen atoms no longer formed an ozone ligand. The oxygen atoms separated to form either dioxygen ligands or just single oxygen atoms or oxides. Starting from the *D*-type structure resulted in a minimum energy structure that is 17.1 kcal mol^{-1} higher in energy than the *A*-type.

Manganese(II), $Mn[O_3]^{2+}$

The lowest energy was calculated for the *A*-type structure. The optimisation starting from the *B* structure yielded a complex where the ozone ligand was bonded through the central oxygen, but with *no* imaginary frequencies. Manganese is the only metal for which a *B*-type structure is a minimum on the potential energy surface of $Mn[O_3]^{2+}$. This structure however is 17.8 kcal mol^{-1} higher in energy than the *A*-type minimum. Once again the *C* structure did not converge but rather formed an oxide with a dioxygen molecule in proximity. Convergence could not be attained starting from a *D*-type structure. The molecule rearranged into the *A* form but the metal then proceeded to move away from the ozone ligand.

Table 3.1 Results of $M[O_3]^{2+}$, calculated with B3LYP/6-31G(d). The value of the $<S^2>$ operator is given as an indication of the amount of spin contamination. The $<S^2>$ value after annihilation is given in parentheses. The lowest energy conformations are highlighted. Energies in Hartree, distances in Å, angles in degrees, wavenumbers in cm^{-1}.

Complex	$Ti[O_3]^{2+}$			
Input	Type A	Type *B*	Type *C*	Type *D*
Energy ^{unstable}	-1074.06846459	-1073.91527205		-1074.06966302
$<S^2>$ ^{unstable}	0.0000	0.0000		0.0000
Instability[a]	None	RHF→UHF, Inter.		None
Energy ^{stable}	-1074.06846459	-1073.97444064		-1074.06966302
$<S^2>$ ^{stable}	0.0000	1.5369 (2.8261)		0.0000
$r(M,O_1)$[b]	1.744	3.034		1.768
$r(M,O_2)$	1.744	3.034	Type A	1.768
$r(M,O_3)$	2.288	2.227		1.914
$r(O_1,O_3)$	1.457	1.269		1.462
$r(O_2,O_3)$	1.456	1.269		1.462
$A(O_1,O_3,O_2)$	99.29	124.46		102.02
NIMAG	0	1		0
Frequency[c]	826.3	130.4		531.8
Complex	$V[O_3]^{2+}$			
Input	Type *A*	Type *B*	Type *C*	Type *D*
Energy ^{unstable}	-1168.53538150	-1168.44774991		
$<S^2>$ ^{unstable}	1.4122 (0.7628)	1.7538 (0.7627)		
Instability[a]	None	Inter.		
Energy ^{stable}	-1168.53538150	-1168.45758471		
$<S^2>$ ^{stable}	1.4122 (0.7628)	2.2948 (2.4473)		
$r(M,O_1)$[b]	1.763	2.931		
$r(M,O_2)$	1.900	2.935	Type A	No convergence
$r(M,O_3)$	2.384	2.118		
$r(O_1,O_3)$	1.435	1.270		
$r(O_2,O_3)$	1.328	1.270		
$A(O_1,O_3,O_2)$	99.58	124.51		
NIMAG	0	2		
Frequency[c]	465.9	229.6		

[a] Instabilities can either be RHF→UHF or internal (Inter.), or both; [b] The terminal oxygens are numbered 1 and 2, the central oxygen 3.[c] The M-O symmetric bond stretching frequency, giving an indication of the bond strength.

Table 3.1 (continued)

Complex	$Cr[O_3]^{2+}$			
Input	Type A	Type *B*	Type *C*	Type *D*
Energy ^{unstable}	-1268.87174023			-1268.87458940
$<S^2>$ ^{unstable}	0.0000			0.0000
Instability[a]	RHF→UHF, Inter.			RHF→UHF, Inter.
Energy ^{stable}	-1268.93631044			-1268.90907040
$<S^2>$ ^{stable}	1.6447 (3.2432)			1.5044 (2.7941)
$r(M,O_1)$[b]	1.864			1.716
$r(M,O_2)$	1.865	No convergence	No convergence	1.714
$r(M,O_3)$	2.398			2.026
$r(O_1,O_3)$	1.327			1.433
$r(O_2,O_3)$	1.328			1.436
$A(O_1,O_3,O_2)$	101.32			109.69
NIMAG	0			0
Frequency[c]	374.8			686.9
Complex	$Mn[O_3]^{2+}$			
Input	Type *A*	Type *B*	Type *C*	Type *D*
Energy ^{unstable}	-1375.41916740	-1375.39083297		
$<S^2>$ ^{unstable}	2.2883 (2.4776)	3.6889 (8.6047)		
Instability[a]	None	None		
Energy ^{stable}	-1375.41916740	-1375.39083297		
$<S^2>$ ^{stable}	2.2883 (2.4776)	3.6889 (8.6047)		
$r(M,O_1)$[b]	1.805	2.933		
$r(M,O_2)$	1.804	3.053	No convergence	No convergence
$r(M,O_3)$	2.337	2.025		
$r(O_1,O_3)$	1.360	1.376		
$r(O_2,O_3)$	1.360	1.369		
$A(O_1,O_3,O_2)$	100.73	114.93		
NIMAG	0	0		
Frequency[c]	507.4	244.1		

[a] Instabilities can either be RHF→UHF or internal (Inter.), or both; [b] The terminal oxygens are numbered 1 and 2, the central oxygen 3.[c] The M-O symmetric bond stretching frequency, giving an indication of the bond strength.

Table 3.1 (continued)

Complex	$Fe[O_3]^{2+}$			
Input	Type *A*	Type *B*	Type *C*	Type *D*
Energy ^{unstable}	-1488.06264455	-1487.98271873		
$<S^2>$ ^{unstable}	0.0000	0.0000		
Instability[a]	RHF→UHF, Inter.	RHF→UHF, Inter.		
Energy ^{stable}	-1488.09826701	-1488.04052706		
$<S^2>$ ^{stable}	1.4232 (2.9416)	2.3187 (6.8413)		
$r(M,O_1)$[b]	1.868	2.736		
$r(M,O_2)$	1.868	2.738	Type *A*	No convergence
$r(M,O_3)$	2.331	1.921		
$r(O_1,O_3)$	1.301	1.266		
$r(O_2,O_3)$	1.300	1.266		
$A(O_1,O_3,O_2)$	106.32	126.32		
NIMAG	0	1		
Frequency[c]	410.1	261.4		
Complex	$Co[O_3]^{2+}$			
Input	Type *A*	Type *B*	Type *C*	Type *D*
Energy ^{unstable}	-1607.12979664	-1607.06781839	-1607.13908144	-1607.14445349
$<S^2>$ ^{unstable}	1.8196 (1.4688)	2.6507 (3.4174)	1.8067 (0.9902)	2.6294 (3.3932)
Instability[a]	Intern.	Inter.	None	None
Energy ^{stable}	-1607.13571616	-1607.06858963	-1607.13908144	-1607.14445349
$<S^2>$ ^{stable}	1.9373 (1.6066)	2.6935 (3.5240)	1.8067 (0.9902)	2.6294 (3.3932)
$r(M,O_1)$[b]	2.008	2.886	1.822	2.052
$r(M,O_2)$	1.959	2.886	3.382	2.049
$r(M,O_3)$	2.437	1.914	3.046	2.639
$r(O_1,O_3)$	1.293	1.372	1.424	1.354
$r(O_2,O_3)$	1.304	1.372	1.185	1.356
$A(O_1,O_3,O_2)$	108.65	115.98	118.93	98.57
NIMAG	0	0	0	0
Frequency[c]	807.4	263.3	454.4	227.8

[a] Instabilities can either be RHF→UHF or internal (Inter.), or both; [b] The terminal oxygens are numbered 1 and 2, the central oxygen 3.[c] The M-O symmetric bond stretching frequency, giving an indication of the bond strength.

Table 3.1 (continued)

Complex	$Ni[O_3]^{2+}$			
Input	Type *A*	Type *B*	Type *C*	Type *D*
Energy ^{unstable}	-1732.60881668	-1732.53430085	-1732.60186932	
$\langle S^2 \rangle^{unstable}$	0.0000	0.0000	0.0000	
Instability[a]	RHF→UHF, Inter.	RHF→UHF, Inter.	RHF→UHF	
Energy ^{stable}	-1732.63322436	-1732.58108464	-1732.63985080	
$\langle S^2 \rangle^{stable}$	1.2086 (1.7835)	1.5126 (2.7608)	1.0022 (0.3380)	
$r(M,O_1)$[b]	1.812	2.634	1.720	
$r(M,O_2)$	1.812	2.632	3.339	Type *A*
$r(M,O_3)$	2.291	1.829	2.976	
$r(O_1,O_3)$	1.303	1.261	1.480	
$r(O_2,O_3)$	1.303	1.261	1.169	
$A(O_1,O_3,O_2)$	104.24	128.71	120.97	
NIMAG	0	1	0	
Frequency[c]	479.4	277.6	554.3	
Complex	$Cu[O_3]^{2+}$			
Input	Type *A*	Type *B*	Type *C*	Type *D*
Energy ^{unstable}	-1864.78097713	-1864.73236451	-1864.78420651	
$\langle S^2 \rangle^{unstable}$	1.1053 (0.7533)	1.4375 (0.7671)	0.8102 (0.7505)	
Instability[a]	None	None	None	
Energy^{stable}	-1864.78097713	-1864.73236451	-1864.78420651	
$\langle S^2 \rangle^{stable}$	1.1053 (0.7533)	1.4375 (0.7671)	0.8102 (0.7505)	
$r(M,O_1)$[b]	2.052	2.821	1.808	
$r(M,O_2)$	1.982	2.848	3.336	No convergence
$r(M,O_3)$	2.466	1.961	3.008	
$r(O_1,O_3)$	1.287	1.308	1.421	
$r(O_2,O_3)$	1.304	1.312	1.181	
$A(O_1,O_3,O_2)$	109.45	122.40	119.73	
NIMAG	0	0	0	
Frequency[c]	323.4	225.7	453.8	

[a] Instabilities can either be RHF→UHF or internal (Inter.), or both; [b] The terminal oxygens are numbered 1 and 2, the central oxygen 3.[c] The M-O symmetric bond stretching frequency, giving an indication of the bond strength.

Table 3.2 The values of the S^2 operator for pure spin states. These values play an important role when assessing the quality of UHF/UKS wave functions.

Multiplicity	S_z	$\langle S^2 \rangle$
singlet	0.0	0.000
doublet	0.5	0.750
triplet	1.0	2.000
quartet	1.5	3.750
quintet	2.0	6.000
hextet	2.5	8.750

Iron(II), $Fe[O_3]^{2+}$

Only two types of structures were found for this fragment. The *A*-type structure resulted in the lowest energy, and the only true minimum. The *B*-type structure converged to yield a fragment that was 50.15 kcal mol^{-1} in energy higher than the *A* minimum. A frequency analysis showed this to be a maximum and following the imaginary frequency would result in an *A* structure.

Cobalt(II), $Co[O_3]^{2+}$

Cobalt is the only metal for which four minimum energy structures were found. The lowest energy was obtained starting from a *D* structure. During the optimisation the ozone ligand rotated out of the starting molecular plane but reached a stationary point in which the ligand is just slightly out of the plane, and not in-plane like the other minima. The *A* structure optimised to a completely in-plane minimum, being 5.5 kcal mol^{-1} higher in energy than the *D*-type. This was however the third lowest energy. Starting from the *C*-type structure yielded a minimum that was bonded through only one oxygen (the central and other terminal oxygen are 3.046 Å and 3.382 Å away from the metal). This structure is 3.4 kcal mol^{-1} higher in energy than the overall, *D*-type minimum. The final minimum was obtained for the *B*-type structure, 48.1 kcal mol^{-1} higher in energy than the *D*-type.

Nickel(II), $Ni[O_3]^{2+}$

The *C*-type structure is the lowest in energy for this fragment, although this was only the situation once the wave functions were checked for instability. The *A*-type unstabilised wave function is 4.4 kcal mol^{-1} lower in energy than the *C*-type unstabilised wave function, however,

when the wave functions were reoptimised the *C*-type structure gave the lowest energy by 4.2 kcal mol^{-1}. The *B* optimisation once again gave a maximum. The imaginary frequency associated with it shows an in-plane rotation of the ligand, which could either mean an *A*-type or *C*-type minimum, as confirmed by the results of the other optimisations.

Copper(II), $Cu[O_3]^{2+}$

The *C* type structure resulted in the lowest energy, but only by 2.0 kcal mol^{-1} relative to the *A*-type minimum. Also interesting to note is that none of the complexes' wave functions were found to have instabilities. Starting from the *D* structure resulted in two oxygens of the ozone ligand moving away and forming a complex consisting of a metal oxide and a dioxygen molecule.

3.3.3 Results: Dissociation energies

Dissociation energies were calculated as the difference in energy between the sum of the metal ion and the optimised ozone molecule, and the optimised complex's. The energies of the different ions were calculated with the B3LYP combination of energy functional and exchange-correlation functional and the 6-31G(d) basis set, as reported in **section 3.3.1**. The energy values of the metal ions are given in **table 3.3**. The ions with an even number of electrons (Ti^{2+}, Cr^{2+}, Fe^{2+} and Ni^{2+}) were calculated as singlets, triplets and quintets. The metals with an uneven number of electrons (V^{2+}, Mn^{2+}, Co^{2+} and Cu^{2+}) were calculated as doublets, quartets and sextets. Stability checks were also done on all the metals. However, for the lowest energy spin states (highlighted in **table 3.3**) the energy lowerings due to stabilisation were at most 0.5 kcal mol^{-1}. **Figure 3.5** shows the lowest energy electron configurations of the ions, illustrating their expected spin states.

Baerends, Branchadell and Sodupe, 1997, have demonstrated that density functionals are not invariant over the set of ground state densities for the 3*d* transition metals. The degenerate set of ground states for an atom corresponds to a set of densities and for the ground state energy to be a functional of the density the functional must map *all the densities to the same ground state.* The five real *d* orbitals do not lead to densities that can be transformed into each other by simple orthogonal spatial transformations and thus the d_{z2} orbitals will not automatically have the same energy as the other *d* orbitals. This may lead to uncertainties of the order 3-5 kcal mol^{-1} in the ground state energy of the metals/ions.

Table 3.3 The B3LYP/6-31G(d) calculated energies of the metals ions. The values of $<S^2>$ are once again given, with the values after annihilation in parentheses. The lowest energy states are highlighted. Energies in Hartree.

Metal	Titanium(II)		
Spin state	Singlet	Triplet	Quintet
Energy ^{unstable}	-848.467060939	-848.545554086	-847.355544407
<S>$^{2\ unstable}$	0.0000	2.0005 (2.0000)	6.0008 (6.0000)
Energy ^{stable}	-848.525238842	-848.545554086	-847.380713369
<S>$^{2\ stable}$	1.0007 (0.0055)	2.0005 (2.0000)	6.0011 (6.0000)
Metal	Vanadium(II)		
Spin state	Doublet	Quartet	Sextet
Energy ^{unstable}	-942.999203308	-942.993577440	-941.749089016
<S>$^{2\ unstable}$	1.7514 (0.7548)	3.7504 (3.7500)	8.7509 (8.7500)
Energy ^{stable}	-942.999208279	-942.993577440	-941.749089016
<S>$^{2\ stable}$	1.7514 (0.7548)	3.7504 (3.7500)	8.7509 (8.7500)
Metal	Chromium(II)		
Spin state	Singlet	Triplet	Quintet
Energy ^{unstable}	-1043.34292075	-1043.41850165	-1043.47119797
<S>$^{2\ unstable}$	0.0000	2.9426 (2.0015)	6.0004 (6.0000)
Energy ^{stable}	-1043.40573648	-1043.41850844	-1043.47183830
<S>$^{2\ stable}$	1.9293 (3.8627)	2.9428 (2.0015)	6.0005 (6.0000)
Metal	Manganese(II)		
Spin state	Doublet	Quartet	Sextet
Energy ^{unstable}	-1149.82916158	-1149.90335127	-1150.02328109
<S>$^{2\ unstable}$	1.7456 (0.7517)	3.7506 (3.7500)	8.7504 (8.7500)
Energy ^{stable}	-1149.90593816	-1149.93904928	-1150.02328109
<S>$^{2\ stable}$	2.7511 (3.6164)	4.7508 (3.7511)	8.7504 (8.7500)
Metal	Iron(II)		
Spin state	Singlet	Triplet	Quintet
Energy ^{unstable}	-1262.49709100	-1262.58202439	-1262.64355656
<S>$^{2\ unstable}$	0.0000	2.9294 (2.0012)	6.0008 (6.0000)
Energy ^{stable}	-1262.56779279	-1262.58202439	-1262.64356377
<S>$^{2\ stable}$	1.9234 (3.8466)	2.9294 (2.0012)	6.0008 (6.0000)

Table 3.3 (Continued)

Metal	Cobalt(II)		
Spin state	Doublet	Quartet	Sextet
Energy ^{unstable}	-1381.51618441	-1381.64209338	-1381.42481734
<S>$^{2\ unstable}$	0.7502 (0.7500)	3.7507 (3.7500)	8.7505 (8.7500)
Energy ^{stable}	-1381.59112053	-1381.64210811	-1381.42481734
<S>$^{2\ stable}$	1.7504 (0.7513)	3.7507 (3.7500)	8.7505 (8.7500)
Metal	Nickel(II)		
Spin state	Singlet	Triplet	Quintet
Energy ^{unstable}	-1506.99967101	-1507.12058146	-1506.86458003
<S>$^{2\ unstable}$	0.0000	2.0004 (2.0000)	6.0003 (6.0000)
Energy ^{stable}	-1507.08885117	-1507.12058568	-1506.87908602
<S>$^{2\ stable}$	1.0002 (0.0015)	2.0004 (2.0000)	6.0003 (6.0000)
Metal	Copper(II)		
Spin state	Doublet	Quartet	Sextet
Energy ^{unstable}	-1639.21308390	-1638.93262834	-1638.15829957
<S>$^{2\ unstable}$	0.7502 (0.7500)	3.7502 (3.7500)	8.7502 (8.7500)
Energy ^{stable}	-1639.21379549	-1638.95066563	-1638.15863083
<S>$^{2\ stable}$	0.7502 (0.7500)	3.7501 (3.7500)	8.7502 (8.7500)

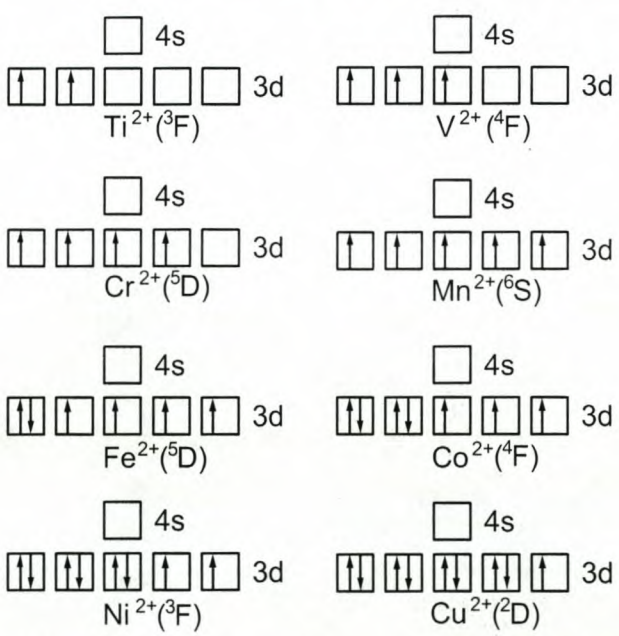

Figure 3.5 The [Ar]$3d^n4s^m$ electron configurations of Ti^{2+}, ..., Cu^{2+}, illustrating their expected ground state spin states.

From **table 3.3** it can be seen that the B3LYP calculations on the metal ions give the appropriate results as expected from **figure 3.5** for the ground states of the ions, with one exception. It is found that vanadium(II) has a doublet ground state instead of the quartet calculated from basic aufbau principles. The energy difference between the quartet and doublet states however is only 3.5 kcal mol^{-1} and based on results by Baerends, Branchadell and Sodupe (1997), can be attributed to the different ground state energy densities of the *d* orbitals, or mere basis set effects. For the dissociation energy the doublet ground state was used.

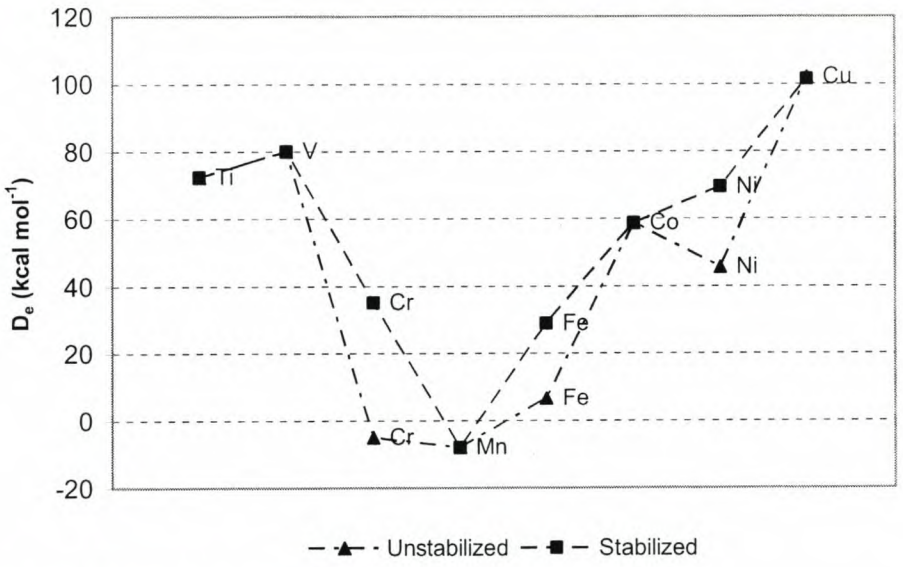

	Unstabilised	Stabilised
$Ti[O_3]^{2+}$	72.4	72.4
$V[O_3]^{2+}$	80.0	80.0
$Cr[O_3]^{2+}$	-5.1	35.0
$Mn[O_3]^{2+}$	-8.0	-8.0
$Fe[O_3]^{2+}$	6.5	28.9
$Co[O_3]^{2+}$	58.8	58.8
$Ni[O_3]^{2+}$	45.5	69.4
$Cu[O_3]^{2+}$	101.9	101.5

Figure 3.6 Dissociation energies of the $M[O_3]^{2+}$, M = Ti, ..., Cu complexes. For the calculation of the energies the metal ions were taken to be in their ground states. Energies are in kcal mol^{-1}.

To give an indication of the effect of testing a wave function for instabilities the dissociation energies were calculated for both the stabilised and unstabilised complexes. However, due to the biradical character of ozone and the subsequent importance of allowing the wave function to be an unrestricted singlet, the energy resulting from a stabilised wave function

was used throughout the calculations. The dissociation energies are shown in **figure 3.6**. *The conclusion is that the stability of transition metal ozone complexes with 2+ charges in singlet and doublet spin states, independent of their ligand environment and relative to the ground state ion and ozone, increases in the order* $Mn^{2+} < Fe^{2+} < Cr^{2+} < Co^{2+} < Ni^{2+} < Ti^{2+} < V^{2+} < Cu^{2+}$.

From the graph of the dissociation energies it can be seen that the unstabilised chromium complex and both manganese complexes have higher energies than the sum of their constituent parts. The chromium and manganese ions in their ground states, however, are in quintet and sextet spin states respectively. Were they to be in the higher energy singlet and doublet states, like in the complexes, the dissociation energy would be 75.4 kcal mol^{-1} and 76.5 kcal mol^{-1} as well as 113.8 kcal mol^{-1} and 65.6 kcal mol^{-1} for the unstabilised and stabilised wave functions respectively. The calculations therefore predict that the manganese doubly ionised ion, in its electronic ground state, will not form an ozone complex without an external energy addition to facilitate a change in spin state.

The complexes were only modelled as singlets and doublets due to time constraints. This decision can now be rationalised by investigating the energies of the valence region of MO's of the complexes. The tendency for complexes to be in higher spin states (to have more unpaired electrons) than singlets and doublets can be seen as a consequence of the degeneracy of the molecular orbitals. In other words, in a highly non-degenerate state the energy loss due to the pairing of electrons will not be more than the loss due to the occupation of higher energy unfilled orbitals. In the highly degenerate case the electrons will stay unpaired since the orbitals have the same energy and occupying the next degenerate orbital does not lead to any energy loss. The degeneracy, compared to that present in the ions, does disappear slightly in the complexes.

A comparison was made between the vibrational frequencies of the symmetrical stretching of the M-O bond (or bonds) and the dissociation energies to establish whether a trend exists between the frequency of the vibration which moves the ion away from the ligand and the energy lowering observed due to the formation of a bond (or bonds) between the ion and the ligand. The results are shown in **figure 3.7**. Using the vibrations for all the molecules no significant trend could be obtained. The structures of the complexes do however differ and when only the vibrational modes that were similar in form were used a linear fit with a R^2 value of 0.1892 (compared to 0.0020 for all the complexes) could be made. Since the complexes with *A*-type minima are in the majority they were used (the *D*-type Co^{2+} complex was included since its

geometry resembles the *A*-type to a much higher extent than the other *D*-type minima). The correlation is however not significant.

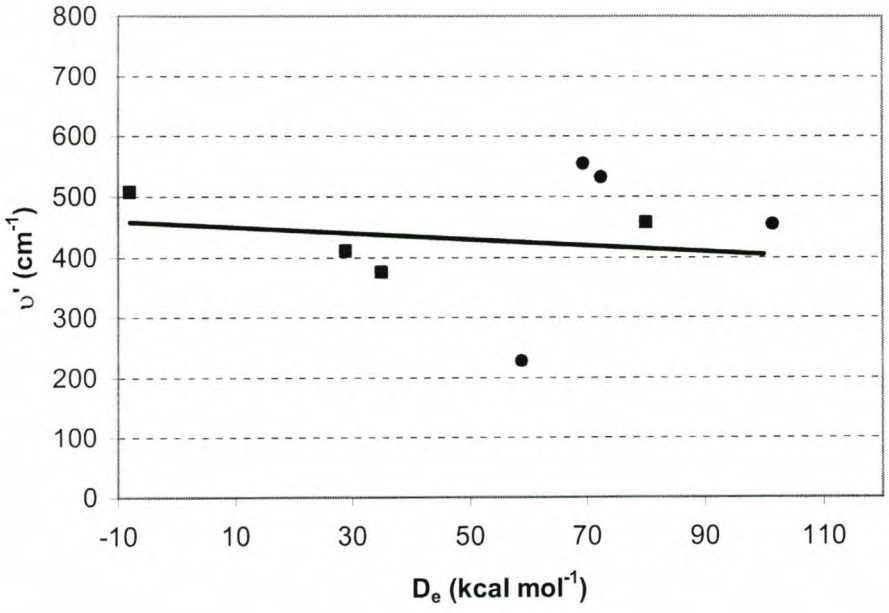

	M-O stretch	D_e
$Ti[O_3]^{2+}$	531.8	72.4
$V[O_3]^{2+}$	456.9	80.0
$Cr[O_3]^{2+}$	374.8	35.0
$Mn[O_3]^{2+}$	507.4	-8.0
$Fe[O_3]^{2+}$	410.1	28.9
$Co[O_3]^{2+}$	227.8	58.8
$Ni[O_3]^{2+}$	554.3	69.4
$Cu[O_3]^{2+}$	453.8	101.5

Figure 3.7 The M-O stretch vibrations in $M[O_3]^{2+}$, M = Ti, ..., Cu plotted versus dissociation energy. Energy in kcal mol^{-1}, wavenumbers in cm^{-1}. The squares show the points that were used and the circles those that were ignored in the fitting, as explained in the discussion.

Another graph was drawn of the vibrational frequencies versus the distance from the metal ion to the centre of mass of the ozone ligand. These results are shown in **figure 3.8**. It is once again important to keep in mind that the Ni^{2+},Cu^{2+} and Ti^{2+} complexes gave structures that differ significantly from the other complexes. In this case a trend line of the form $y = x^n$ with a R^2 value of 0.9857 could be fitted. The relation between vibrational frequency and the force constant, and hence the distance, is expected to have a power function form, according to Badger's Rule (Badger, 1934, 1935).

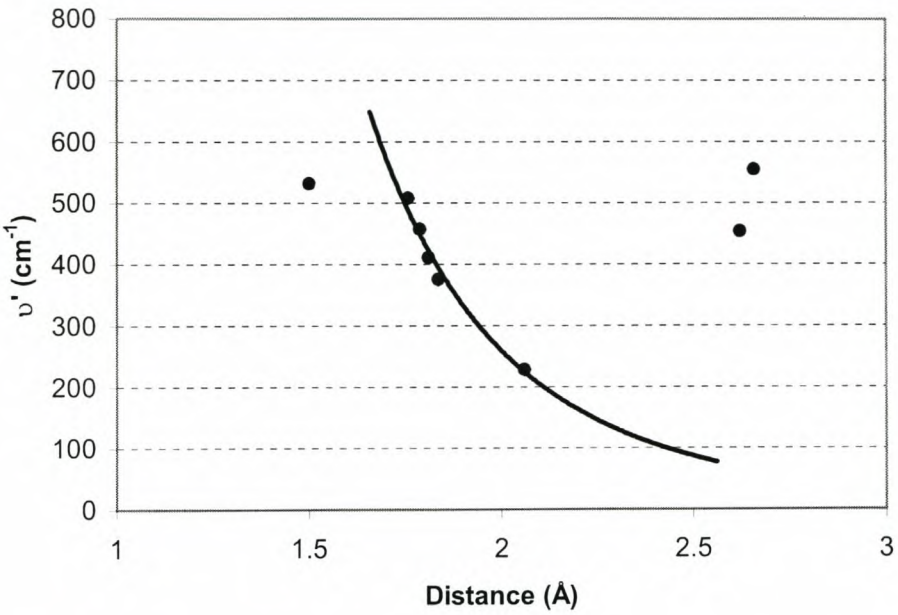

	M-O stretch	Distance
$Ti[O_3]^{2+}$	531.8	1.502
$V[O_3]^{2+}$	456.9	1.789
$Cr[O_3]^{2+}$	374.8	1.837
$Mn[O_3]^{2+}$	507.4	1.759
$Fe[O_3]^{2+}$	410.1	1.811
$Co[O_3]^{2+}$	227.8	2.061
$Ni[O_3]^{2+}$	554.3	2.659
$Cu[O_3]^{2+}$	453.8	2.622

Figure 3.8 The M-O stretch vibrations in $M[O_3]^{2+}$, M = Ti, ..., Cu plotted versus the distance from the metal to the centre of mass of the ozone ligand. Distances in Å, wavenumbers in cm^{-1}.

3.4 Modelling of $M(CO)_nH_m(O_3)$

3.4.1 Computational Procedure

Complexes of the form $M(CO)_nH_m(O_3)$ were modelled, where n = 2,3,4,5,6 and m = 0,1. The values of n and m, in other words the number of carbonyl and atomic hydrogens present in the complexes, were determined by the 18-electron rule (Shriver and Atkins, 1999). According to this rule the number of valence electrons of the central atom are counted (in its neutral state), together with the electrons donated by each of the ligands present. If the complex is charged, the appropriate number of electrons are simply subtracted or added to the total amount. The total

number of electrons should then amount to 18. Ozone was prematurely counted as a four electron donor, two electrons through each of the terminal oxygens. In cases where 18 electrons could not be obtained by just adding CO's and an O_3 ligand, an atomic hydrogen ligand was used, as a single electron donor. Two illustrative examples are:

$Cr(CO)_4(O_3)$:		*$Mn(CO)_3H(O_3)$*:	
Cr	= 6 e^-	Mn	= 7e^-
4CO (4 x 2)	= 8 e^-	3CO (3 x 2)	= 6 e^-
O_3	= 4 e^-	H	= 1 e^-
	18 e^-	O_3	= 4 e^-
			18 e^-

The complexes were once again modelled with the B3LYP combination of functionals. The lanl2dz basis set was used (Hay and Wadt, 1985a; Hay and Wadt, 1985b; Wadt and Hay, 1985). This is an ECP basis set, substituting the 10 core electrons of the metal with pseudopotentials. The remaining valence electrons are described by a $(8s,5p,5d) \rightarrow [3s,3p,2d]$ contraction, contracted in a (341,311,41) manner. The O, C and H atoms are described by the basis set of Dunning and Huzinaga (Dunning, Hay, 1976). For details of this basis set see **section 3.2.1**.

Stationary points on the potential energy surfaces were characterised by an analysis of the Hessian matrix. The wave functions were *not* tested for instabilities and the optimisations were done without symmetry constraints. All complexes were built as singlets.

The fragment calculations (**section 3.2**) in which the ozone ligand was modelled with the 6-31G(d) basis set resulted in ozone geometries that compared very well with the literature. The first set of calculations where the non-metallic atoms are described by the Dunning/Huzinaga set delivered results in which the ozone bond lengths were overestimated, based on the results of the fragment calculations. This led to a next set of calculations in which the metal atoms were described with the Los Alamos pseudopotentials and accompanying valence basis functions of Hay and Wadt (1985) and the other atoms by the 6-31G(d) set. The ECP basis set with the basis set of Dunning/Huzinaga for the non-metals will be referred to as basis set I, and the ECP basis set with the 6-31G(d) basis set will be referred to as basis set II.

The results of the fragment calculations showed that the type *A* orientation of ligand to metal was the only orientation that resulted in a minimum for *all* the complexes. Where the type

A geometry was not the lowest energy, the difference between the lowest energy geometry and the *A*-type was less than 4 kcal mol^{-1}. This led to the decision to model all the complexes with the ozone ligand in a type *A* orientation.

Dissociation energies were calculated for these complexes. The Basis Set Superposition Error (BSSE) was also calculated and in **Chapter 4** a discussion of the electronic structure of these complexes is given.

3.4.2 Results: Geometries

The results for the determination with basis set I are given in **table 3.4**. All the stationary points were confirmed as minima by the absence of imaginary eigenvalues in the Hessian matrix.

Table 3.4 The B3LYP calculated energies and geometries of the complexes. The metal was described by the Los Alamos ECP basis set and the non-metals with the DZ basis set of Dunning and Huzinaga (basis set I). Energies are in Hartree, distances and angles in Å and degrees.

Complex	$Ti(CO)_5(O_3)$	$V(CO)_4H(O_3)$	$Cr(CO)_4(O_3)$	$Mn(CO)_3H(O_3)$
Energy	-850.187241716	-750.704612821	-765.07058811	-669.939698951
r(M,O_1)	1.999	1.921	1.893	1.857
r(M,O_2)	1.982	1.921	1.894	1.876
r(M,O_3)	2.614	2.542	2.495	2.457
r(O_1,O_2)	1.469	1.465	1.459	1.450
r(O_1,O_3)	1.464	1.465	1.459	1.453
A(O_1,O_3,O_2)	98.19	97.41	98.19	98.39
Complex	$Fe(CO)_3(O_3)$	$Co(CO)_2H(O_3)$	$Ni(CO)_2(O_3)$	$Cu(CO)H(O_3)$
Energy	-688.895636926	-597.774223279	-621.420124963	-535.480644524
r(M,O_1)	1.852	1.824	1.821	1.968
r(M,O_2)	1.853	1.824	1.821	1.899
r(M,O_3)	2.434	2.405	2.419	2.457
r(O_1,O_2)	1.468	1.481	1.511	1.521
r(O_1,O_3)	1.468	1.481	1.511	1.512
A(O_1,O_3,O_2)	98.26	97.96	97.48	103.58

Two titanium complexes were built and the results compared. One complex was seven coordinate, having 5 CO ligands and conforming to the 18-electron rule, the other was six

coordinate, having 4 CO ligands with only 16 electrons in the valence shell. Increasing the number of CO ligands increases the M-O bond length. The chromium complex was also modelled with three, four and five CO ligands. Once again, an increase in coordination number of the metal leads to an increase in the metal-ozone bond length. This is an expected result since the availability of metal d orbitals for overlap and hence the bond strength should decrease as more ligands are involved in the coordination.

As mentioned in **section 3.4.1** the results of a calculation on an ozone molecule hinted that the basis set for O used in the lanl2dz combination does not give an accurate description of ozone. The calculations with basis set I were, therefore, repeated with what proved to be a much more accurate basis set, based on ozone bond lengths. These results with basis set I can be compared with the results with basis set II, given in **table 3.5**. Graphical representations of the complexes, as determined with basis set II, are given in **figure 3.9**.

Table 3.5 The B3LYP calculated energies and geometries of the complexes. The metal was described by the Los Alamos ECP basis set and the non-metals with the 6-31G(d) basis set (basis set II). Energies are in Hartree, distances and angles in Å and degrees.

Complex	$Ti(CO)_5(O_3)$	$V(CO)_4H(O_3)$	$Cr(CO)_4(O3)$	$Mn(CO)_3H(O_3)$
Energy	-850.281825571	-750.780164173	-765.144808835	-669.997212014
$r(M,O_1)$	1.985	1.907	1.879	1.857
$r(M,O_2)$	1.971	1.907	1.879	1.859
$r(M,O_3)$	2.549	2.479	2.431	2.394
$r(O_1,O_2)$	1.394	1.391	1.385	1.369
$r(O_1,O_3)$	1.393	1.391	1.385	1.369
$A(O_1,O_3,O_2)$	100.80	99.79	100.66	101.35
Complex	$Fe(CO)_3(O_3)$	$Co(CO)_2H(O_3)$	$Ni(CO)_2(O_3)$	$Cu(CO)H(O_3)$
Energy	-688.951560724	-597.807554633	-621.449757553	-535.498232094
$r(M,O_1)$	1.827	1.794	1.781	2.065
$r(M,O_2)$	1.827	1.794	1.781	2.064
$r(M,O_3)$	2.367	2.335	2.346	2.503
$r(O_1,O_2)$	1.395	1.407	1.444	1.315
$r(O_1,O_3)$	1.395	1.407	1.444	1.315
$A(O_1,O_3,O_2)$	100.23	99.77	98.61	109.68

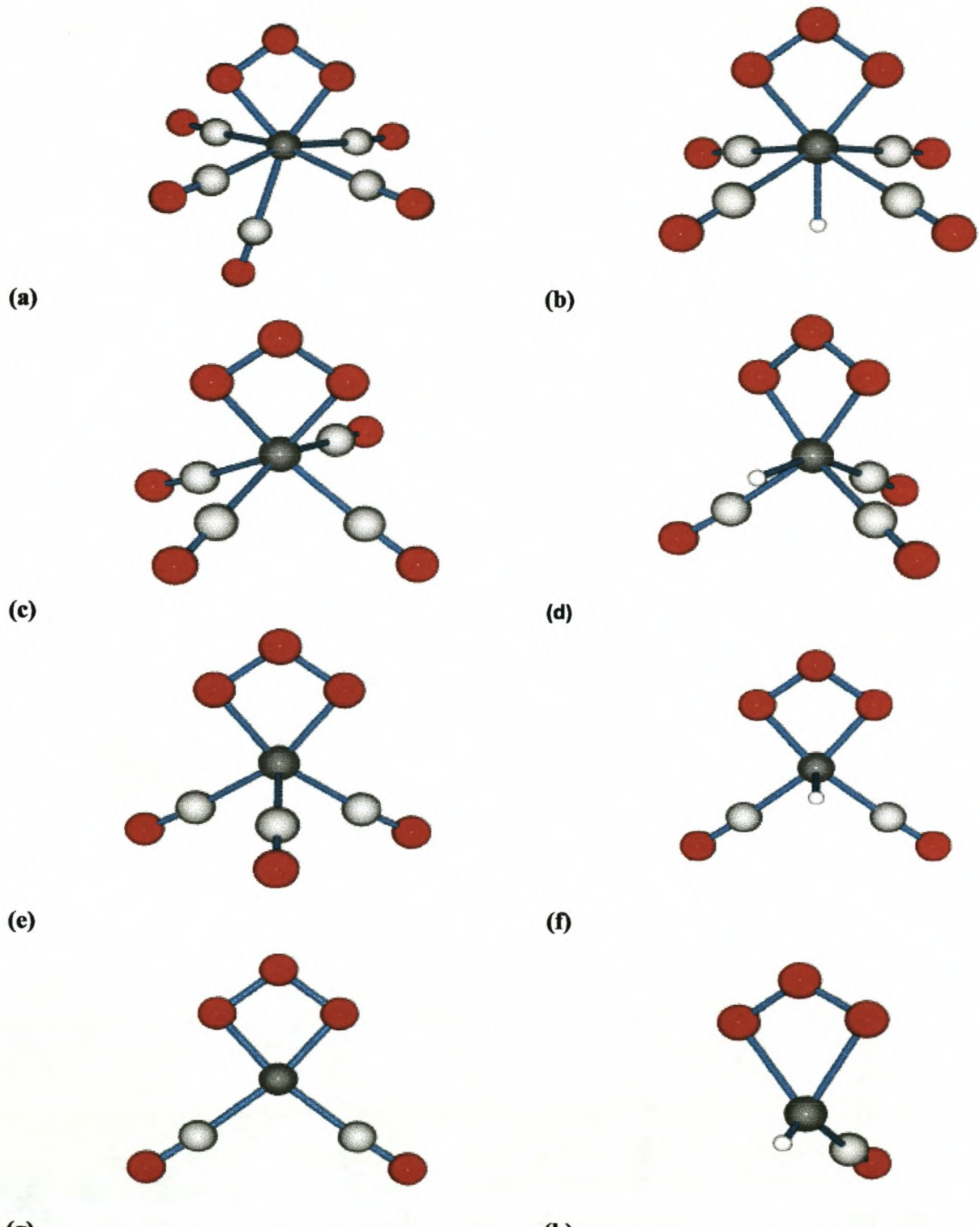

Figure 3.9 (a) $Ti(CO)_5(O_3)$, (b) $V(CO)_4H(O_3)$, (c) $Cr(CO)_4(O_3)$, (d) $Mn(CO)_3H(O_3)$, (e) $Fe(CO)_3(O_3)$, (f) $Co(CO)_2H(O_3)$, (g) $Ni(CO)_2(O_3)$ and (h) $Cu(CO)H(O_3)$, determined with B3LYP/II.

The metal-ozone bond length calculated with basis set II differed at most by 0.05 Å from the results with basis set I. The ozone bonds, however, were determined to be much shorter in general. Carbonyl-metal bond distances can be compared with those from the literature determined from a $Cr(CO)_6$ crystal structure as 1.916 Å (Whitaker and Jeffrey, 1967).

Calculations with basis set I showed that stationary points do exist for some of the structures where the ozone ligand is in-plane with two of the carbonyl ligands. However, frequency analysis showed these points to be maxima for some of the complexes that could be turned into minima by moving the ozone out of the plane. A short discussion of each of the complexes follows:

Titanium, $Ti(CO)_5(O_3)$

Two different metal-carbonyl bonds were found. Two *cis* carbonyls have Ti-CO bonds of 2.124 Å, whereas the other two *cis* carbonyls have bond distances of 2.156 Å. The most interesting feature is that the near-symmetric structure is deformed by the carbonyl lying *trans* to the ozone ligand, which forms an angle of 163° with the central oxygen of the ozone ligand (**fig. 3.9a**). The ozone ligand lies staggered with respect to the carbonyls and forms an angle of 43° with the eclipsed form.

Vanadium, $V(CO)_4H(O_3)$

This complex was built with the hydrogen ligand both *trans* and *cis* to the ozone ligand. The *trans* form proved to be the lower in energy. It is also the complex with the highest degree of symmetry, D_{2h}; all the carbonyl-metal bonds are 2.010 Å, the ozone ligand lies staggered by 45.6° compared to the eclipsed form, and the hydrogen forms an angle of 180.0° via the metal with the central oxygen atom of the ozone ligand.

Chromium, $Cr(CO)_4(O_3)$

The chromium complex is once again in a staggered form with respect to the ozone and two of the linear carbonyls, the angle being 37.2°. The four carbonyls are also not symmetrical, two *trans* ligands having Cr-CO bond distances of 1.939 Å , the other two 1.923 Å. The other difference between the two pairs of *trans* ligands is the angle between the *trans* pairs: the one

angle is 146.9°, the other angle is much smaller, only 114.3°. This can be seen from the graphical representations (**fig. 3.9c**).

Manganese, $Mn(CO)_3H(O_3)$

This complex was built with the hydrogen ligand *trans* to the ozone ligand as well as *cis* to it. The *trans* conformation resulted in a structure with the hydrogen *cis* to the ozone ligand, but not in plane with the linear hydrogen-carbonyl pair. The *cis*-starting conformation optimised to a minimum where the ozone is in plane with the hydrogen-carbonyl pair. The energy of this eclipsed form is 0.5 kcal mol^{-1} higher than the staggered form. Two carbonyls have bond distances that are nearly the same, 1.856 Å and 1.855 Å, the third one, lying trans to the hydrogen, is 1.848Å.

Iron, $Fe(CO)_3(O_3)$

This complex is similar in form to the manganese complex, without the hydrogen. The carbonyl perpendicular to the plane of the ozone ligand has an Fe-CO bond length of 1.780 Å, the other two carbonyls are both 1.846 Å away from the central metal.

Cobalt, $Co(CO)_2H(O_3)$

Two stationary points, both minima, were found for this complex.The one structure has the ozone ligand in plane with the carbonyls, the other one not. The in-plane structure is 3.5 kcal mol^{-1} lower in energy than the out-of-plane structure. For the lower energy structure, the Co-CO bond lengths are 1.854 Å. The hydrogen lies 10° away from perpendicular to the ozone-carbonyl plane (**fig. 3.9f**).

Nickel, $Ni(CO)_2(O_3)$

The complex was modelled with the ozone ligand once again in- and out-of-plane. However only one minimum was found, that of the planar structure. The Ni-CO bond lengths are 1.881 Å. This picture is consistent with molecular orbital theory which predicts that Ni favours planar four coordination when bonded to strong field ligands in oxidation state II.

Copper, $Cu(CO)H(O_3)$

Only the staggered structure resulted in convergence for this complex. The Cu-CO bond distance is 1.949 Å. The three ozone oxygen atoms and the carbon and oxygen of the carbonyl are nearly in a plane (the angle between the central ozone oxygen, the carbon atom of the carbonyl and the oxygen atom of the carbonyl is 176.4°). The Cu atom is then slightly elevated out of this plane, the Cu-C-O angle being 166.9° (**fig. 3.9h**). The hydrogen ligand is perpendicular to the plane formed by the oxygen atoms in the complex.

3.4.3 Results: Dissociation energies

Dissociation energies were calculated as the difference in energy between the sum of the ozone ligand and the $M(CO)_nH_m$ complex, and the optimised $M(CO)_nH_m(O_3)$ complex. Both fragments were optimised as singlets. Optimisation of the complexes was done without any symmetry constraints. The energies were calculated with the B3LYP combination of density functionals and basis set II. The BSSE was also calculated for the complexes and the dissociation energy adjusted by the appropriate values. The BSSE for the chromium complex was calculated to be *negative* suggesting that the energy is not lowered but in fact *increased* by allowing the electrons to occupy the basis functions of the neighbouring atoms. The reason for this anomalous result could not be established and thus the value is omitted. The structures for the $M(CO)_nH_m$ complexes are shown in **figure 3.10**. A graph of the dissociation energies can be seen together with the BSSE values in **figure 3.11**. A short discussion of the structures obtained for the complexes follows.

Titanium, $Ti(CO)_5$

A trigonal bipyramidal arrangement of the ligands was obtained as a stationary point on the potential energy surface of the complex. Frequency analysis showed it to be a maximum, with the imaginary frequency indicating an out-of-plane vibration of the three equatorial carbonyls. Building the complex with four ligands in plane and one perpendicular to this plane resulted in the conformation shown in **figure 3.10a**, which is 5.6 kcal mol^{-1} lower in energy.

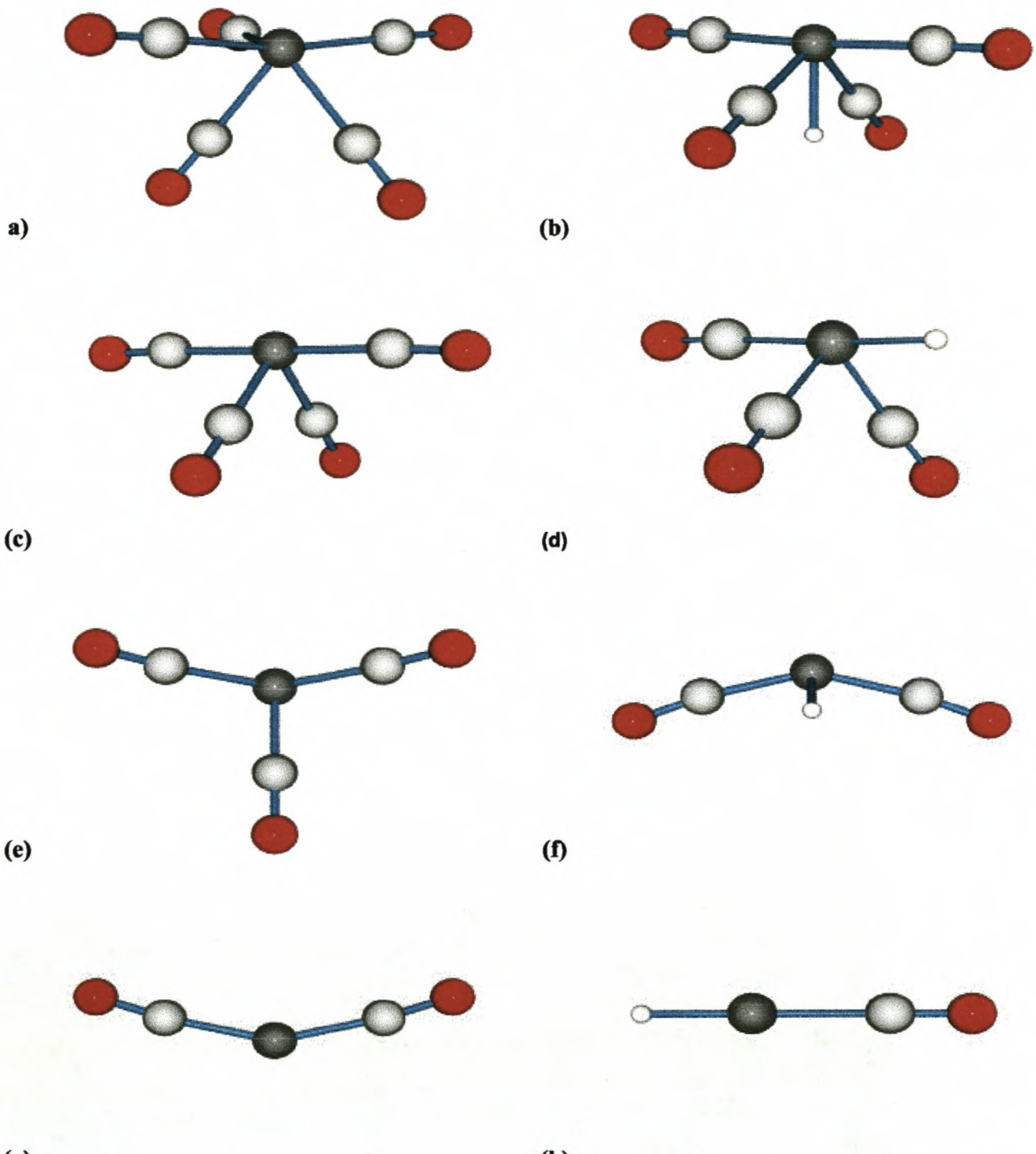

Figure 3.10 (a) $Ti(CO)_5$, (b) $V(CO)_4H$, (c) $Cr(CO)_4$, (d) $Mn(CO)_3H$, (e) $Fe(CO)_3$, (f) $Co(CO)_2H$, (g) $Ni(CO)_2$ and (h) Cu(CO)H, determined with B3LYP/II.

Vanadium, $V(CO)_4H$

The complex was built with the atoms in the positions they have in the ozone complex, without the ozone ligand. This led to an energy minimum with the carbonyls in a plane and the hydrogen atom skew to this plane. Interchanging the position of the hydrogen atom *trans* to the ozone ligand in the ozone complex with one of the carbonyls, and optimising from this position lead to a minimum with the hydrogen and two carbonyls in a plane and the other two carbonyls below this plane, making an angle of 80.7° with each other. Starting with the four carbonyls in a plane and the hydrogen perpendicular to this plane afforded the lowest energy structure (**fig. 3.10b**). Starting from a trigonal bipyramidal structure, with three carbonyls in the equatorial plane, gave a structure with one imaginary frequency. Placing two carbonyls and the hydrogen in the equatorial plane led to a distorted trigonal bipyramidal energy minimum 7.1 kcal mol^{-1} higher in energy than the lowest energy structure.

Chromium, $Cr(CO)_4$

Two stationary points were obtained for this structure, both minima. The one is a square planar structure, the other, shown in **figure 3.10c**, is the lower in energy, 9.5 kcal mol^{-1} lower than the square planar form.

Manganese, $Mn(CO)_3H$

For this structure, three different minima were found. The highest energy minimum corresponds to the planar structure. The structure is not ideally square planar, with the two carbonyls *cis* to the hydrogen making an OC-Mn-CO angle of 158.6°. The second minimum is one in which the hydrogen and two carbonyls lie in a plane, with the third carbonyl perpendicular to this plane. Once again the two carbonyls *cis* to the hydrogen are not collinear and they form an angle of 162.7° via the metal. In both the distortion from linearity is in the direction of the hydrogen. The final minimum, the lowest in energy, is 4.0 kcal mol^{-1} and 1.1 kcal mol^{-1} lower than the previous forms, respectively. The structure is similar to the $Cr(CO)_4$ minimum with one of the carbonyls replaced by a hydrogen.

Iron, $Fe(CO)_3$

Two minima were obtained, a planar structure and one in which two carbonyls are in a plane and the third perpendicular to this plane, 3.6 kcal mol^{-1} lower in energy. As with the previous structures, the two in-plane carbonyls and the metal are not collinear, making a OC-Fe-CO angle of 136.4°.

Cobalt, $Co(CO)_2H$

A planar minimum could not be obtained for this complex. The structure shown in **figure 3.10f** follows the same general trend as observed for the other complexes in that the two carbonyls are not collinear. The angle between them is 150.4°. Also, as observed for the other complexes containing hydrogens, the hydrogen is not completely perpendicular to the plane of the carbonyls.

Nickel, $Ni(CO)_2$

Again two minima were obtained, one nearly linear (OC-Ni-CO angle of 178.2°) and one, 0.5 kcal mol^{-1} lower in energy, with a OC-Ni-CO angle of 152.6°, as seen in **figure 3.10g**.

Copper, Cu(CO)H

For copper only a linear conformation could be obtained (**fig. 3.10h**).

The trend observed for the dissociation energies of the complexes (**fig. 3.11**) does not suggest the same result as for the fragment calculations in terms of the most stable complexes. Note that copper now forms the complex that is the least stable, with iron being the most stable. Vanadium and titanium are also, as with the fragment calculations, high up in the series. The complete trend of dissociation energies is Cu < Ni < Co < Cr < Mn < V < Ti < Fe. The BSSE values are also very small, the highest value being 6.1 kcal mol^{-1}, the lowest 2.7 kcal mol^{-1}.

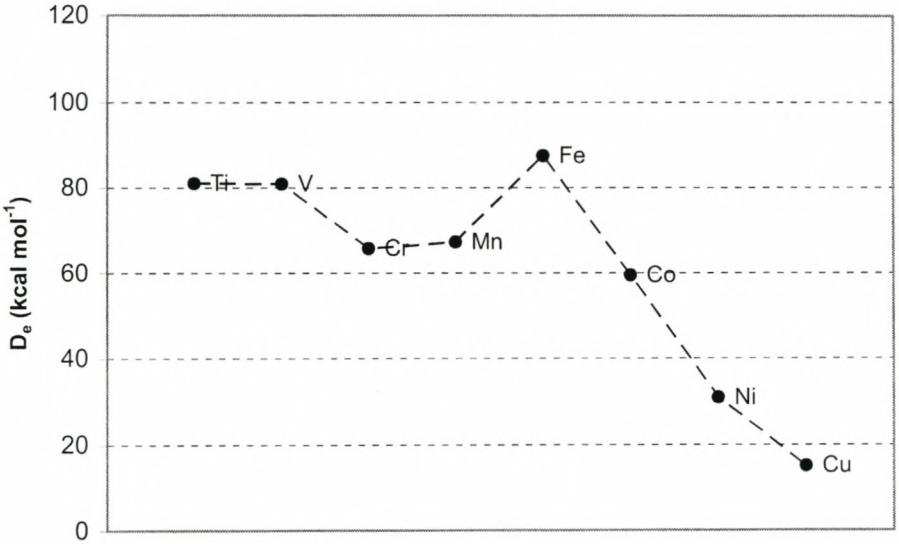

	D_e	BSSE
$Ti(CO)_5(O_3)$	81.0	4.3
$V(CO)_4H(O_3)$	80.9	6.1
$Cr(CO)_4(O_3)$	65.7	-
$Mn(CO)_3H(O_3)$	72.9	5.7
$Fe(CO)_3(O_3)$	91.5	4.1
$Co(CO)_2H(O_3)$	59.4	4.5
$Ni(CO)_2(O_3)$	30.9	4.7
$Cu(CO)H(O_3)$	15.0	2.7

Figure 3.11 Dissociation energies of $M(CO)_mH_n(O_3)$, M = Ti, ..., Cu complexes. All complexes are built as singlets. The Basis Set Superposition Error is also listed. Energies are in kcal mol^{-1}.

Chapter 4: Electronic Structure and Bonding Analysis

4.1 Introduction

After the prediction of reliable molecular geometries, bond energies and vibrational frequencies of transition metal compounds (Frenking et al., 1996; Cundari et al., 1996; Ziegler, 1991; Jonas and Thiel, 1995, 1996), the necessary first steps of any quantum chemical study, the abstract data need to be analyzed in terms of known chemical models. Haaland (1989) has shown that it is possible *and* can be very useful to distinguish between covalent and donor-acceptor bonds in main-group chemistry. The term *covalent* refers to bonds where each bonding partner provides one electron to the two-electron bond. The term *donor-acceptor* refers to Lewis acid-base adducts (acceptor-donor). He showed that understanding bonds in this way can explain many of the trends observed in main-group chemistry.

Frenking and Pidun (1997) explain the importance of donor-acceptor bonds in transition metal chemistry with the example of WCl_6 and $W(CO)_6$. These compounds are usually discussed as interactions between closed shell fragments, W^{6+} and $6Cl^-$ and W and 6CO. Hardly anyone would discuss the bonding of CCl_4 in terms of interactions between C^{4+} and $4Cl^-$, but rather as covalent bonding with an sp^3-hybridized carbon.

In this chapter the bonding of the optimized ozone complexes is investigated with the help of three theoretical techniques, Atoms in Molecules (AIM) developed by Bader (1990), Charge Decomposition Analysis (CDA) developed by Dapprich and Frenking (1995) and Natural Bond Orbital (NBO) analysis developed by Reed et al. (1988).

All calculations relating to Atoms in Molecules were done with the AIMPAC suite of programs (Biegler-König, Bader, Ting-Hau, 1982). The programs used were GRIDV (for calculating contour maps), CONTORPG (for generating postscript output files from GRIDV results), GRDVECPG (for calculating gradient vector paths and generating postscript output) and PROAIMV (for integrating over atomic basins). The wave function was generated by using the `output=wfn` option in *Gaussian98*.

The Charge Decomposition analysis was done with the CDA 2.1.2 software package developed by Dapprich and Frenking (1995).

Natural Bond Orbital calculations were performed with the Gaussian NBO 3.1 package included within *Gaussian98 A.7*.

4.2 The Electronic Structure and Bonding of the Ozone Molecule

The ozone molecule was modelled as described in **Chapter 3** at the B3LYP/6-31G(d) level of theory. **Figure 4.1** shows the contour plots of the electron density, the Laplacian of the electron density as well as a graph indicating the atomic basins of each of the oxygen atoms.

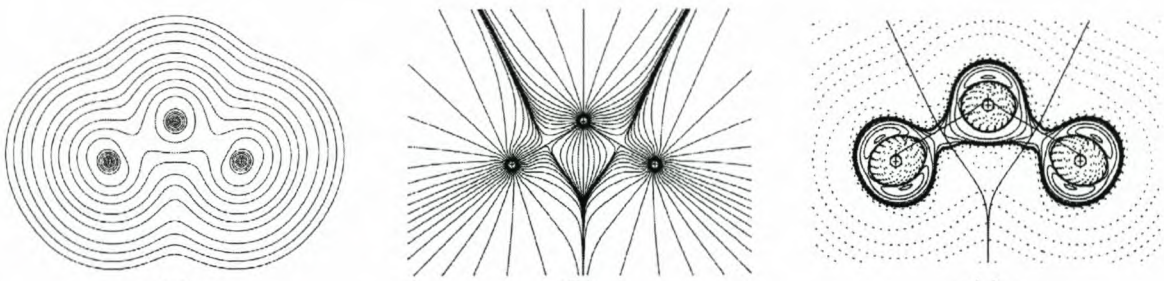

(a) (b) (c)

Figure 4.1 (a) A contour plot of the electron density, $\rho(\mathbf{r})$, in the molecular plane of ozone; (b) The gradient vector field of the electron density in the molecular plane. Each set of lines originating at infinity and terminating at a nucleus defines the atomic basin of that nucleus. The set of unique paths connecting the nuclei, the bond paths, are also shown; (c) A contour plot of the Laplacian of the electron density, $\nabla^2\rho(\mathbf{r})$, in the molecular plane. Solid lines indicate areas of charge concentration, where $\nabla^2\rho(\mathbf{r}) < 0$; dotted lines indicate areas of charge depletion, where $\nabla^2\rho(\mathbf{r}) > 0$. The unique set of gradient paths defining the zero-flux surfaces is also shown.

The total value of the electron density can be obtained for each of the atomic basins shown in **figure 4.1b** by integration over the three-dimensional volume enclosed by the zero-flux surface. If the nuclear charge of the particular atom is added to the total negative charge obtained through integration, atomic partial charges become available. PROAIMV calculated the total number of electrons located within the terminal oxygen to be 8.105 e and within the central oxygen, 7.793 e. This implies an atomic partial charge of -0.105 e on the terminal oxygens and +0.207 e on the central oxygen. The natural populations calculated by NBO analysis were 8.137 e on the terminal oxygens and 7.726 e on the central oxygen, resulting in atomic charges of -0.137 e on the terminal oxygens and +0.274 e on the central oxygen. The Mulliken charges on the terminal and central oxygens are -0.116 e and 0.231 e respectively.

The O-O bonds can be characterized by looking at the values of $\nabla^2\rho(r)$ as well as the total energy density defined by Cremer and Kraka (1984) at the bond critical point. The value of the Laplacian at the bond critical point is -0.314416 e $Bohr^{-5}$. This indicates a charge concentration on the bond critical point which implies a shared electron covalent open-shell interaction. The total energy density, H_b is -0.5130 Hartree $Bohr^{-1}$. According to Cremer and Kraka (1984) this is an indication that an open-shell covalent interaction is taking place. As expected the bonds are thus characterized as covalent bonds by AIM techniques.

4.3 The Electronic Structure and Bonding of $M(CO)_mH_n(O_3)$

4.3.1 Atoms in Molecules Analysis

The wave functions were generated for the minimum energy structures as described in **Chapter 3** with the B3LYP combination of functionals and the Los Alamos pseudo potentials for the transition metals and the 6-31G(d) basis set for the organic atoms.

Figure 4.2 shows the contour line diagrams for the complexes. For the calculation of the bond paths only the critical points associated with the ozone bonds, the ozone-metal bonds and the ring critical point were taken into account. The zero-flux surfaces were likewise calculated as two descending paths only from the critical points within and around the ozone ligand. An exception is the $Ni(CO)_2(O_3)$ complex. This complex is completely planar in form, and, therefore, the AIM analysis on it could conveniently be done for all the atoms. Information about the electron density and other relevant data is given in **table 4.1**. Calculating the partial atomic charges by integration using PROMEGA gave rise to errors due to (3,-3) and (3,1) critical points in the electron density found in the metal atomic basin. This problem was overcome by clearly specifying the relevant critical points using the PROAIM algorithm which uses critical points as input to determine the atomic basin and not the PROMEGA algorithm which determines the atomic basin from scratch. The results are shown in **table 4.2**. A test calculation was done with the chromium complex by calculating a full electron wave function, using the full electron basis set of Wachters (1970) on the metal centre. This set is a $(14s,11p,6d,3f) \rightarrow [8s,6p,4d,1f]$ contraction, contracted (6,2,1,1,1,1,1,1/3,3,1,2,1,1/3,1,1,1/3). The 6-31G(d) basis set was used for the other atoms. The critical points found using the ECP basis set vanished when the full electron

set was used, however, the location of the remaining critical points did not vary from those calculated with the ECP set. Most importantly however the values of the electron density,

Table 4.1 The electron density $\rho(\mathbf{r_b})$, Laplacian of the electron density $\nabla^2\rho(\mathbf{r_b})$, and the total energy density $H(\mathbf{r_b})$ at the bond critical points of the bound ozone ligand. Electron density is in e Bohr^{-3}, the Laplacian in e Bohr^{-5} and the energy density in Hartree Bohr^{-1}.

Complex	$Ti(CO)_5(O_3)$	$V(CO)_4H(O_3)$	$Cr(CO)_4(O_3)$	$Mn(CO)_3H(O_3)$
$\rho(\mathbf{r_b})_{1\text{-}3}$	0.3273	0.3300	0.3351	0.3497
$\rho(\mathbf{r_b})_{2\text{-}3}$	0.3283	0.3300	0.3351	0.3500
$\rho(\mathbf{r_b})_{1\text{-}M}$	0.0929	0.1131	0.1197	0.1187
$\rho(\mathbf{r_b})_{2\text{-}M}$	0.0953	0.1131	0.1197	0.1194
$\nabla^2\rho(\mathbf{r_b})_{1\text{-}3}$	-0.1217	-0.1354	-0.1326	-0.1625
$\nabla^2\rho(\mathbf{r_b})_{2\text{-}3}$	-0.1244	-0.1355	-0.1326	-0.1633
$\nabla^2\rho(\mathbf{r_b})_{1\text{-}M}$	0.4914	0.5796	0.6006	0.6489
$\nabla^2\rho(\mathbf{r_b})_{2\text{-}M}$	0.5349	0.5796	0.6006	0.6515
$\mathbf{H(r_b)_{1\text{-}3}}$	-0.2957	-0.3001	-0.3081	-0.3320
$\mathbf{H(r_b)_{2\text{-}3}}$	-0.2973	-0.3001	-0.3082	-0.3324
$\mathbf{H(r_b)_{1\text{-}M}}$	-0.0012	-0.0188	-0.0323	-0.0336
$\mathbf{H(r_b)_{2\text{-}M}}$	-0.0015	-0.0188	-0.0323	-0.0341
Complex	$Fe(CO)_3(O_3)$	$Co(CO)_2H(O_3)$	$Ni(CO)_2(O_3)$	$Cu(CO)H(O_3)$
$\rho(\mathbf{r_b})_{1\text{-}3}$	0.3267	0.3169	0.2876	0.3985
$\rho(\mathbf{r_b})_{2\text{-}3}$	0.3271	0.3168	0.2877	0.3986
$\rho(\mathbf{r_b})_{1\text{-}M}$	0.1286	0.1361	0.1389	0.06106
$\rho(\mathbf{r_b})_{2\text{-}M}$	0.1287	0.1360	0.1389	0.06098
$\nabla^2\rho(\mathbf{r_b})_{1\text{-}3}$	-0.1209	-0.1026	-0.0440	-0.2288
$\nabla^2\rho(\mathbf{r_b})_{2\text{-}3}$	-0.1213	-0.1024	-0.0441	-0.2289
$\nabla^2\rho(\mathbf{r_b})_{1\text{-}M}$	0.6700	0.7117	0.6967	0.4437
$\nabla^2\rho(\mathbf{r_b})_{2\text{-}M}$	0.6710	0.7109	0.6967	0.4429
$\mathbf{H(r_b)_{1\text{-}3}}$	-0.2952	-0.2792	-0.2330	-0.4126
$\mathbf{H(r_b)_{2\text{-}3}}$	-0.2955	-0.2791	-0.2330	-0.4127
$\mathbf{H(r_b)_{1\text{-}M}}$	-0.0438	-0.0480	-0.0460	0.0089
$\mathbf{H(r_b)_{2\text{-}M}}$	-0.0439	-0.0479	-0.0460	0.0089

The metals are labelled M, the oxygens are labelled 1 for O_1 and 2 for O_2 9the terminal oxygens) and 3 for O_3, the central oxygen.

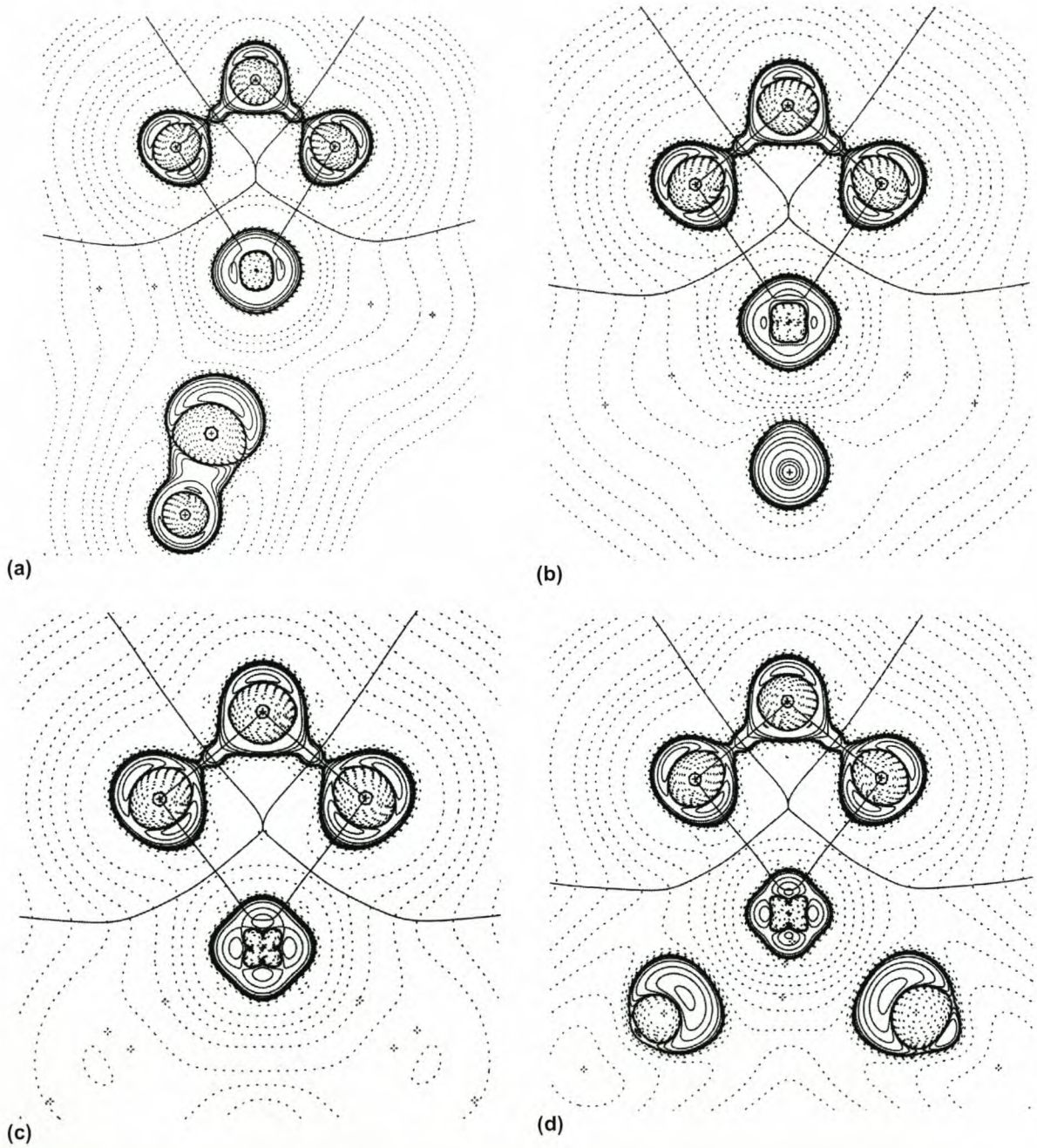

Figure 4.2 Contour plots of the Laplacian of the electron density, $\nabla^2\rho(\mathbf{r})$ in the plane of the ozone ligand for (a) $Ti(CO)_5(O_3)$, (b) $V(CO)_4H(O_3)$, (c) $Cr(CO)_4(O_3)$ and (d) $Mn(CO)_3H(O_3)$. Solid lines indicate areas of charge concentration where $\nabla^2\rho(\mathbf{r}) < 0$; dotted lines indicate areas of charge depletion where $\nabla^2\rho(\mathbf{r}) > 0$. The bond paths and interatomic surfaces *for the ozone part of the complexes* are also shown.

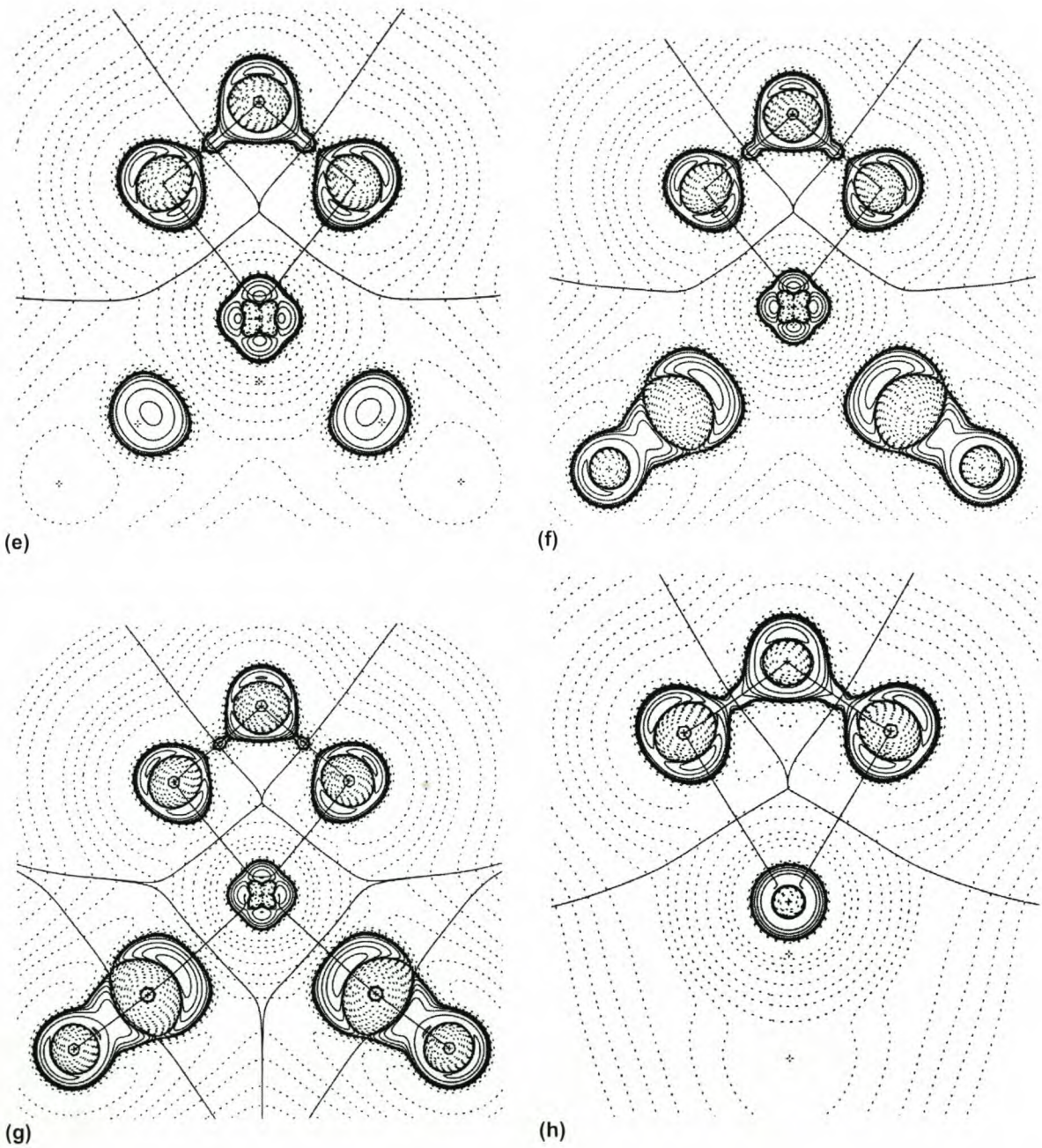

Figure 4.2 (continued) (e) $Fe(CO)_3(O_3)$, (f) $Co(CO)_2H(O_3)$, (g) $Ni(CO)_2(O_3)$ and (h) $Cu(CO)_2H(O_3)$. Since all the atoms of the nickel complex are in the same plane this complex was analyzed more thoroughly and the interatomic surfaces and bond paths for *all* the atoms are shown.

Laplacian and energy density varied by less than 0.002 in their respective units indicating that the quality of the ECP wave functions was sufficient. A complete discussion of the properties that can be derived from the AIM analysis of each of the complexes follows. (cf. **fig. 4.2**, **table 4.1** and **table 4.2**)

From the line diagrams of the Laplacian it can be seen that the electron density does show a very slight deformation around the terminal oxygens in the direction of the metal atom along the bond path. The deformation however is not very large. Frenking and Pidun (1997) have noted that a marked distortion of the ligand Laplacian distribution may indicate covalent bonding. A distribution that changes little from the free ligand to the bound ligand should be an indication of non-covalent interaction - in metal complexes, donor-acceptor interaction.

The asymmetric nature of the ozone part of the $Ti(CO)_5(O_3)$ complex is reflected in the electron density of the relevant bond critical points (bcp's). The shorter bond shows a smaller $\rho(\mathbf{r}_b)$ compared to the longer bond (0.0929 e $Bohr^{-3}$ compared to 0.0953 e $Bohr^{-3}$). All other complexes have electron densities at the ozone bcp's which reflect their symmetric nature. The values of $\rho(\mathbf{r}_b)$ at the metal-ozone bcp's increases from the titanium complex to the chromium complex, the manganese complexes having similar $\rho(\mathbf{r}_b)$ values to the chromium complex. The values then increase further until a sharp decline for the copper complex. Bonding of the ligand to the metal should lead to a decrease in the electron density available for the ozone interatomic bonds, which is the observed behaviour. The values decrease from 0.4532 e $Bohr^{-3}$ for unbound ozone to between 0.3985 e $Bohr^{-3}$ and 0.2876 e $Bohr^{-3}$ for the bound ozone. Although the $\rho(\mathbf{r}_b)$ values cannot be compared significantly within the series, it is observed that the complex with the lowest $\rho(\mathbf{r}_b)$ at the metal-ozone bcp's shows the highest value of $\rho(\mathbf{r}_b)$ at the ozone bcp's and the complex with the highest $\rho(\mathbf{r}_b)$ value at the metal-ozone bcp's has the lowest value of $\rho(\mathbf{r}_b)$ at the ozone bcp's. These two complexes are $Cu(CO)H(O_3)$ and $Ni(CO)_2(O_3)$ respectively. This is an expected result since a decrease in electron density on the ozone ligand should make more electron density available for the metal-ozone bonds.

Looking at the atomic charges, AIM calculated an atomic charge on the metals which is very high. For the calculation the metal zero-flux surfaces were determined following the gradient paths descending from the bcp's surrounding the metal plus the ring critical point (see **fig. 4.2g** for an example of this). To determine whether this was a problem arising from the use of ECP basis sets the integration was also done with the full electron test wave function of the

chromium complex. The metal charge however remained high. A positive charge of 1.4133 e was calculated for the chromium atom. A further discussion of the charges follows in **section 4.3.3**. Once again the asymmetric nature of $Ti(CO)_5(O_3)$ is portrayed by the charges that are not symmetric. The bound ozone shows a near-zero charge on the central oxygen, with large negative charges in the region of -0.4 e on the terminal oxygens. This picture differs from the unbound ozone in the sense that the ozone ligand now has an overall negative charge which seems to be localized on the terminal oxygens of the ligand. The unbound ozone shows terminal oxygens which are much more electronegative and a central oxygen that has an electron deficiency. This picture is the same with the bound ozone, except that the molecule has gained more charge which has been distributed in the same fashion as in the unbound molecule. This is analogous to the O_2-metal bond in which O_2^- or O_2^{2-} is formally created from the metal. It may also be a consequence of back donation. A very large charge separation such as observed here might also indicate a degree of ionic bonding present (Bytheway et al., 1996).

Table 4.2 Partial atomic charges determined by integration of the electron density over the atomic basin. Charges are given in e.

Complex	$Ti(CO)_5(O_3)$	$V(CO)_4H(O_3)$	$Cr(CO)_4(O_3)$	$Mn(CO)_3H(O_3)$
q(M)	1.6836	1.5353	1.2952	1.1460
$q(O_1)$	-0.4647	-0.4501	-0.4182	-0.3819
$q(O_2)$	-0.4946	-0.4501	-0.4182	-0.3816
$q(O_3)$	-0.0070	-0.0003	0.0114	0.0414
Complex	$Fe(CO)_3(O_3)$	$Co(CO)_2H(O_3)$	$Ni(CO)_2(O_3)$	$Cu(CO)H(O_3)$
q(M)	1.0885	1.0047	1.0092	0.8200
$q(O_1)$	-0.4228	-0.4176	-0.4533	-0.3186
$q(O_2)$	-0.4228	-0.4177	-0.4534	-0.3183
$q(O_3)$	0.0026	-0.0014	-0.0439	0.1263

The metals are labelled M, the terminal oxygens are O_1 and O_2 and the central oxygen O_3.

The most significant result which can be deduced from the AIM analysis however is the type of bonding present. As mentioned the values of the Laplacian and the energy densities can be used to conclude the bonding type. All the complexes have energy densities at the metal-ozone bond which are positive or near-zero, indicating that non-covalent interactions are present. This result is supported by the values of the Laplacian of the electron density, which are all positive,

indicating that there is a local charge depletion at the bcp. For non-covalent bonds in which an electron pair is donated into an empty orbital, it is expected that the charge concentration be slightly towards the accepting atom. The ozone bcp's all show energy densities which are clearly negative. Once again this result is supported by the Laplacian values which are also negative and therefore indicate a local charge concentration in the region where the electrons from a covalent bond are shared.

A comparison was made between the average values of $\rho(\mathbf{r_b})$ between the two ozone-metal bcp's and the dissociation energies of the complexes. The results are shown in **figure 4.3**

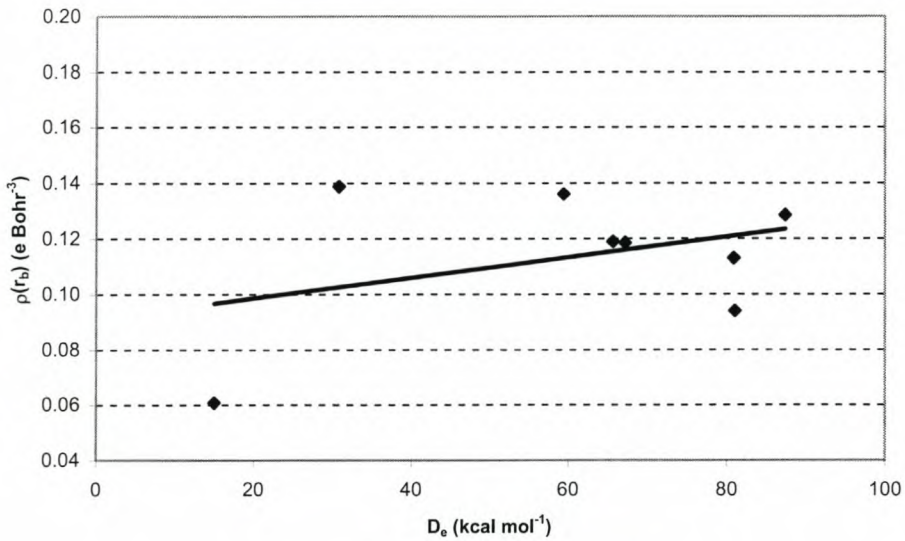

	Average $\rho(r_b)$	D_e
$Ti(CO)_5(O_3)$	0.0941	81.0
$V(CO)_4H(O_3)$	0.1131	80.9
$Cr(CO)_4(O_3)$	0.1191	65.7
$Mn(CO)_3H(O_3)$	0.1187	72.9
$Fe(CO)_3(O_3)$	0.1286	91.5
$Co(CO)_2H(O_3)$	0.1361	59.4
$Ni(CO)_2(O_3)$	0.1389	30.9
$Cu(CO)H(O_3)$	0.0610	15.0

Figure 4.3 The average $\rho(\mathbf{r_b})$ values between the two metal-ozone bcp's for $M(CO)_mH_n(O_3)$, M = Ti, ..., Cu plotted versus dissociation energy. Energy in kcal mol^{-1}, $\rho(\mathbf{r_b})$ in e $Bohr^{-3}$.

A linear correlation was made between the values that resulted in a poor fit with a R^2 value of 0.1339. The poor correlation may be explained by the fact that the calculated D_e values are relative to the *lowest energy singlet states* of the metal fragments, which may not necessarily be

the *lowest energy ground states*. If the D_e values were calculated relative to the ground states of the fragments the trend might change. The electron density at the bcp is indicative of the amount of charge accumulating in the bonding region which is not influenced in any degree by the spin states of one or other of the respective fragments. It therefore remains difficult to compare relative bond strengths as given by D_e values with "absolute" ones as given by the electron density.

4.3.2 Charge Decomposition Analysis

The Charge Decomposition Analysis considers orbital mixing to determine the amount of donation through σ orbitals from a ligand to a metal and the amount of back donation from the metal to the ligand through π orbitals. A theoretical background of the method and the Dewar-Chatt-Duncanson (DCD) model is given in **chapter 2**. Frenking and Pidun (1997) and Ehlers et al. (1996) have shown that CDA analysis can be used as a quantitative expression of the DCD model of σ-donation and π-back donation.

Table 4.3 CDA results in terms of donation *d*, back donation *b*, repulsive polarization, *r* and the rest term, Δ. Units are e.

Complex	$Ti(CO)_5(O_3)$	$V(CO)_4H(O_3)$	$Cr(CO)_4(O_3)$	$Mn(CO)_3H(O_3)$
d	0.462	0.477	0.440	0.237
b	0.188	0.192	0.147	-0.012
r	-0.395	-0.421	-0.328	-0.113
Δ	0.021	0.014	0.077	0.230
Complex	$Fe(CO)_3(O_3)$	$Co(CO)_2H(O_3)$	$Ni(CO)_2(O_3)$	$Cu(CO)H(O_3)$
d	0.494	0.305	0.331	0.353
b	0.159	-0.012	-0.020	0.107
r	-0.353	-0.065	-0.042	-0.157
Δ	0.034	0.204	0.173	0.005

The CDA software uses three separate output files used generated by *Gaussian98*. The first file contains the molecular orbitals of the whole complex, the second file contains the molecular orbitals of the donating fragment and the third file the molecular orbitals of the

accepting fragment. The coordinates of the atoms are taken from the minimised energy geometries.

Table 4.3 gives the values of the total donation, back donation, repulsive polarization and the rest term calculated for the complexes. According to the CDA analysis the bonding in $Ti(CO)_5(O_3)$, $V(CO)_4H(O_3)$, $Cr(CO)_4(O_3)$, $Fe(CO)_3(O_3)$ and $Cu(CO)H(O_3)$ can be interpreted according to the DCD model. All these complexes show positive values for the donation and back donation and very small rest terms. $Mn(CO)_3H(O_3)$, $Co(CO)_2H(O_3)$ and $Ni(CO)_2(O_3)$ have large values for the donation term, *but* negative values for the back donation and rest terms that differ to some extent from zero. The back donation however may be negative but in actual fact is *less* than the numerical value of the rest term for the DCD complexes and may, therefore, be regarded as negligible. The rest term, which represents the overlap of empty ligand orbitals with empty metal orbitals, however is still quite large. This term indicates that the overlap of the unoccupied metal orbitals and the unoccupied ligand orbitals contribute significantly to the overall charge interaction. This means that the bond formation involves the promotion of an electron from the ground state to the excited state of one or both of the fragments and that normal covalent bonds between two open shell fragments are present. The bond formation can in principle also be between a *doubly excited* closed shell fragment and a ground state fragment, which might seem reasonable considering the nature of the ground state of ozone which does contain a doubly excited configuration.

Analysis of the orbitals contributing to the different overlapping terms can clarify this situation. The orbitals that are involved in the positive residual terms are shown in **figure 4.4**, they are MO 40 for $Mn(CO)_3H(O_3)$ and MO 35 for both $Co(CO)_2H(O_3)$ and $Ni(CO)_2(O_3)$. These orbitals are the HOMO-1 for the Mn complex and the HOMO for the Co and Ni complexes. It can be seen that molecular orbital fragments which are centred on the oxygen atoms and forms bonding combinations with the metal orbitals bear a resemblance to the $2b_1$ orbital of free ozone. This ozone orbital becomes doubly occupied in the $[core]1a_2^2 4b_2^2 6a_1^0 2b_1^2$ doubly excited configuration which forms part of the ground state (see **section 3.2.1**). The apparent contradictory results of the CDA compared to the AIM predictions in terms of the bonding type can thus be partly clarified by the intricate nature of the ground state electron configuration of ozone.

Further discussions are based on the complexes that showed pure DCD behaviour. **Table 4.4** lists the orbitals which contribute most to the different terms and **figure 4.5** shows some of

the orbitals that are involved in the donation and back donation. The complete list of contributing orbitals as displayed in the output generated by CDA 2.1.2 is given in **addendum B**.

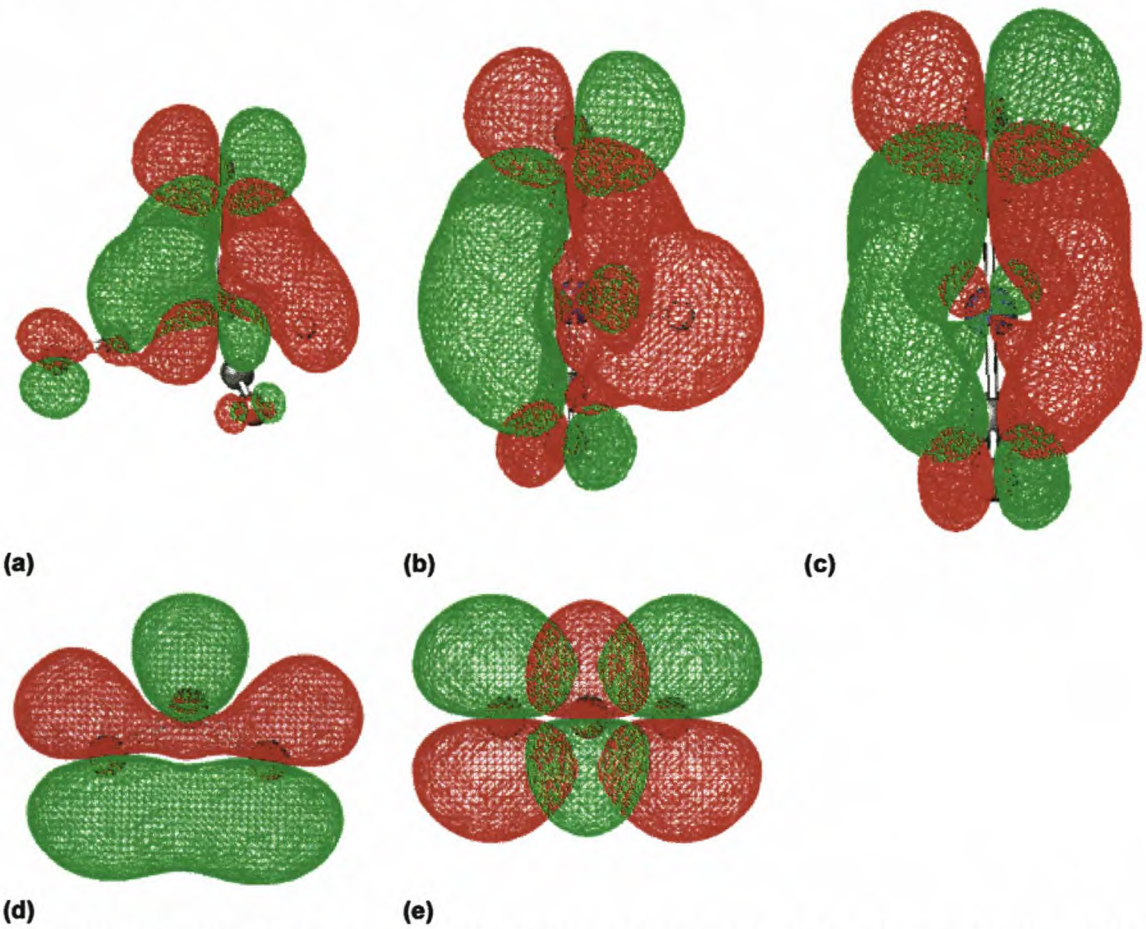

Figure 4.4 The molecular orbitals of the (a) $Mn(CO)_3H(O_3)$, the (b) $Co(CO)_2H(O_3)$ and the (c) $Ni(CO)_2(O_3)$ complexes that are involved in the positive residual term generated by CDA. The ozone molecular plane is orientated perpendicular to the plane of the paper. For reference the (d) $6a_1$ and (e) $2b_1$ orbitals of ozone are also shown.

For $Ti(CO)_5(O_3)$ the orbitals shown for the donation are MO 49, MO 50 and MO 51. They are the dominant orbitals in the partitioning scheme, donating respectively 0.114, 0.124 and 0.124 e. MO 49 constitutes the donation of 0.114 electrons from the $6a_1$ MO of ozone into the d_{z2} orbital of the metal. MO 50 shows donation of 0.124 electrons from the $4b_2$ MO of ozone into the d_{xz} orbital of the metal. MO 51 that is responsible for the donation of 0.124 electrons appears to be a combination of ozone and metal orbitals that do not appear to be involved in any bonding interaction. The overlap from these orbitals thus remains unexplained. The dominant orbital in the back donation partitioning is MO 52. This is the same orbital in the large amount of

unoccupied-unoccupied overlap for the complexes that do not show pure DCD behaviour. In the case of $Ti(CO)_5(O_3)$ 0.203 e is being back donated from the metal d_{yz} orbital into the $2b_1$ π^* orbital of ozone.

Table 4.4 Dominant MO contributions to the donation *d*, back donation *b*, repulsive polarization, *r* and the rest term, Δ.

Molecule	MO	*d*	*b*
$Ti(CO)_5(O_3)$	49	0.114	
	50	0.124	
	51	0.124	
	52		0.203
$V(CO)_4H(O_3)$	27	0.104	
	42	0.080	
	43	0.122	
	45	0.078	
	46		0.230
$Cr(CO)_4(O_3)$	27	0.087	
	42	0.083	
	43	0.110	
	46		0.164
$Fe(CO)_3(O_3)$	19	0.062	
	23	0.130	
	35	0.070	
	37	0.115	
	41		0.146
$Cu(CO)H(O_3)$	13	0.043	
	15	0.047	
	26	0.072	
	29	0.056	0.104

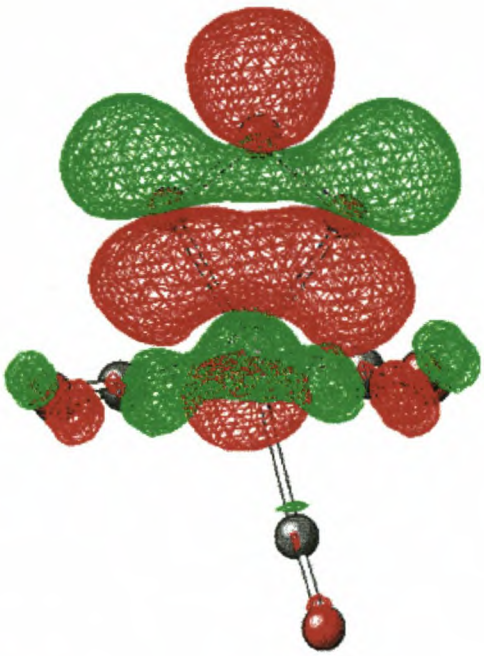

(a) MO 49

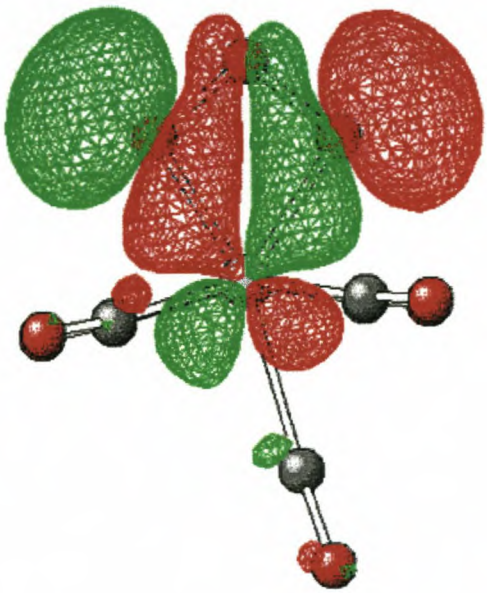

(b) MO 50

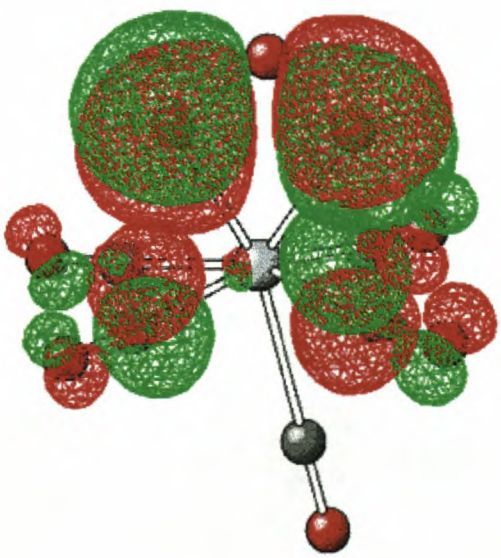

(c) MO 51

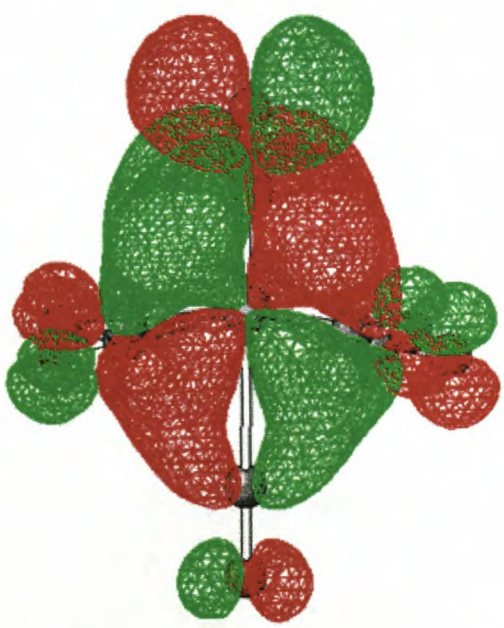

(d) MO 52

Figure 4.5 Schematic representations of some of the orbitals involved in the donation (a)-(c) and back donation (d) of the ozone-titanium bond in $Ti(CO)_5(O_3)$.

(a) MO 27

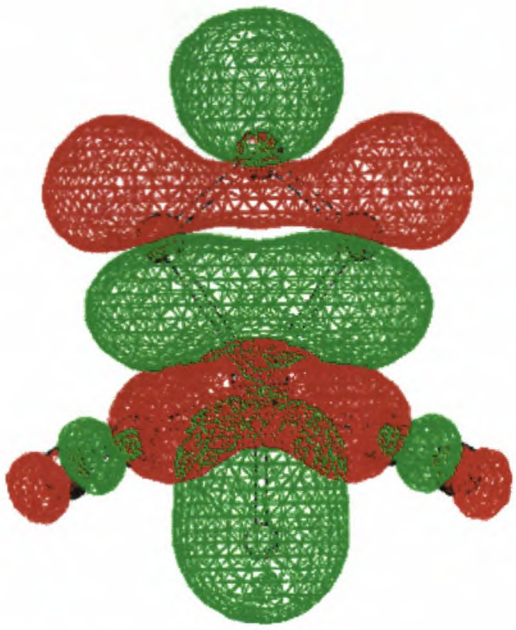

(b) MO 42

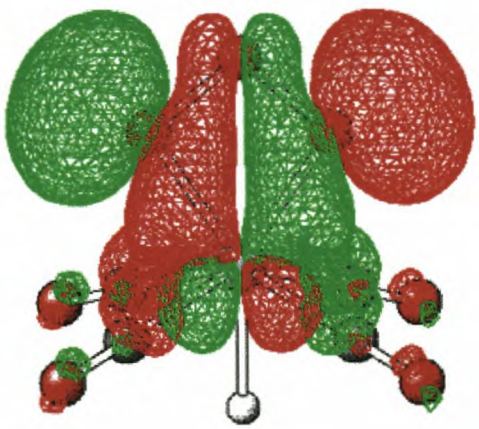

(c) MO 43

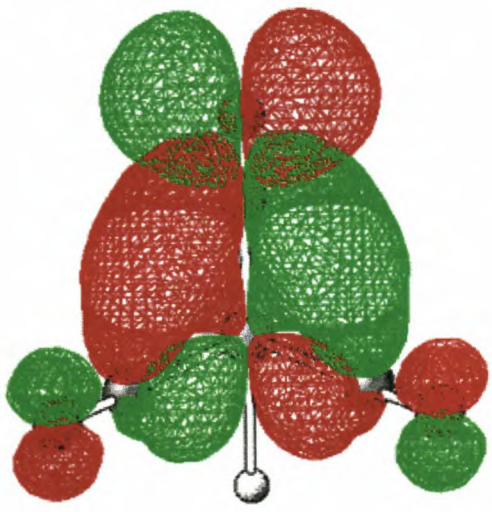

(d) MO 46

Figure 4.5 (continued) Schematic representations of some of the orbitals involved in the donation (a)-(c) and back donation (d) of the ozone-vanadium bond in $V(CO)_4H(O_3)$.

(a) MO 27

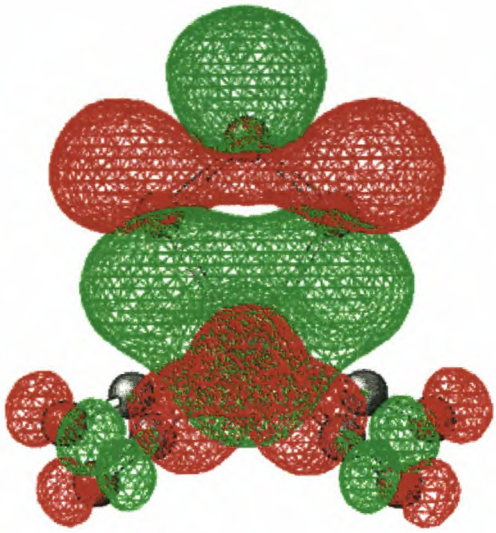

(b) MO 42

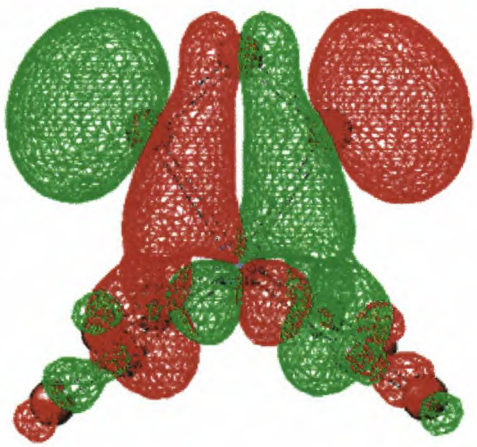

(c) MO 43

(d) MO 46

Figure 4.5 (continued) Schematic representations of some of the orbitals involved in the donation (a)-(c) and back donation (d) of the ozone-chromium bond in $Cr(CO)_4(O_3)$.

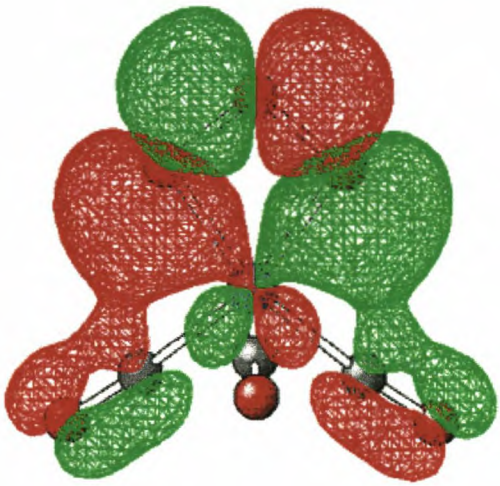

(a) MO 23

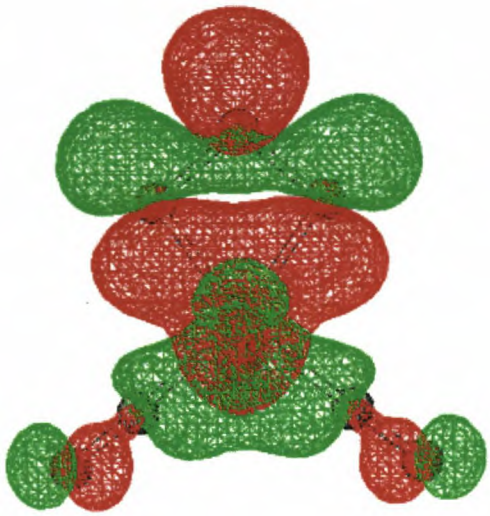

(b) MO 35

(c) MO 37

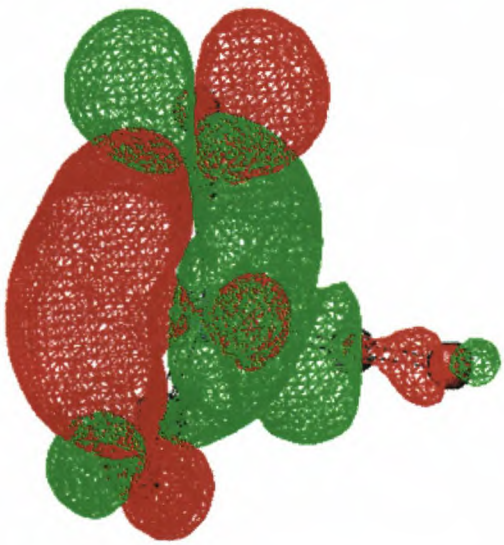

(d) MO 41

Figure 4.5 (continued) Schematic representations of some of the orbitals involved in the donation (a)-(c) and back donation (d) of the ozone-iron bond in $Fe(CO)_3(O_3)$.

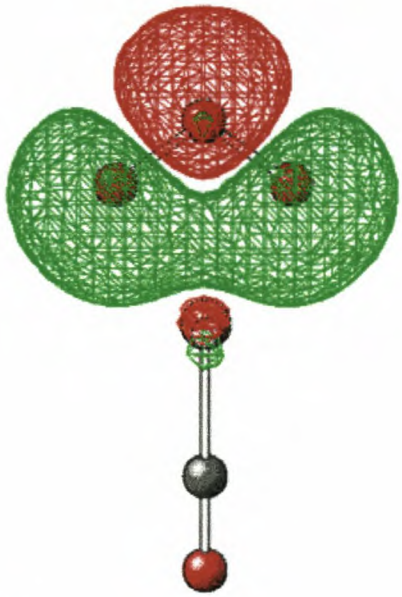

(a) MO 13

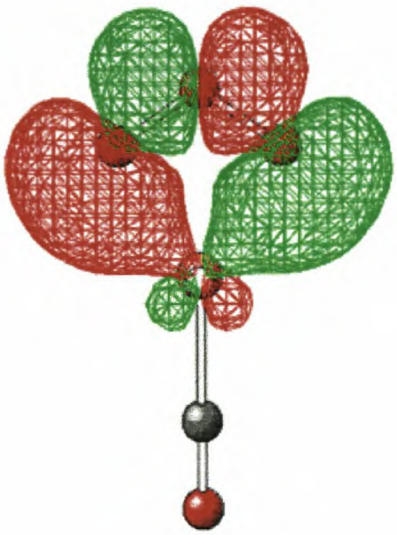

(b) MO 15

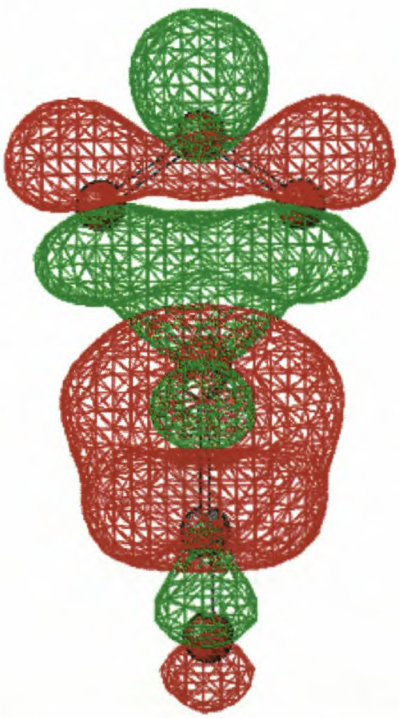

(c) MO 26

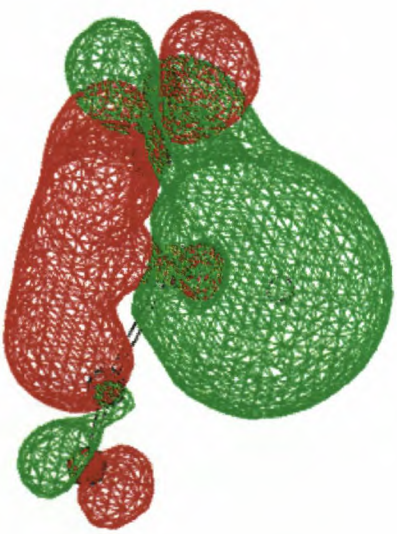

(d) MO 29

Figure 4.5 (continued) Schematic representations of some of the orbitals involved in the donation (a)-(c) and back donation (d) of the ozone-copper bond in $Cu(CO)H(O_3)$.

For the next three complexes, $V(CO)_4H(O_3)$, $Cr(CO)_4(O_3)$ and $Fe(CO)_3(O_3)$, the orbitals in the donation-back donation scheme all have the same shape, and hence, they will be discussed simultaneously. The orbitals listed in **table 4.4** for the donation in the vanadium complex can be considered dominant, but for the chromium and iron complexes the contributions to the terms are spread over a wider range of orbitals and only the three/four highest donating orbitals are given. In **figure 4.5** only the highest three orbitals are shown. It can be seen that the first type (MO 27 for $V(CO)_4H(O_3)$ and $Cr(CO)_4(O_3)$ and MO 23 for $Fe(CO)_3(O_3)$) consists of the $3b_2$ (MO 8) orbital of the ozone ligand donating respectively 0.104, 0.087 and 0.130 e into the d_{xz} orbital of the metal. The second MO's (MO 42 for $V(CO)_4H(O_3)$ and $Cr(CO)_4(O_3)$ and MO 35 for $Fe(CO)_3(O_3)$) consists of the $6a_1$ (MO 12) orbital of ozone donating respectively 0.080, 0.083 and 0.070 e into the d_{z2} orbital of the metal. The last set of MO's (MO 43 for $V(CO)_4H(O_3)$ and $Cr(CO)_4(O_3)$ and MO 37 for $Fe(CO)_3(O_3)$) shows the donation of 0.122, 0.110 and 0.115 e also into the d_{xz} metal orbital. The dominant back donation orbitals (MO 46 for $V(CO)_4H(O_3)$ and $Cr(CO)_4(O_3)$ and MO 41 for $Fe(CO)_3(O_3)$) shows back donation of 0.230, 0.164 and 0.146 e from the d_{yz} orbital of the metal into the π^* $2b_1$ orbital of the ozone.

In the case of the copper complex the diagram seems to suggest that MO 13 is not involved in ozone-metal interaction. MO 15 shows donation of 0.047 electrons into the d_{xz} orbital and MO 26 shows 0.072 electrons being donated into the d_{z2} orbital. It is interesting to note that MO 29 shows large contributions to *both* donation *and* back donation terms. The MO is indicative of the same form of behaviour as the other back donation MO's described.

Pidun and Frenking, 1996, have demonstrated that the CDA can also be used to elucidate information about the amount of electron pairs involved in the donation-back donation between acetylene and the metal in $WCl_5(HCCH)^-$ and $W(CO)_5(HCCH)$. The range of orbitals involved in the scheme for the ozone complexes makes such determinations for this example inaccurate. The observation that the majority donation occurs into *two* orbitals (d_{z2} and d_{xz}), however, hints that ozone acts as a four electron donor.

Once again, a comparison was made between the results of the CDA with the dissociation energies. The amount of charge donated was used as an indicator of the bond strength and the *d* values were compared with the D_e values. The results are shown in **figure 4.6**. The AIM calculated electron densities showed no correlation with D_e due to the relative nature of the dissociation energies. In the case of the CDA the donation and back donation terms are calculated

relative to *the same spin states* as the dissociation energies. Also due to the large residual terms calculated for the Mn, Co and Ni complexes indicating that the CDA method does not describe the bonding in these species accurately, they were omitted from the correlation (these values are shown with solid triangles in **fig. 4.6**). A linear fit with a R^2 value of 0.9796 was obtained.

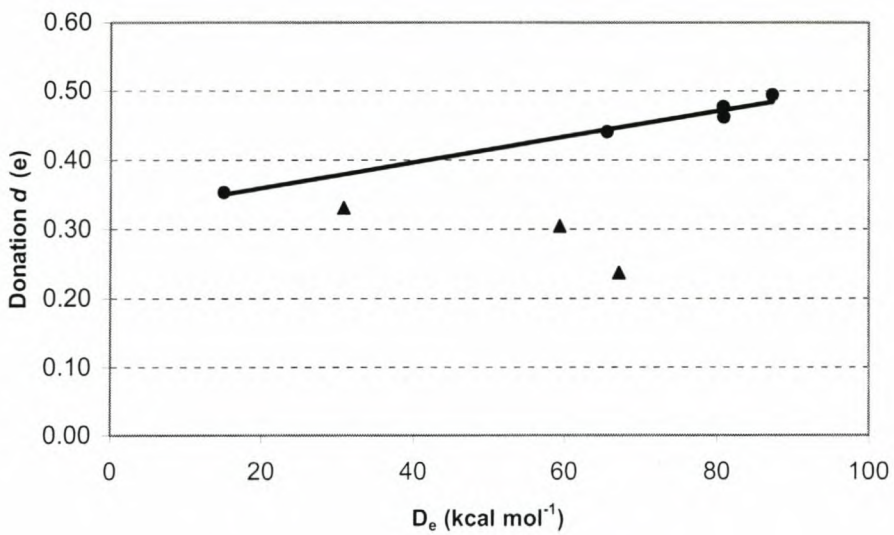

	Donation *d*	D_e
$Ti(CO)_5(O_3)$	0.462	81.0
$V(CO)_4H(O_3)$	0.477	80.9
$Cr(CO)_4(O_3)$	0.440	65.7
$Mn(CO)_3H(O_3)$	0.237	72.9
$Fe(CO)_3(O_3)$	0.494	91.5
$Co(CO)_2H(O_3)$	0.305	59.4
$Ni(CO)_2(O_3)$	0.331	30.9
$Cu(CO)H(O_3)$	0.353	15.0

Figure 4.6 The CDA calculated donation for $M(CO)_mH_n(O_3)$, M = Ti, ..., Cu plotted versus dissociation energy. Energy in kcal/mol, donation in e.

4.3.3 Natural Bond Orbital Analysis

The partial atomic charges were calculated using the NBO method and can be compared with the values obtained by the Mulliken population analysis as well as the values obtained through integration over the respective atom basins (**table 4.5**). The AIM method calculated very large positive metal charges, the Mulliken scheme calculated values that were positive but much lower in magitude than the AIM method. The NBO method found values ranging from negatively

charged to positively charged. The trend observed for the ozone oxygen atoms is the same according to all the methods, the terminal oxygens are negatively charged with the central oxygen having either small positive or small negative values. Charges of -0.1369 e on the terminal oxygens and 0.2739 e on the central oxygen were calculated for free ozone.

Table 4.5 The atomic partial charges on the ozone oxygens and metal atoms, calculated with the NBO method and by Mulliken population analysis. The total ozone charge is also given (*cf.* **table 4.2**). Charges are given in e.

	Complex	$Ti(CO)_5(O_3)$	$V(CO)_4H(O_3)$	$Cr(CO)_4(O_3)$	$Mn(CO)_3H(O_3)$
NBO	**q(M)**	-0.3170	-0.6079	-0.4635	-0.3116
	q(O_1)	-0.3140	-0.2665	-0.2532	-0.2405
	q(O_2)	-0.3344	-0.2665	-0.2532	-0.2391
	q(O_3)	0.0554	0.0539	0.0664	0.1043
	q(ozone)	-0.5931	-0.4791	-0.4401	-0.3753
Mulliken	**q(M)**	0.2519	0.0123	0.2191	0.1405
	q(O_1)	-0.3520	-0.3345	-0.3127	-0.2837
	q(O_2)	-0.3839	-0.3345	-0.3127	-0.2837
	q(O_3)	0.0321	0.0385	0.0513	0.0812
	Complex	$Fe(CO)_3(O_3)$	$Co(CO)_2H(O_3)$	$Ni(CO)_2(O_3)$	$Cu(CO)H(O_3)$
NBO	**q(M)**	0.0862	0.3955	0.7046	0.7986
	q(O_1)	-0.3250	-0.3448	-0.4260	-0.3364
	q(O_2)	-0.3248	-0.3448	-0.4261	-0.3363
	q(O_3)	0.0608	0.0543	0.0005	0.2168
	q(ozone)	-0.5890	-0.7237	-0.8517	-0.4559
Mulliken	**q(M)**	0.2096	0.1204	0.4250	0.1343
	q(O_1)	-0.3171	-0.3131	-0.3561	-0.2347
	q(O_2)	-0.3172	-0.3130	-0.3561	-0.2346
	q(O_3)	0.0399	0.0381	-0.0102	0.1787

The metals are labelled M, the terminal oxygens are labelled O_1 and O_2 and O_3 for the central oxygen.

The aim of the NBO method is to calculate the "best" localised set of orbitals for a structure. High occupancy of antibonding orbitals (BD^*) and low occupancy of bonding orbitals (BD's) or lone pairs (LP's) indicates a structure that is highly delocalised. This is the situation that is portrayed by the NBO analysis. High occupancy for BD's and LP's is defined as >1.90 e. High occupancy for antibonding orbitals is defined as anything larger than 0.1 e.

The NBO partitioning calculated a low occupancy (<1.90 e) BD between the Ti atom and one of the terminal oxygens together with a high occupancy antibonding orbital (BD*) occupied by 0.347 e but no other bonding orbitals between the two fragments. Between each of the terminal oxygens and the central oxygen a BD was calculated. Two LP's were calculated on the bonding oxygen, one having an occupancy of only 1.732 e. On the central oxygen two LP's were calculated, one having low occupancy. The other terminal oxygen was found to have three LP's of which two were occupied by less than 1.90 e. The vanadium complex, once again, showed BD between the ozone oxygens but no BD's between the ozone and metal. Two LP's were calculated for the central oxygen, one having low occupancy, and three for each of the terminal oxygens, once again with two of them being occupied by less than 1.7 e. The other orbitals of note are two BD*'s between the adjacent oxygens, each having an occupancy of 0.034 e. From chromium to cobalt the NBO results all had the same trend: a BD between each of the terminal oxygens and the central oxygen of the ozone, no BD's between the ozone and metal fragment, low occupancy second and third LP's on the terminal oxygens and two LP's on the central oxygen, with two relatively highly occupied BD*'s between the oxygens.

This picture of ozone differs from free ozone in that free ozone has BD's between the adjacent oxygens, two highly occupied LP's on each of the oxygens and a *highly* (>1.90 e) occupied BD* between the two terminal oxygens which can be linked with the excited ground state configuration of ozone. There is also a low occupancy (0.635 e) BD between these two oxygens. For the chromium, manganese, iron and cobalt complexes localization of these π electrons when ozone is bound leads to the BD* and BD disappearing to form the two low occupancy LP's.

The nickel complex shows an interesting NBO partitioning. BD's are calculated between the Ni and terminal O's, with relatively low occupancies of < 1.80 e. Accompanying them are two BD*'s with occupancies of 0.375 e. The oxygens each have two LP's and there are four LP's on the metal, all highly occupied. No BD's are found between the carbonyl and the Ni.

For the copper complex a 1.605 e occupied BD is calculated between the Cu and H atom with a 0.234 e occupied BD*. No BD's are found between the CO and the Cu. The partitioning for the O_3 fragment surprisingly is similar to unbound ozone. The BD* orbital between the two terminal oxygens remains, as well as the BD. This partitioning, indicating an unchanged ozone

compared to the free ozone is reflected in the D_e values, with the copper complex having a D_e value of only 15.0 kcal mol^{-1}.

Throughout the scheme the carbonyl-metal bonds were explicitly partitioned into BD's, with high occupancy BD*'s. The exception is the copper complex which was partitioned as described above.

The NBO program also carries out second-order perturbation estimates of the donor-acceptor interactions in the NBO basis. All possible interactions between filled/donor/Lewis-type orbitals and empty/acceptor/non-Lewis-type orbitals are examined and their *energetic importance* estimated by second order perturbation theory.

$Ti(CO)_5(O_3)$ reveals large (10-60 kcal mol^{-1}) contributions due to delocalisation of the Ti-C BD's into the Ti-C BD*'s. Large values obtained for BD*-BD* and BD*-RY* (RY=Rydberg orbitals) are insignificant since these orbitals are not even approximately doubly occupied. The same observation indicative of a large degree of delocalisation in the M-CO system is made for the other complexes. Of note however are the delocalisations of the ozone LP's. Looking only at the systems in which no BD's were determined between the ozone and the metal large delocalisations were calculated between the LP's on the terminal oxygens and the M-C BD*'s. In each of these cases one of the three LP's on the terminal oxygens showed large values (between 50 and 120 kcal mol^{-1}) for delocalisation into M-C BD*'s or RY*'s.

The NBO method is thus unable to obtain a minimal Lewis basis for the systems due to the high degree of delocalisation present. This is perhaps best illustrated by the amount of charge that lies outside the Lewis space (the Lewis space being the orbitals contained in the minimal Lewis basis). For the complexes these values range between 1.337 e (for the nickel complex) and 3.089 e (for the vanadium complex). The non-Lewis space makes up between 1.6 % and 4.0 % of the total electronic population. An attempt was made to investigate the possibility of a different Lewis structure. This was done by explicitly assigning part of the Lewis structure, as explained in **Addendum B**. BD's were assigned between the metal and the carbons/hydrogens as well as between the metal and the terminal oxygens. Three BD's were assigned between each of the carbons and oxygens of the carbonyls. For the ozone BD's were assigned between the adjacent oxygens and two LP's on each of the oxygens. The NBO algorithm then proceeds to find a Lewis structure containing the assigned BD's and LP's and assigns the remaining electrons accordingly. This however did not improve the situation and only led to a *higher* occupancy of the non-Lewis

space. The Natural Atomic Orbitals (NAO's) and the Natural Population Analysis (NPA) are not affected by this and their values can be used without concern.

Chapter 5: Conclusion

The results of this work can be summarised as follows:

- Reviewing the literature on the modelling of ozone and specifically the calculation of the vibrational frequencies revealed that very high levels of theory such as CCSD(T) and large basis sets are needed to accurately calculate the vibrational modes. The biradical electronic configuration forming part of the ozone ground state is used in many quantum chemical texts (Jensen, 2001; Klapötke and Schultz, 1998) as example of RHF→UHF instabilities and great care has to be taken when deciding on a level of theory to model the molecule.
- Investigating the possible orientations of the ozone ligand for the MO_3^{2+}, M = [Ti, ..., Cu] series showed that for vanadium, chromium, iron and manganese a planar structure with coordination through the terminal oxygens is preferred. Titanium and cobalt preferred an out-of-plane structure. The cobalt structure is very similar to the in-plane structures with only a very small deviation from planarity. For both structures however the coordination still seemed to be through the terminal oxygens. Both nickel and copper showed complexes coordinated through only *one* of the terminal oxygens to be the lowest in energy. For this series the order of stability was $Mn^{2+} < Fe^{2+} < Cr^{2+} < Co^{2+} < Ni^{2+} < Ti^{2+} < V^{2+} < Cu^{2+}$.
- Enlarging the complexes by adding carbonyls and hydrogen ligands resulted in a completely different order of stability. For the $M(CO)_nH_m(O_3)$, M = [Ti, ..., Cu], n = [1, ..., 5], m = [0,1] series the complexes were built with the ozone ligand coordinating through the terminal oxygens in a planar geometry with regard to the ozone ligand and the metal. The basis set of Dunning and Huzinaga proved to deliver poor results with respect to the 6-31G(d) results and experimental ozone geometries. The order of stability for this series was Cu < Ni < Co < Cr < Mn < V < Ti < Fe. BSSE values were also calculated but proved to be small in comparison with the dissociation energies.
- The *Atoms in Molecules* technique for analysing the wave function produced atomic charges that were very high indicating possible ionic contributions to the bonding mechanism. The Mulliken and NPA charges however showed no sign of this behaviour. Bond critical points were found between the terminal oxygens and the

metal for each of the complexes, indicating that coordination *does indeed* occur through the terminal oxygens. The values of the Laplacian as well as the total energy densities at the bond critical points confirmed that the interactions are of donor-acceptor type.

- The *Charge Decomposition Analysis* could not calculate acceptable values for the charge donation, charge back donation and rest terms in the manganese, cobalt and nickel complexes indicating that describing the complexes as closed shell fragments fails and that donor-acceptor-type bonding is not relevant for the respective species. The failure of the CDA method to describe the above mentioned complexes could however be explained by investigating the molecular orbitals responsible for the erroneous back donation and rest terms. These showed that the biradical ground state of ozone and the inclusion of a doubly excited configuration in describing this ground state may be responsible for the failures. A linear relationship between the donation values for the complexes and the dissociation energies was obtained.
- The *Natural Bond Orbital* analysis of the complexes failed to calculate acceptable Lewis structures. This is due to the high degree of delocalisation present in the complexes, as illustrated by second order perturbation energy calculations. The atomic charges calculated with this method however are not affected by this.
- In future the challenge now remains for these complexes to be synthesised.

References

Adler-Golden, S. M., Langhoff, S. R., Bauschlicher Jr., C. W., Carney, G. D. (1985). *J. Chem. Phys.* **83**, 255.

Allen, H. H., Kennard, O. (1993). *Chemical Design Automation News*. **8**, 31.

Allinger, N. L., Yuh, Y. H., Lii, J-H. (1989). *J. Am. Chem. Soc.* **111**, 8551.

Allinger, N. L., Chen, K., Lii, J-H. (1996). *J. Comput. Chem.* **17**, 642.

Almlöf, J., Taylor, P. R. (1987). *J. Chem. Phys.* **86**, 4070.

Bader, R. F. W. (1990). Editor. *Atoms in Molecules. A Quantum Theory*. Oxford: Oxford University Press.

Bachrach, S. M. (1994). *Reviews in Computational Chemistry*, edited by K. B. Lipkowitz and D. B. Boyd, Vol. V, p. 171. New York: VCH.

Badger, R. M. (1934). *J. Chem. Phys.* **2**, 128.

Badger, R. M. (1935). *J. Chem. Phys.* **3**, 710.

Baerends, E. J., Branchadell, V., Sodupe, M. (1997). *Chem. Phys. Lett.* **265**, 481.

Bauernschmitt, R., Ahlrichs, R. (1996). *J. Chem. Phys.* **104**, 9047.

Becke, A. D. (1986). *J. Chem. Phys.* **84**, 4524.

Becke, A D. (1988). *Phys. Rev. A* **38**, 3098.

Becke, A. D. (1989). *Int. J. Quantum Chem., Quantum Chem. Symp.* **23**, 599

Becke, A. D. (1993a). *J. Chem. Phys.* **98**, 1372.

Becke, A. D. (1993b). *J. Chem. Phys.* **98**, 5648.

Biegler-König, F. W., Bader, R. F. W., Ting-Hau, T. (1982). *J. Comput. Chem.* **3**, 317.

Blanchet, C., Duarte, H. A., Salahub, D. R. (1997). *J. Chem. Phys.* **106**, 8778.

Born, M., Oppenheimer, J. R. (1927). *Ann. Physik.* **84**, 457.

Boys, S. F. (1950). *Proc. Roy. Soc (London).* **A200**, 542.

Boys, S.F., Bernardi, F. (1970). *Mol. Phys.* **19**, 553.

Brooks, R., Bruccoleri, R. E., Olafson, B. D., States, D. J., Swaminathan, S., Karplus, M. (1983). *J. Comput. Chem.* **4**, 187.

Burke, K., Perdew, J. P., Wang, Y. (1998). *Electronic Density Functional Theory, Recent Progress and New Directions*, edited by J. F. Dobson, G. Vignale and M. P. Das, p. 81. New York: Plenum Press.

Bytheway, I., Popelier, P. L. A., Gillespie, R. J. (1996). *Can. J. Chem.* **74**, 1059.

Chalasinski, G., Szczesniak, M. M. (1994). *Chem. Rev.* **94**, 1723.

Chatt, J., Duncanson, L. A. (1953). *J. Chem. Soc.* 2939.

Colmont, J-M., Demaison, J., Cosléou, J. (1995). *J. Mol. Spectrosc.* **171**, 453.

Cornell, W. D., Cieplak, P., Bayly, C. I., Gould, I. R., Merz Jr., K. M., Ferguson, D. M., Spellmeyer, D. C., Fox, T., Caldwell, J. W., Kollman, P. A. (1995). *J. Am. Chem. Soc.* **117**, 5179.

Cotton, F. A., Wilkinson, G. (1988). *Advanced Inorganic Chemistry*, 5th ed. New York : John Wiley & Sons.

Cramer, C. J., Dulles, F. J., Giesen, D. J., Almlöf, J. (1995). *Chem. Phys. Lett.* **245**, 165.

Cremer, D., Kraka, E. (1984). *Angew. Chem.* **23**, 627.

Cundari, T. R., Benson, M. T., Lutz, M. L., Sommerer, S. O. (1996). *Reviews in Computational Chemistry*, edited by K. B. Lipkowitz and D. B. Boyd, Vol. VIII, p. 145. New York: VCH.

Dapprich, S., Frenking, G. (1995). *J. Phys. Chem.* **99**, 9352.

Davidson, E. R., Feller, D. (1986). *Chem. Rev.* **86**, 681.

Davidson, E. R. (1991). *Chem. Rev.* **91**, 649.

Dewar, M. J. S. (1951). *Bull. Soc. Chim. France*, C71.

Dewar, M. J. S., Zoebisch, E. G., Healy, E. F., Stewart, J. J. P. (1985). *J. Am. Chem. Soc.* **107**, 3902.

Dickson, R. M., Becke, A. D. (1993). *J. Chem. Phys.* **99**, 3898.

Ditchfield, R., Hehre W. J., Pople, J. A. (1971). *J. Chem. Phys.* **54**, 724.

Dunning Jr., T. H., Hay, P. J. (1976). *Modern Theoretical Chemistry*, edited by H.F. Schaefer III, p. 1. New York: Plenum.

Eckart, C. E. (1930). *Phys. Rev.* **36**, 878.

Ehlers, A. W., Dapprich, S., Vyboishchikov, S. F., Frenking, G. (1996). *Organometallics.* **15**, 105.

Fan, H-J., Liu, C-W. (1999). *Chem. Phys. Lett.* **300**, 351.

Feller, D., Davidson, E. R. (1990). *Reviews in Computational Chemistry*, edited by K. B. Lipkowitz and D. B. Boyd, Vol. I, p. 1. New York: VCH.

Fermi, E. (1927). *Rend. Accad. Lincei.* **6**, 602.

Fock, V. (1930). *Z. Physik.* **61**, 161.

Fournier, R., Andzelm, J., Salahub, D. R. (1989). *J. Chem. Phys.* **90**, 6371.

Frenking, G., Antes, I., Böhme, M., Dapprich, S., Ehlers, A. W., Jonas, V., Neuhaus, A., Otto, M., Stegmann, R., Veldkamp, A., Vyboishchikov, S. F. (1996). *Reviews in Computational Chemistry*, edited by K. B. Lipkowitz and D. B. Boyd, Vol. VIII, p. 63. New York: VCH.

Frenking, G., Pidun, U. (1997). *J. Chem. Soc. Dalton Trans.* 1653.

Frenking, G., Frölich, N. (2000). *Chem. Rev.* **100**, 717.

Frisch, M. J., Trucks, G. W., Schlegel, H. B., Scuseria, G. E., Robb, M. A., Cheeseman, J. R., Zakrzewski, V. G., Montgomery Jr., J. A., Stratmann, R. E., Burant, J. C., Dapprich, S., Millam, J. M., Daniels, A. D., Kudin, K. N., Strain, M. C., Farkas, O., Tomasi, J., Barone, V., Cossi, M., Cammi, R., Mennucci, B., Pomelli, C., Adamo, C., Clifford, S., Ochterski, J., Petersson, G. A., Ayala, P. Y., Cui, Q., Morokuma, K., Malick, D. K., Rabuck, A. D., Raghavachari, K., Foresman, J. B., Cioslowski, J., Ortiz, J. V., Baboul, A. G., Stefanov, B. B., Liu, G., Liashenko, A., Piskorz, P., Komaromi, I., Gomperts, R., Martin, R. L., Fox, D. J., Keith, T., Al-Laham, M. A. , Peng, C. Y., Nanayakkara, A., Gonzalez, C., Challacombe, M., Gill, P. M. W., Johnson, B. G., Chen, W., Wong, M. W., Andres, J. L., Head-Gordon, M., Replogle E. S., Pople, J. A. (1998). *Gaussian 98, Rev. A.7.* Gaussian Inc., Pittsburgh, PA.

Gordon, M. S. (1980). *Chem. Phys. Lett.* **76**, 163.

Haaland, A. (1989). *Angew. Chem. Int. Ed. Engl.* **28**, 992.

Hall, G. G. (1951). *Roy. Soc. London.* **A205**, 541.

Hariharan, P. C., Pople, J. A. (1973). *Theor. Chim. Acta.* **28**, 213.

Hariharan, P. C., Pople, J. A. (1974). *Mol. Phys.* **27**, 209.

Hartree, D. R. (1928). *Proc. Camb. Phil. Soc.* **24**, 89.

Hay, P. J., Wadt, W. R. (1985). *J. Chem. Phys.* **82**, 270.

Hehre, W. J., Ditchfield, R., Pople, J. A. (1972). *J. Chem. Phys.* **56**, 2257.

Helgaker, T., Taylor, P. R. (1995). *Modern Electronic Structure Theory*. Part II, edited by D. Yarkony. Singapore: World Scientific.

Hohenberg, P., Kohn, W. (1964). *Phys. Rev. B.* **136**, 864.

Jensen, F. (2001). *Introduction to Computational Chemistry*. Editor, p. 115. Chichester: John Wiley & Sons.

Jonas, V., Thiel, W. (1995). *J. Chem. Phys.* **102**, 8474.

Jonas, V., Thiel, W. (1996). *J. Chem. Phys.* **105**, 3636.

Jones, R. O. (1985). *J. Chem. Phys.* **82**, 325.

Klapötke, T. M., Schultz, A. (1998). *Quantum Chemical Methods In Main-Group Chemistry*, p. 45. Chichester: John Wiley & Sons.

Koch, W., Frenking, G., Steffen, G., Reinen, D., Jansen, M., Assenmacher, W. (1993). *J. Chem. Phys.* **99**, 1271.

Koch, W., Holthausen, M. C. (2000). *A Chemist's Guide To Density Functional Theory*, p. 55. Weinheim: Wiley-VCH.

Kohn, W., Sham, L. J. (1965). *Phys. Rev. A.* **140**, 1133.

Korber, N., Jansen, M. (1990). *Chem. Commun.* 1654.

Krauss, M., Stevens, W. J. (1984). *Ann. Rev. Phys. Chem.* **35**, 357.

Lee, C., Yang, W., Parr, R. G. (1988). *Phys. Rev. B.* **37**, 785.

Lee, T. J., Allen, W. D., Schaefer III, H. F. (1987). *J. Chem. Phys.* **87**, 7062.

Lee, T. J., Scuseria, G. E. (1990). *J. Chem. Phys.* **93**, 489.

Levy, M. (1979). *Proc. Natl. Acad. Sci. USA.* **76**, 6062.

Levy, M. (1982). *Phys. Rev. A.* **26**, 1200.

Møller, C., Plesset, M.S. (1934). *Phys. Rev.* **46**, 618.

Morin, M., Foti, A. E., Salahub, D. R. (1985). *Can. J. Chem.* **63**, 1982.

Mulliken, R. S. (1962). *J. Chem. Phys.* **36**, 3428.

Murray, C. W., Handy, N. C., Amos, R. D. (1993). *J. Chem. Phys.* **98**, 7145.

Nakao, Y., Hirao, K., Taketsugu, T. (2001). *J. Chem. Phys.* **114**, 7935.

Pauli, W. (1925). *Z. Physik.* **31**, 765.

Perdew, J. P. (1986). *Phys. Rev. B.* **33**, 8822.

Perdew, J. P. (1991). *Electronic Structure of Solids*, edited by P. Ziesche and H. Eschrig, p. 11. Berlin: Akademie Verlag.

Perdew, J. P., Wang, Y. (1986). *Phys. Rev. B.* **33**, 8800.

Perdew, J. P., Wang, Y. (1992). *Phys. Rev. B.* **45**, 13244.

Pidun, U., Frenking, G. (1996). *J. Organometallic Chem.* **525**, 269.

Popelier, P. (2000). Editor. *Atoms in Molecules: An Introduction.* Harlow: Prentice Hall.

Popelier, P., Bader, R. F. W. (1998). *J. Phys. Chem.* **102**, 7314.

Pople, J. A., Beveridge, D. L., Dobosh, P. (1967). *J. Phys. Chem.* **47**, 2026.

Pople, J. A., Beveridge, D. L. (1970). *Approximate Molecular Orbital Theory.* New York: McGraw-Hill.

Pople, J. A., Gill, P. M. W., Handy, N. C. (1995). *Int. J. Quantum Chem.* **56**, 303.

Raghavachari, K., Trucks, G. W., Pople, J. A., Replogle, E. (1989). *Chem. Phys. Lett.* **158**, 207.

Rappé, A. K., Casewit, C. J., Colwell, K. S., Goddard III, W. A., Skiff, W. M. (1992). *J. Am. Chem. Soc.* **114**, 10024.

Reed, A. E., Curtiss, L. A., Weinhold, F. (1988). *Chem. Rev.* **88**, 899.

Roothaan, C. C. J., (1951). *Rev. Mod. Phys.* **23**, 69.

Schaftenaar, G., Noordik, J. H. (2000). *J. Comput.-Aided Mol. Design.* **14**, 123.

Schrödinger, E. (1926a). *Ann. Physik.* **79**, 361.

Schrödinger, E. (1926b). *Ann. Physik.* **80**, 437.

Schrödinger, E. (1926c). *Ann. Physik.* **81**, 109.

Scott, A. P., Radom, L. (1996). *J. Phys. Chem.* **100**, 16502.

Scuseria, G. E., Lee, T. J., Scheiner, A. C., Schaefer III, H. F. (1989). *J. Chem. Phys.* **90**, 5635.

Seeger, R., Pople, J. A. (1977). *J. Chem. Phys.* **66**, 3045.

Segal, G., Pople, J. A. (1966). *J. Chem. Phys.* **44**, 3289.

Shriver, D. F., Atkins, P. W. (1999). *Inorganic Chemistry*, 3rd edition, p. 539. Oxford: Oxford Univ Press.

Slater, J. C. (1929). *Phys. Rev.* **34**, 1293.

Slater, J. C. (1930). *Phys. Rev.* **35**, 509.

Slater, J. C. (1930). *Phys. Rev.* **36**, 75.

Sodupe, M., Branchadell, V., Rosi, M., Bauschlicher, Jr., C. W. (1997). *J. Phys. Chem. A.* **101**, 7854.

Stanton, J. F., Magers, W. N. (1988). *J. Chem. Phys.* **88**, 7650.

Stanton, J. F., Lipscomb, W. N., Magers, D. H., Bartlett, R. J. (1989). *J. Chem. Phys.* **90**, 1077.

Stewart, J. J. P. (1989). *J. Comput. Chem.* **10**, 209.

Thomas, L. H. (1927). *Proc. Camb. Phil. Soc.* **23**, 542.

Thomas, J. L. C., Bauschlicher Jr., C. W., Hall, M. B. (1997). *J. Phys Chem. A.* **101**, 8530.

Van Duijneveldt, F. B., Van Duijneveldt-van de Rijdt, J. G. C. M., Van Lenthe, J. H. (1994). *Chem. Rev.* **94**, 1873.

Versluis, L., Ziegler, T. (1988). *J. Chem. Phys.* **88**, 322.

Vosko, S. H., Wilk, L., Nusair, M. (1980). *Can. J. Phys.* **58**, 1200.

Wachters, A. J. H. (1970). *J. Chem. Phys.* **52**, 1033 .

Wadt, W. R., Hay, P. J. (1985a). *J. Chem. Phys.* **82**, 299.

Wadt, W. R., Hay, P. J. (1985b). *J. Chem. Phys.* **82**, 284.

Weinhold, F. (1998). *Encyclopedia of Computational Chemistry,* edited by P. v. R. Schleyer, N. L. Allinger, T. Clark, P. A. Kollman, H. F. Schaefer III, P. R. Scheiner, Vol. 3, p.1793. Chichester: Wiley-VCH.

Whitaker, A., Jeffrey, J. W. (1967). *Acta Cryst.* A**31**, 1649.

Wilson, S. (1987). *Adv. Chem. Phys.* **67**, 439.

Yamaguchi, Y., Frisch, M. J., Lee, T. J., Schaefer III, H. F., Binkley, J. S. (1968). *Theor. Chim. Acta.* **69**, 337.

Ziegler, T. (1991). *Chem. Rev.* **91**, 651.

Addendum A: Gaussian98 Input

Example of *Gaussian98* input file for O_3 optimisation and frequency calculation

```
%chk=checkpoint.chk
#b3lyp/6-31G(d) opt scf(maxcycle=512,nosymm) nosymm guess=mix
iop(6/7=3) gfinput
```

(`iop(6/7=3)` ***and*** `gfinput` ***is needed in order for the Molden graphical package to display structures and densities)***

```
Title

0 1
O
O 1 1.272
O 2 1.272 1 116.8
```

(The checking of a wave function for instabilities cannot be done together with an optimisation or frequency calculation and therefore the job was split into three parts using the `--link1-` ***command)***

```
--link1-
%chk=checkpoint.chk
#b3lyp/6-31G(d) stable=Opt scf(maxcycle=512, nosymm) nosymm
guess=read geom=allcheck iop(6/7=3) gfinput

--link1-
%chk=checkpoint.chk
#b3lyp/6-31G(d) freq scf(maxcycle=512, nosymm) nosymm guess=read
geom=allcheck iop(6/7=3) gfinput
```

Example of input file for $M[O_3]^{2+}$ optimisation and frequency calculation

```
%chk=checkpoint.chk
#B3LYP/6-31G(d) opt guess=mix scf(maxcycle=512, conver=6) nosymm
gfinput iop(6/7=3)

Title

2 1
M
M 1 1.5
O 2 1.28 1 95.0
O 3 1.28 2 116.8 1 0.0

--link1--
%chk=checkpoint.chk
#B3LYP/6-31G(d) stable=opt geom=allcheck guess=read nosymm
scf(maxcycle=512, conver=6, nosymm) nosymm gfinput iop(6/7=3)

--link1--
%chk=checkpoint.chk
#B3LYP/6-31G(d) freq geom=allcheck guess=read  scf(maxcycle=512,
conver=6, nosymm) nosymm gfinput iop(6/7=3)
```

Example of input file for $M(CO)_nH_m(O_3)$ optimisation and frequency calculation with basis set II

(The basis set is specified using the `gen` ***command which prompts the program to read the basis set from the input file. This is needed because two basis sets, and not one standard set, are used. Specifying the lanl2dz basis set at the end of the molecule specification and not in the route section only specifies what AO functions should be used. The pseudopotentials for the***

core need to be specified in the route section using `pseudo`. ***The wave function needed for the AIMPAC suite of programs is generated using*** `output=wfn` ***and then specifying the file name at the end of the molecule specification.)***

```
%chk=checkpoint.chk
#b3lyp/gen opt freq scf(maxcycle=512, nosymm) pseudo=lanl2
pop=nboread gfnput IOP(6/7=3) nosymm output=wfn

Title

0  1
Molecule Specification

M 0
LanL2DZ
****
C O H 0
6-31G(d)
****

wavefunction.wfn
```

(In cases where the Lewis structure found by the NBO algorithm did not conform to the expected structure, e.g. no bonding orbitals between the metal and ozone, the lone pairs, single, double and triple bonds were explicitly specified, using `pop=nboread`. ***The bonded atom pairs are specified*** `xn` ***and*** `xm`***)***

```
$nbo $end
$choose
lone x1 amount x2 amount x3 amount ... end
bond s x4 y4  s x5 y5  s x6 y6 ...
     d x7 y7  d x8 y8  d x9 y9 ...
     t x10 y10  t x11 y11  t x12 y12 ... end
```

```
$end
```

Example of input file for the calculation of the Basis Set Superposition Error of $M(CO)_nH_m(O_3)$

```
#b3lyp/gen sp scf(maxcycle=512, conver=6, nosymm) nosymm
pseudo=lanl2 pop=none gfnput iop(6/7=3)

Metal fragment

0  1
```
Molecule specification ***(Only the metal and carbonyls are specified here)***

```
M 0
LanL2DZ
****
C O H 0
6-31G(d)
****

--link1--

#b3lyp/6-31G(d) sp scf(maxcycle=512,conver=5, nosymm) nosymm
pop=none gfInput iop(6/7=3)

Ligand fragment

0 1
```
Molecule Specification ***(Only the ozone is specified here)***

```
--link1--
```

```
#b3lyp/gen sp scf(maxcycle=512, conver=6, nosymm) pseudo=lanl2
pop=none gfinput iop(6/7=3) massage
```

(the massage ***command together with the*** Nuc ***specification is used to remove the particles associated with the required atoms in order to leave behind just the basis functions centred on those atoms)***

```
Metal fragment with ligand functions

0  1
```

Molecule specification ***(The whole complex is specified here)***

```
Ti 0
LanL2DZ
****
C O 0
6-31G(d)
****

[ozone atom1] Nuc 0.0
[ozone atom2] Nuc 0.0
[ozone atom3] Nuc 0.0

--link1--

#b3lyp/gen sp scf(maxcycle=512, conver=6, nosymm) pseudo=lanl2
pop=none gfinput iop(6/7=3) massage

Ligand fragment with metal fucntions

0  1
```

Molecule specification ***(The whole complex is specified here)***

```
M 0
LanL2DZ
****
C O H 0
6-31G(d)
****

[atom1] Nuc 0.0
[atom2] Nuc 0.0
[atom3] Nuc 0.0
     ...
     ...
     ...
```

Addendum B: CDA 2.1.2 Analysis Output

The contributions of all the occupied molecular orbitals of the complexes to the donation d, back donation b, repulsive polarisation r and rest terms Δ. The molecular orbitals are arranged from lowest to highest energy.

CDA 2.1.2 results for $Ti(CO)_5(O_3)$

--- donation q[d](i) ---

```
-0.000  0.001 -0.000 -0.000 -0.000 -0.000  0.003  0.004 -0.000 -0.000
-0.000 -0.000 -0.000 -0.000 -0.004 -0.000 -0.002 -0.001 -0.133 -0.000
-0.000 -0.000 -0.000 -0.041  0.041  0.000 -0.001 -0.000 -0.001 -0.000
 0.070  0.000  0.001 -0.002  0.013  0.009  0.006 -0.000  0.006  0.007
 0.021  0.000  0.019  0.024  0.008  0.002  0.013  0.023  0.114  0.124
 0.124  0.002  0.014  0.000  0.000  0.000  0.000  0.000  0.000  0.000
```

Total value *q[d]*: 0.462 Electrons

--- back donation q[b](i) ---

```
-0.000 -0.000 -0.000 -0.000 -0.000 -0.000 -0.000 -0.000 -0.000 -0.000
 0.000  0.000  0.000 -0.001 -0.007  0.002  0.001 -0.000 -0.005 -0.000
-0.000 -0.000 -0.000 -0.002 -0.001 -0.002 -0.004  0.001 -0.002  0.001
 0.003  0.000 -0.001 -0.007  0.003 -0.001  0.012 -0.000 -0.001  0.008
-0.002 -0.000 -0.006  0.002 -0.001 -0.004  0.001 -0.001 -0.001 -0.002
-0.001  0.203  0.002  0.000  0.000  0.000  0.000  0.000  0.000  0.000
```

Total value *q[b]*: 0.188 Electrons

--- repulsive polarisation q[r](i) ---

```
-0.000 -0.000 -0.000  0.000 -0.000  0.000  0.000  0.000 -0.000 -0.000
 0.000 -0.000  0.000  0.006  0.035  0.001  0.016 -0.000 -0.033 -0.000
```

```
-0.000 -0.000 -0.000 -0.012 -0.002 -0.008 -0.012  0.002  0.005  0.007
 0.049  0.000 -0.000 -0.008  0.027  0.010  0.045  0.000 -0.006  0.051
-0.030  0.002 -0.050  0.018 -0.030  0.045 -0.045 -0.075 -0.119 -0.017
-0.101 -0.080 -0.085  0.000  0.000  0.000  0.000  0.000  0.000  0.000

 Total value q[r]:  -0.395 Electrons

--- residual q[Δ](i) ---

-0.000 -0.000 -0.000 -0.000 -0.000 -0.000 -0.000 -0.000 -0.000 -0.000
-0.000 -0.000 -0.000 -0.000 -0.000 -0.000 -0.000 -0.000 -0.002 -0.000
-0.000 -0.000 -0.000  0.000  0.001  0.000 -0.000 -0.000 -0.000 -0.000
 0.004 -0.000  0.000 -0.000  0.001  0.000  0.001 -0.000  0.000  0.001
 0.000  0.000  0.001  0.002 -0.001  0.000  0.000 -0.000 -0.002  0.008
 0.001  0.005  0.002  0.000  0.000  0.000  0.000  0.000  0.000  0.000

 Total value q[Δ]:   0.021 Electrons
```

CDA 2.1.2 results for $V(CO)_4H(O_3)$

```
--- donation q[d](i) ---

 0.001 -0.000 -0.000 -0.000 -0.000  0.003  0.002 -0.000 -0.000 -0.000
-0.000 -0.000 -0.002 -0.000 -0.002 -0.056 -0.000 -0.000 -0.000 -0.000
-0.022  0.050 -0.004 -0.000  0.000 -0.000  0.104 -0.010  0.031  0.008
 0.001  0.001  0.011 -0.000  0.030  0.015  0.000  0.023  0.001  0.004
 0.012  0.080  0.122 -0.019  0.078  0.002  0.013  0.000  0.000  0.000

Total value q[d]:   0.477 Electrons

--- back donation q[b](i) ---

-0.000 -0.000 -0.000 -0.000 -0.000 -0.000 -0.000  0.000  0.000  0.000
 0.000  0.001 -0.008  0.002  0.003 -0.003 -0.000 -0.000 -0.001 -0.000
```

```
-0.002 -0.001 -0.012  0.001  0.001 -0.000  0.001 -0.016  0.006 -0.000
 0.002  0.000  0.016 -0.000 -0.007 -0.004  0.000  0.001 -0.003  0.000
 0.004  0.005 -0.001 -0.020 -0.002  0.230 -0.001  0.000  0.000  0.000

 Total value q[b]:    0.192 Electrons

--- repulsive polarisation q[r](i) ---

-0.000 -0.000 -0.000  0.000  0.000  0.000  0.000 -0.000  0.000 -0.000
 0.000  0.007  0.025  0.000  0.014 -0.024 -0.000 -0.000 -0.000 -0.000
-0.014  0.003 -0.035  0.002  0.011  0.004  0.020 -0.025  0.055  0.004
 0.005 -0.001  0.070  0.015 -0.046 -0.044  0.000  0.015  0.044 -0.016
-0.023 -0.079 -0.019 -0.105 -0.093 -0.096 -0.096  0.000  0.000  0.000

 Total value q[r]:  -0.421 Electrons

--- residual q[Δ](i) ---

-0.000 -0.000 -0.000 -0.000 -0.000 -0.000 -0.000 -0.000 -0.000 -0.000
-0.000 -0.000  0.000 -0.000 -0.000 -0.000 -0.000 -0.000 -0.000 -0.000
 0.001  0.000 -0.000 -0.000  0.000  0.000  0.006 -0.002  0.001  0.000
 0.000 -0.000  0.001  0.000  0.001  0.001  0.000  0.002 -0.000  0.000
-0.001 -0.007  0.008 -0.001  0.001  0.002  0.002  0.000  0.000  0.000

 Total value q[Δ]:    0.014 Electrons
```

CDA 2.1.2 results for $Cr(CO)_4(O_3)$

```
--- donation q[d](i) ---

 0.001 -0.000 -0.000 -0.000 -0.000  0.003  0.002 -0.000 -0.000 -0.000
-0.000 -0.000 -0.000 -0.002 -0.001 -0.056 -0.000 -0.000 -0.000  0.000
-0.019  0.055 -0.003 -0.000 -0.001 -0.000  0.087 -0.003  0.020  0.002
 0.014  0.003  0.039  0.013  0.002  0.004  0.022  0.000 -0.001 -0.002
```

```
 0.003  0.083  0.110  0.049  0.008 -0.009  0.016  0.000  0.000  0.000

 Total value q[d]:    0.440 Electrons

--- back donation q[b](i) ---

-0.000 -0.000 -0.000 -0.000 -0.000 -0.000 -0.000  0.000  0.000 -0.000
-0.000 -0.000  0.002 -0.004  0.001 -0.002 -0.000 -0.000 -0.000 -0.000
-0.001 -0.001 -0.012  0.001  0.001 -0.000  0.002 -0.012  0.005  0.001
 0.000  0.001  0.013 -0.002 -0.001 -0.002 -0.003  0.000  0.002 -0.003
 0.001  0.001  0.003 -0.001  0.006  0.164 -0.010  0.000  0.000  0.000

 Total value q[b]:    0.147 Electrons

--- repulsive polarisation q[r](i) ---

 0.000  0.000 -0.000  0.000 -0.000  0.000  0.000 -0.000  0.000 -0.000
 0.000  0.004  0.004  0.020  0.007 -0.017 -0.000 -0.000  0.000  0.000
 0.000  0.005 -0.031  0.005  0.002  0.002  0.041 -0.014  0.045  0.003
 0.011 -0.002  0.063 -0.015 -0.002 -0.019 -0.019  0.000  0.006  0.032
-0.011 -0.061 -0.002 -0.047 -0.101 -0.092 -0.144  0.000  0.000  0.000

 Total value q[r]:  -0.328 Electrons

--- residual q[Δ](i) ---

-0.000 -0.000 -0.000 -0.000 -0.000 -0.000 -0.000 -0.000 -0.000 -0.000
-0.000 -0.000 -0.000 -0.000 -0.000 -0.001 -0.000 -0.000 -0.000 -0.000
 0.000  0.000 -0.000 -0.000 -0.000 -0.000  0.003 -0.000  0.000  0.000
 0.000 -0.000  0.005  0.000  0.000  0.000  0.002 -0.000 -0.000 -0.002
-0.000 -0.002  0.004  0.001 -0.000  0.064  0.003  0.000  0.000  0.000

 Total value q[Δ]:    0.077 Electrons
```

CDA 2.1.2 results for $Mn(CO)_3H(O_3)$

--- donation q[d](i) ---

```
 0.001 -0.000 -0.000 -0.000  0.002  0.002 -0.000 -0.000 -0.000 -0.000
-0.001 -0.000 -0.000 -0.067  0.000 -0.000 -0.000 -0.037  0.065 -0.005
-0.001 -0.001  0.016  0.046 -0.004  0.095  0.000  0.001  0.007  0.007
 0.000  0.000 -0.001 -0.000  0.077  0.013  0.068  0.034  0.011 -0.091
-0.001  0.000  0.000  0.000  0.000  0.000  0.000  0.000  0.000  0.000
```

Total value *q[d]*: 0.237 Electrons

--- back donation q[b](i) ---

```
-0.000 -0.000 -0.000 -0.000 -0.000 -0.000 -0.000 -0.000  0.000  0.002
-0.001  0.001  0.001 -0.002 -0.000 -0.000 -0.000  0.000 -0.001 -0.013
-0.000  0.001  0.003  0.005 -0.014  0.002  0.000  0.000 -0.003 -0.001
-0.000  0.000  0.001  0.000  0.005  0.002  0.003 -0.004  0.005  0.004
-0.007  0.000  0.000  0.000  0.000  0.000  0.000  0.000  0.000  0.000
```

Total value *q[b]*: -0.012 Electrons

--- repulsive polarisation q[r](i) ---

```
 0.000 -0.000 -0.000 -0.000  0.000  0.000 -0.000 -0.000 -0.000  0.005
 0.013  0.000  0.006 -0.010 -0.000 -0.000 -0.000  0.030  0.003 -0.025
-0.001  0.002  0.115  0.054 -0.016  0.014  0.003  0.002 -0.020 -0.017
-0.000 -0.003  0.007  0.004 -0.063  0.129  0.017 -0.080 -0.110 -0.018
-0.155  0.000  0.000  0.000  0.000  0.000  0.000  0.000  0.000  0.000
```

Total value *q[r]*: -0.113 Electrons

--- residual q[Δ](i) ---

```
-0.000 -0.000 -0.000 -0.000 -0.000 -0.000 -0.000 -0.000 -0.000 -0.000
-0.000 -0.000 -0.000 -0.001 -0.000 -0.000 -0.000 -0.000  0.000 -0.001
-0.000 -0.000  0.000  0.000 -0.001  0.012 -0.000  0.000  0.000  0.000
-0.000  0.000 -0.000 -0.000 -0.005  0.000  0.001  0.003  0.004  0.199
 0.020  0.000  0.000  0.000  0.000  0.000  0.000  0.000  0.000  0.000

 Total value q[Δ]:    0.230 Electrons
```

CDA 2.1.2 results for $Fe(CO)_3(O_3)$

```
--- donation q[d](i) ---

 0.001 -0.000 -0.000 -0.000  0.002  0.003 -0.000 -0.000 -0.000 -0.000
-0.001 -0.000  0.000 -0.074 -0.001 -0.000  0.000  0.012  0.062 -0.007
-0.001 -0.000  0.130 -0.003  0.014  0.003 -0.000  0.008  0.011  0.029
 0.000  0.009  0.017 -0.003  0.070  0.012  0.115  0.004  0.041  0.027
 0.014  0.000  0.000  0.000  0.000  0.000  0.000  0.000  0.000  0.000

 Total value q[d]:    0.494 Electrons

--- back donation q[b](i) ---

-0.000 -0.000 -0.000 -0.000 -0.000 -0.000 -0.000  0.000 -0.000  0.001
 0.001  0.002  0.001 -0.002 -0.000 -0.000 -0.000 -0.001 -0.000 -0.016
 0.001  0.000  0.001 -0.015  0.001  0.000  0.000  0.008  0.000 -0.002
 0.000  0.001  0.002  0.003  0.004  0.002 -0.001  0.002  0.032 -0.010
 0.146  0.000  0.000  0.000  0.000  0.000  0.000  0.000  0.000  0.000

 Total value q[b]:    0.159 Electrons

--- repulsive polarisation q[r](i) ---

 0.000  0.000 -0.000 -0.000  0.000  0.000 -0.000 -0.000 -0.000  0.003
 0.011  0.006  0.000 -0.006 -0.000  0.000 -0.000 -0.005  0.025 -0.035
```

```
 0.003  0.001  0.012 -0.012  0.036  0.008  0.004  0.043 -0.018 -0.003
 0.000  0.004  0.025  0.011 -0.038  0.134 -0.017 -0.112 -0.151 -0.197
-0.085  0.000  0.000  0.000  0.000  0.000  0.000  0.000  0.000  0.000

 Total value q[r]:  -0.353 Electrons

--- residual q[Δ](i) ---

-0.000 -0.000 -0.000 -0.000 -0.000 -0.000 -0.000 -0.000 -0.000 -0.000
-0.000 -0.000 -0.000 -0.001 -0.000 -0.000 -0.000  0.001  0.000 -0.001
-0.000 -0.000  0.004 -0.001 -0.000  0.000 -0.000  0.001 -0.000  0.000
-0.000  0.001  0.002 -0.001 -0.003  0.000  0.005  0.000 -0.002  0.003
 0.026  0.000  0.000  0.000  0.000  0.000  0.000  0.000  0.000  0.000

 Total value q[Δ]:   0.034 Electrons
```

CDA 2.1.2 results for $Co(CO)_2H(O_3)$

```
--- donation q[d](i) ---

-0.000 -0.000  0.000  0.002  0.002 -0.000 -0.000 -0.000 -0.001 -0.000
-0.000  0.002 -0.000 -0.050 -0.029  0.075 -0.006 -0.001  0.014 -0.003
 0.000 -0.000  0.000  0.002  0.045 -0.003  0.077  0.020 -0.001  0.046
 0.011  0.074  0.065  0.025 -0.061  0.000  0.000  0.000  0.000  0.000

Total value q[d]:   0.305 Electrons

--- back donation q[b](i) ---

-0.000 -0.000 -0.000 -0.000 -0.000 -0.000  0.000  0.005  0.002  0.001
 0.001 -0.000  0.000 -0.002  0.001 -0.000 -0.012  0.001  0.005 -0.013
-0.004 -0.000  0.000  0.001  0.003  0.003  0.007  0.001  0.002  0.006
 0.001  0.001  0.021 -0.006 -0.038  0.000  0.000  0.000  0.000  0.000
```

Total value *q[b]*: -0.012 Electrons

--- *repulsive polarisation q[r](i)* ---

```
-0.000 -0.000  0.000  0.000  0.000 -0.000 -0.000  0.004  0.009  0.005
 0.000  0.001  0.000 -0.010  0.052  0.019 -0.028  0.001  0.127 -0.008
 0.012  0.001  0.002 -0.005  0.032  0.009  0.044 -0.038  0.137 -0.029
-0.109  0.020 -0.146 -0.172  0.004  0.000  0.000  0.000  0.000  0.000
```

Total value *q[r]*: -0.065 Electrons

--- *residual q[Δ](i)* ---

```
-0.000 -0.000 -0.000 -0.000 -0.000 -0.000 -0.000 -0.000 -0.000 -0.000
-0.000 -0.000 -0.000 -0.000 -0.000  0.000 -0.001 -0.000  0.000 -0.001
 0.000 -0.000 -0.000 -0.000  0.001 -0.000  0.012  0.000 -0.000 -0.002
-0.000  0.002  0.002  0.001  0.192  0.000  0.000  0.000  0.000  0.000
```

Total value *q[Δ]*: 0.204 Electrons

CDA 2.1.2 results for $Ni(CO)_2(O_3)$

--- *donation q[d](i)* ---

```
-0.000 -0.000  0.000  0.001  0.002 -0.000 -0.000 -0.000 -0.001 -0.000
-0.000 -0.000 -0.000 -0.049 -0.031  0.072 -0.005 -0.001 -0.005 -0.002
 0.000 -0.000 -0.000  0.015 -0.005  0.035  0.065  0.022 -0.008  0.067
 0.018  0.093  0.067  0.026 -0.046  0.000  0.000  0.000  0.000  0.000
```

Total value *q[d]*: 0.331 Electrons

--- *back donation q[b](i)* ---

```
-0.000 -0.000 -0.000 -0.000 -0.000 -0.000  0.000  0.004  0.004  0.003
 0.001 -0.000 -0.000 -0.001  0.001  0.000 -0.010  0.002 -0.013 -0.009
 0.000  0.005 -0.000 -0.001  0.009  0.012  0.017 -0.009  0.002  0.003
 0.020 -0.001 -0.002 -0.005 -0.053  0.000  0.000  0.000  0.000  0.000

 Total value q[b]:  -0.020 Electrons

--- repulsive polarisation q[r](i) ---

-0.000  0.000 -0.000  0.000  0.000 -0.000 -0.000  0.004  0.008  0.004
 0.000 -0.000  0.000 -0.006  0.064  0.026 -0.027  0.002 -0.016 -0.012
-0.000  0.041  0.001  0.040  0.059  0.090  0.067 -0.131  0.124 -0.079
-0.091 -0.005 -0.067 -0.152  0.013  0.000  0.000  0.000  0.000  0.000

 Total value q[r]:  -0.042 Electrons

--- residual q[Δ](i) ---

-0.000 -0.000 -0.000 -0.000 -0.000 -0.000 -0.000 -0.000 -0.000 -0.000
-0.000 -0.000 -0.000 -0.000 -0.000  0.000 -0.001 -0.000 -0.001  0.000
-0.000 -0.000  0.000 -0.000 -0.000  0.000  0.013  0.001 -0.000 -0.003
-0.003  0.003  0.001  0.001  0.162  0.000  0.000  0.000  0.000  0.000

 Total value q[Δ]:   0.173 Electrons
```

CDA 2.1.2 results for Cu(CO)H(O_3)

```
--- donation q[d](i) ---

 0.000 -0.000  0.000  0.001 -0.000 -0.000 -0.000 -0.000 -0.000 -0.040
-0.000  0.002  0.043  0.000  0.047  0.036  0.023  0.000  0.000 -0.001
 0.021  0.007  0.005  0.001  0.032  0.072  0.008  0.041  0.056  0.000

 Total value q[d]:   0.353 Electrons
```

--- *back donation q[b](i)* ---

```
-0.000 -0.000 -0.000 -0.000 -0.000  0.001  0.000  0.003  0.002 -0.000
-0.000  0.000  0.000 -0.001  0.001  0.001  0.001 -0.001 -0.000 -0.004
-0.002 -0.001 -0.001  0.001  0.004  0.009 -0.001 -0.009  0.104  0.000
```

Total value *q[b]*: 0.107 Electrons

--- *repulsive polarisation q[r](i)* ---

```
 0.000 -0.000  0.000  0.000 -0.000  0.000  0.000  0.002  0.001 -0.001
-0.000  0.004  0.019 -0.000  0.035  0.025  0.021 -0.005  0.000 -0.011
 0.050  0.040  0.097  0.047 -0.009 -0.097 -0.056 -0.189 -0.130  0.000
```

Total value *q[r]*: -0.157 Electrons

--- *residual q[Δ](i)* ---

```
-0.000 -0.000 -0.000 -0.000 -0.000 -0.000 -0.000 -0.000 -0.000 -0.000
-0.000  0.000  0.000 -0.000  0.001  0.001  0.001  0.000 -0.000 -0.000
-0.002 -0.001  0.000 -0.000 -0.002 -0.006  0.000  0.002  0.013  0.000
```

Total value *q[Δ]*: 0.005 Electrons